DEVELOPING LIGNIN-BASED EPOXY AND POLYURETHANE RESINS

By

Saeid Nikafshar

A DISSERTATION

Submitted to
Michigan State University
in partial fulfillment of the requirements
for the degree of

Forestry-Doctor of Philosophy

2022

ABSTRACT

DEVELOPING LIGNIN-BASED EPOXY AND POLYURETHANE RESINS

By

Saeid Nikafshar

Lignin, the most abundant natural aromatic polymer, is currently produced as by-product during biorefinery and chemical pulping processes. Lignin is rich in hydroxyl functional groups (both phenolic and aliphatic OH), making it an excellent raw material for synthesizing epoxy and polyurethane resins. However, there are several challenges in utilizing unmodified lignins as feedstock for product development, including high polydispersity/heterogeneity, low reactivity, poor accessibility of hydroxyl groups for reaction with co-monomers low solubility in common organic solvents, and dark color. There are significant variations in lignin characteristics, depending on the source of biomass and isolation methods. Therefore, in-depth lignin characterization is needed to provide the basic knowledge of the structural, chemical, and thermal properties to facilitate lignin valorization.

This study was focused on lignin characterization and development of lignin-based epoxy and polyurethane resins. First, a wide range of lignin samples was fully characterized by measuring their ash contents, elemental analyses, hydroxyl contents, chemical structures, molar mass distributions, and thermal properties. Next, a novel method was developed to measure the reactivity of thirteen different unmodified lignins toward biobased epichlorohydrin (ECH). A partial least square regression (PLS-R) model (with 92 % fitting accuracy and 90 % prediction ability) was created to study the correlation between lignin properties and epoxy content. The results showed that lignins with higher phenolic hydroxyl contents and lower molecular weights were more suitable for replacing 100 % of toxic bisphenol A (BPA) in the formulation of resin

precursors. Additionally, two epoxidized lignin samples (with the highest epoxy contents) were cured using a biobased hardener (Cardolite from cashew nutshell), showed comparable thermomechanical performances and thermal stabilities to a petroleum-based epoxy system.

Biobased waterborne polyurethane resins (PUDs) were also developed by entirely replacing the petroleum-based polyol and the internal emulsifier with either alkaline pre-extraction lignins or enzymatic hydrolysis lignins as well as tartaric acid (a biobased diacid). The formulated resins had zero VOC (volatile organic compound), which was achieved by replacing toxic *n*-methyl-2-pyrrolidone (NMP) with cyrene (a biobased solvent). To further improve the mechanical properties of our biobased PUD resins, 20 wt.% of lignin was substituted with low hydroxyl value soy-polyol, which increased their tensile strength and elongation at break to 87% and 68% of a commercial PUD resin.

The results of this study demonstrated that it is imperative to fully characterize lignin and choose the right lignin for each specific application. This approach enabled us to entirely replace petroleum-based raw materials (BPA and polyol) with lignin and formulate biobased epoxy and polyurethane resins.

Dedicated to my beloved wife, Horieh,
&
My amazing parents, Ali & Mahvash,
For your endless encouragement, support, and love

ACKNOWLEDGMENTS

Words cannot express the depth of my gratitude to my supervisor Dr. Mojgan Nejad for her suggestions, valuable guidance, endless support, advice, insightful criticism, and patience. She always has gone above and beyond to make sure I was on the right track, and she helped me improve myself in all aspects, such as personality, research, writing, and networking. Moreover, special thanks must go to my committee members, Dr. Eric Hegg (Department of Biochemistry & Molecular Biology), Dr. John Dorgan (Chemical Engineering & Material Science Department), and Dr. Mohammad Rabnawaz (School of Packaging) for their valuable comments, feedback, and suggestions.

I gratefully acknowledge Mr. Michael Rich (Composite Materials and Structures Center) and Mr. Aaron Walworth (School of Packaging) for training me to set up lab equipment used in this research study. I would also like to thank my colleague Dr. Nusheng Chen, Dr. Zhen Fang, Dr. Zhaoyang Yuan, Dr. Maryam Arefmanesh, Christian Henry, Mona Alinejad, Mohsen Siahkamari, Kevin Dunne, Jiarun Wang, Akash Gondalyia, and Sasha Bell for their help and support.

Of course, I am so grateful to my family. To my kind and always compassionate mother, my strong and supportive father, and my talented brother: Thank you for everything; I truly appreciate it. I could never have done this without you. I am a blessed son to have you by my side. And last, to my beautiful, brilliant, and fantastic wife, Horieh: I love you. Thank you for your patience, inspiration, support, care, and unconditional love for the last few years. You are my favorite.

TABLE OF CONTENTS

LIST OF TABLES

LIST OF FIGURES

LIST OF SCHEMES

CHAPTER 1

1.1 Introduction

Lignin is the second most abundant natural polymer produced as a by-product during chemical pulping and biorefinery processes. It is found in the middle lamella and the primary and secondary cell walls of plants, and it provides rigidity, strength, and protection from microorganism attacks.[1-4] Lignin is defined as a heterogeneous polymer derived from three phenylpropanoid monomers: *p*-coumaryl, coniferyl, and sinapyl alcohols (the 'so-called' H-, G-, and S- monolignols) that radically couple through carbon-carbon or ether linkages (*i.e.*, β-*O*-4, β-5, and β-β), Scheme 1. The β-*O*-4 bond is the most common linkage, accounting for almost 50% of the linkages in the lignin structure.[5] Monomer composition in lignin varies by different biomass sources. For instance, softwood lignins are primarily composed of G units.[1] On the other hand, hardwood lignins are rich in G and S units with low levels of H units,[6] while herbaceous plants, like wheat straw, consist of all three monomers with a high amount of H units.[7] In addition to the type of monomers, the lignin content significantly depends on plant sources and generally increases in the order of grasses (17 - 24 wt.%), hardwood (18 - 25 wt.%), and softwood (27- 33 wt.%).[8]

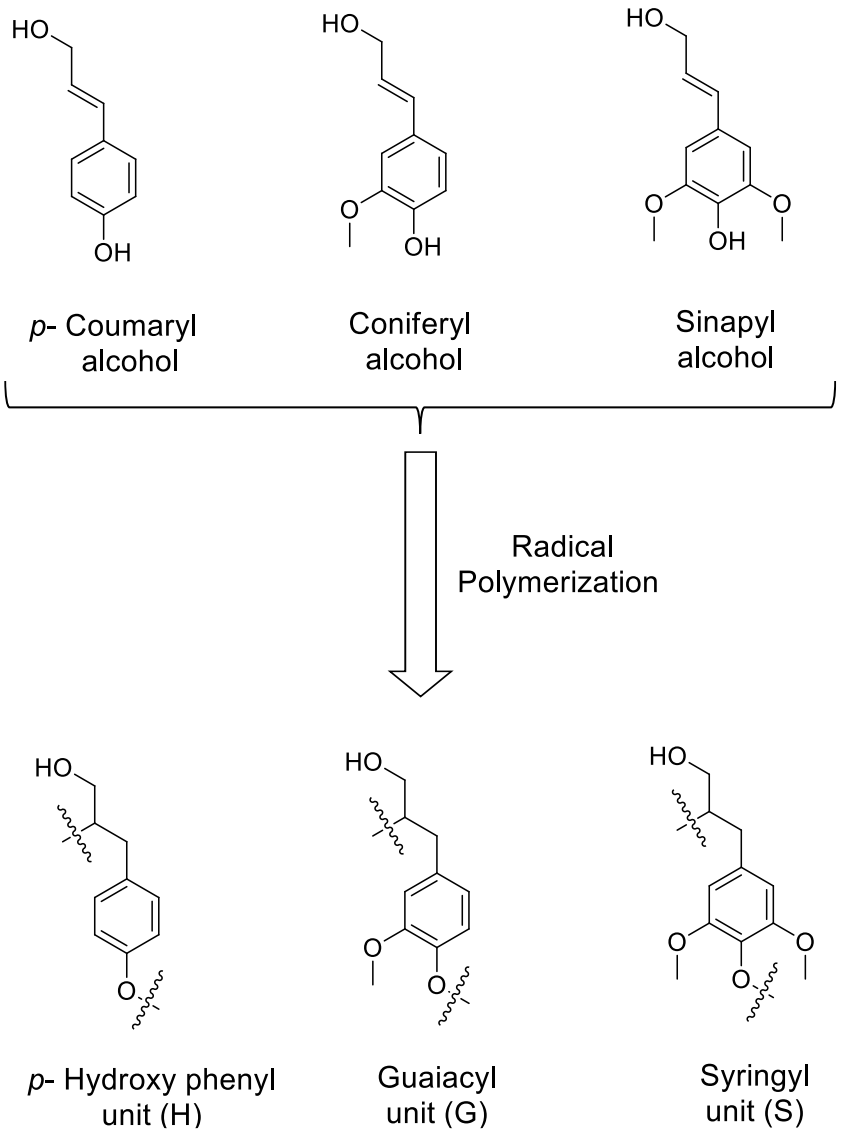

Scheme 1. Three main monolignols (precursors) and their structures in lignin

A variety of lignin isolation methods have been used [9-12] to extract lignin from biomass by breaking linkages in lignin carbohydrate complexes (LCCs), resulting in smaller polymer chains solubilized in the pulping media.[10] During the isolation process, multiple chemical modifications and transformations occur, which significantly change the lignin properties, highlighting the importance of studying the effects of the isolation process on lignin properties. Isolation processes for technical lignins mainly target the maximum valorization of carbohydrates in the biomass

without any concern for the fate of lignin. Several commercial isolation methods, including the sulfite (lignosulfonate), kraft, organosolv, and soda processes, are readily available to produce lignin on the commercial-scale, and the properties of these technical lignins significantly differ based on the isolation processes.[9, 13-15] In addition, several other methods have also been used for lignin isolation from biomass, including ionic liquid, enzymatic hydrolysis, alkaline wet oxidation, and pyrolysis, but those lignins are mainly available at either the lab or pilot scales.[10-12]

The global commercial production of technical lignin (excluding bioenergy production) is approximately 1.65 million tons annually, with lignosulfonate accounting for about 80% of the market.[16] Approximately 16% of production is kraft lignin,[17] and the remainder (4%) is shared between hydrolysis and soda lignins.[18] The majority of the lignin produced is burned and used at its lowest value as fuel despite the fact that it has significant potential as a renewable raw material for producing value-added products.[19] Therefore, there is a great interest in developing lignin-based products by replacing petroleum-based raw materials using cost-effective and environmentally friendly processes.

1.2 Lignin Applications

Lignin has excellent potential to be incorporated into a wide range of products, including as additives or as a raw material for synthesis of polymeric resins. As additives, lignin has been used as an antioxidant,[20] an ultraviolet light-stabilizer,[21] a flame retardant,[22] an antimicrobial,[23] an antibacterial,[24] and a plasticizer.[25] As raw materials in polymeric resins, lignin has been used to partially replace bisphenol A, phenol, and polyol in synthesizing epoxy,[26] polyurethane,[27] phenolic,[28] acrylic,[29] and polyester resins.[30] In addition, lignin has been used as a sustainable feedstock for the production of low molecular weight aromatic compounds such as vanillin,[31]

vanillic acid,[32] syringic aldehyde,[33] syringic acid,[34] *p*-hydroxybenzoic acid.[35] Lignin is also used as a raw material to produce carbon fibers for advanced composite applications. [36]

1.2.1 Lignin-Based Epoxy

Epoxy resins refer to low molecular weight prepolymers that contain one or more epoxy groups (oxirane rings).[37] They are conventionally prepared by reacting epichlorohydrin (ECH) with the hydroxyl groups of bisphenol A (BPA) under alkaline conditions using sodium hydroxide as a catalyst.[38] Epoxy resins are used for the production of adhesives, coatings, and composites due to their excellent chemical, thermal, and mechanical properties.[39, 40] One of the most common types of epoxy resin is diglycidyl ether bisphenol A (DGEBA), as shown in Scheme 2.[39] This resin forms a crosslinked network by adding different curing agents like polyamines, polyamides, anhydrides, and mercaptans, to cure epoxy resin at different temperatures.[38] The final properties of the epoxy system depend on several factors such as curing agents, catalysts, and additives in addition to the curing parameters (*i.e.*, temperature and time).[41]

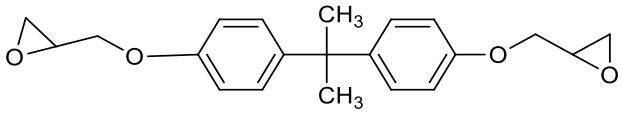

Scheme 2. Chemical structure of diglycidyl ether bisphenol A (DGEBA)

Due to increased greenhouse gas emissions, and health and environmental concerns, there have been serious efforts to replace fossil fuel-based chemicals with biobased materials.[42-44] BPA, which is used as the main raw material in the production of DGEBA epoxy resin, comprises more than 67% of the molar mass of DGEBA.[43] BPA has detrimental effects on human health and the environment and has been shown to act as an endocrine disruptor that is highly toxic for living organisms.[45] BPA-based products have been banned in food packaging, food-related materials,

and baby bottles.[46-48] BPA can be leached out by hydrolysis of carbonate linkages in the presence of a base in mild conditions,[49] since the ester linkages are hydrolyzed easier and faster compared to ether linkages.[50] Therefore, it is of great interest to identify alternative, renewable, and sustainable raw materials that can substitute BPA in the epoxy resin formulation.

Several biobased aromatic compounds have been used to synthesize epoxy resin, including itaconic acid,[43] eugenol,[51] rosins,[52] gallic acid,[46] vanillin,[53] vanillic acid,[54] as well as lignin. [26, 55-62] Renewable compounds like lignin, which are widely available, sustainable, and inedible, are more desirable because they do not compete with food resources like other renewable materials (*e.g.,* vegetable oils). Due to the presence of phenolic hydroxyl groups in lignin's structure (S, G, and H), lignin is widely recognized as an alternative raw material to substitute BPA in epoxy resin formulations.[63]

Although many studies have focused on utilizing lignin in epoxy resin,[64-67] they mostly used modified lignin (fractionated or lignin monomers).[66-68] It was reported that the cured epoxy thermosets made with lignin-derived monomers/dimers had comparable properties to DGEBA thermosets, and properties of the epoxy systems can be tunable by using various curing agents.[69-74] However, the extra cost associated with lignin fractionation and using lignin monomers in epoxy resin formulation has not been viewed favorably by the industry. There have been few studies that used unmodified lignin to replace BPA in epoxy resins. [57-62] Sasaki et al.[57] epoxidized lignin isolated from bamboo by the steam-explosion process and reported that the lignin-based epoxy thermosets had lower thermal stability and flexural strength compared with a petroleum-based epoxy system. Other studies used lignin from different isolation methods and sources to epoxidize lignin and replaced up to 42 wt.% DGEBA in epoxy resin. [60-62] They found the epoxy contents of epoxidized lignins were lower than DGEBA. In addition, the thermal stability and mechanical

properties of lignin-based epoxy networks were decreased by incorporating a higher amount of DGEBA (more than 42 wt.%) with epoxidized lignin. They could not replace a higher amount of DGEBA in epoxy resin due to lower reactivity and higher molecular weight of epoxidized lignin. In contrast, the factors affecting the suitability of lignin in epoxidation reaction have not been directly evaluated.

The structure of lignin is much larger and more complicated than BPA. The high polydispersity index (PDI), low solubility in organic solvents and water, as well as the presence of various functional groups (different types of hydroxyl groups) of lignin are challenges that have limited its application as a BPA replacement.[66] These attributes not only result in a non-homogenous network it also impacts lignin reactivity with epichlorohydrin (ECH).

1.2.2 Lignin-Based Polyurethane

Polyurethanes (PU) are synthesized based on the chemical reaction between a diisocyanate with a di or polyol, a compound containing more than one hydroxyl group, as shown in Scheme 3.[75] Isocyanate compounds are categorized based on their structures (aromatic and aliphatic). MDI (methylene diphenyl diisocyanate) and TDI (toluene diisocyanate) are the aromatic isocyanates most commonly used in PU globally. HDI (hexamethylene diisocyanate) and IPDI (isophorone diisocyanate) are aliphatic isocyanates commonly used for coating formulations because coatings formulated with aromatic isocyanates are sensitive to UV degradation.[76] Aromatic isocyanates are more reactive than aliphatic isocyanates due to the delocalization of electron density in the aromatic rings and are usually used in PU adhesive and foam formulations.

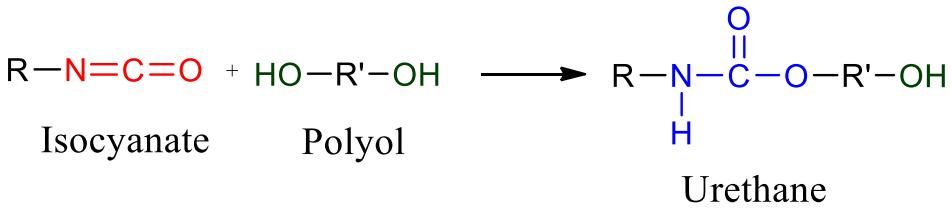

Scheme 3. Urethane synthesis reaction

PU coatings are used for wood, metal, plastic, leather, and textile applications. The automotive and transportation industries are the leading consumer of PU coatings due to their high dielectric strength and high chemical, heat, and weather resistance properties.[77] The global market size of PU was $60.5 billion in 2017, with an estimated annual growth rate of 8-10%.[78] As the global market of polyols shows strong growth, the demand for biobased polyols is increasing, representing an excellent opportunity for renewable and sustainable feedstocks like lignin. The abundance of hydroxyl groups (aliphatic and phenolic), availability, sustainability, and relatively lower price than most petroleum-based polyols makes lignin an excellent candidate for substituting polyols in polyurethane formulations.[79-82]

There are several challenges in incorporating lignin into polyurethane. Lignin has a complex structure in which all hydroxyl groups are not accessible to react with isocyanate due to steric hindrance.[83] In addition, lignin has three different hydroxyl groups, including aliphatic, aromatic, and carboxylic acid groups, which have different reactivity toward isocyanate in the following order: primary aliphatic > secondary aliphatic >> phenolic >-COOH.[84] Therefore, these variations limit the control of the reaction and the performance of final products. Besides, lignin has a relatively high polydispersity index (PDI), which causes the final products to have inconsistent properties due to the low homogeneity of lignin polymeric chains.[85, 86]

1.3 Objectives

The main objectives of this thesis are summarized as below, which resulted in multiple side projects for creating value-added products from lignin:

1) Characterizing the structure of a wide range of commercially available lignins isolated from different biomass sources and isolation processes

2) Replacing toxic bisphenol A with unmodified technical lignins in epoxy resin

   - Investigating the correlation between lignin properties and the epoxy content of epoxidized lignin
   - Measuring chemical, thermal, and mechanical properties of epoxidized lignin thermosets in comparison with a commercial epoxy network (diglycidyl ether bisphenol A, DGEBA)

3) Formulating lignin-based polyurethane resins

   - Exploring the possibility of entirely replacing petroleum-based polyol with hardwood lignin isolated through alkaline pre-extraction and enzymatic hydrolysis processes
   - Increasing the biobased carbon content of resin by substituting other petroleum-based chemicals in polyurethane dispersion formulation (PUD), including internal emulsifier and solvent with biobased compounds
   - Formulating zero-VOC, high-performance resin

1.4 Hypothesis

To successfully develop high-performance lignin-based bioproducts, the first critical step is to start with the right lignin for each specific product. Studying correlations between measured lignin properties and the performance of the developed lignin-based resins can help evaluate the

suitability of new lignin for a particular application based on the simple properties of that lignin measured in the lab. The objectives of these proposed projects were as follows:

1) Lignin with higher phenolic hydroxyl content and lower molecular weight, PDI, and ash content are better candidates for replacing BPA in epoxy resin
2) Lignins with a lighter color and higher aliphatic hydroxyl content have great potential to replace petroleum-based polyol in formulating lignin-based PU resins

CHAPTER 2 (Lignin Characterization)

2.1 Introduction

Choosing the right lignin for a specific application is the most crucial step in lignin valorization. To facilitate the utilization of commercial lignin in different products, in-depth characterization of lignins is needed to provide basic knowledge of the structural, chemical, and thermal properties of each sample lignin. Although lignin's randomness is derived from the radical coupling of H, G, and S monomers, the relative abundance of these monomers and the technique by which lignin is extracted also contribute to variation in lignin properties.

Ash content and elemental analysis provide quantitative information about impurities and lignin composition, such as nitrogen, sulfur, carbon, and sodium contents. These compounds can affect physical (like odor caused by sulfur),[86] or chemical properties of lignin. For instance, a high amount of sodium and potassium in lignin can act as catalysts to both increase the reaction of lignin with isocyanate,[87] and cause trimerization of isocyanate.[88]

Molar mass distribution of lignin is an important structural property that significantly impacts lignin valorization, and it is commonly determined by gel permeation chromatography (GPC). The molecular weight of lignin can play a crucial role in defining the reactivity of lignin with co-monomers and also its suitability for carbon fiber application.[1]

Hydroxyl groups play critical roles in determining the physical and chemical properties of lignin.[89, 90] Therefore, having a reliable method to quantify and qualify different hydroxyl functional groups of lignin is essential. Phosphorous 31-NMR spectroscopy is a technique where hydroxyl functional groups of lignin are selectively labeled with phosphorus as an active nucleus. This technique is advantageous because of a wide chemical shift, less overlap, and less interference from the homonuclear coupling compared to ^{1}H NMR.[91] The ^{31}P NMR technique provides quantitative data

for various types of hydroxyl groups (aliphatic, phenolic, and carboxylic acid) that are critical for employing lignin as raw materials in polymeric resin applications.

The thermal properties of lignin are usually measured by differential scanning calorimetry (DSC) and thermogravimetric analysis (TGA). As an amorphous thermoplastic polymer, it is vital to measure the glass transition temperature (T_g) of lignin to evaluate its flexibility/brittleness at certain temperatures. Source and isolation method, moisture content, molecular weight, and dispersity (Đ), as well as thermal history, significantly affect the T_g of lignin.[92] In addition to T_g that is usually measured by TGA, this technique can also be used to analyze the thermal stability of lignin and its ash content.[93, 94]

2.2 Experimental

2.2.1 Materials

Seventeen commercially available lignins from different biomass sources and isolation processes were purchased or kindly provided by lignin producers Table 1.

Table 1. The list of lignin samples from various isolation processes and sources

Lignin No.*	Source	Isolation Process	Supplier
1-SW-K	Softwood	Kraft	Ingevity
2-SW-K	Softwood	Kraft	Arauco
3-SW-K	Softwood	Kraft	UPM Biochemicals
4-SW-K	Softwood	Kraft	West Fraser
5-SW-K	Softwood	Kraft	Domtar
6-SW-K	Softwood	Kraft	Stora Enso
7-SW-K	Softwood	Kraft	Metsa
8-HW-K	Hardwood	Kraft	Suzano
9-HW-K	Hardwood	Kraft	American Science Technology
10-SW-O	Softwood	Organosolv	Fibria (Lignol)
11-HW-O	Hardwood	Organosolv	Fibria (Lignol)
12-HW-O	Hardwood	Organosolv	American Science Technology
13-WS-O	Wheat Straw	Organosolv	CIMV
14-PS-O	Peanut Shell	Organosolv	American Science Technology
15-CS-O	Corn Stover	Organosolv	American Science Technology
16-SW-L	Softwood	Sulfite (Lignosulfonate)	Borregaard (Lignotech)
17-WS-S	Wheat Straw	Soda	Green Value LCC

*K: kraft, O: organosolv, L: lignosulfonate, S: soda, SW: softwood, HW: hardwood, WS: wheat straw, PS: peanut shell, and CS: corn stover

For ^{31}P NMR, chloroform-d, 99.8% (Cambridge Isotope Laboratories, Inc.), pyridine, anhydrous, 99.8% (Sigma Aldrich), *N*, *N*-dimethylformamide, anhydrous, 99.8% (Sigma Aldrich),

cyclohexanol, 99% (Sigma Aldrich), chromium (III) acetylacetonate 97% (Sigma Aldrich), and 2-chloro-4,4,5,5-tetramethyl-1,3,2-dioxaphopholane 95%, (Sigma Aldrich) were used.

For GPC (THF column), various polystyrene standards ranging from 162-42000 g/mol were purchased from Agilent. All lignin samples were acetylated by acetic anhydride (ACS reagent, 99.7%, Chem-Impex INT'L INC.) and pyridine (99.9%, Sigma Aldrich). Tetrahydrofuran (HPCL grade, J.T. Baker) was used as the mobile phase.

2.3 Characterization

2.3.1 Ash Content

Firstly, crucibles were rinsed with DI water and placed in an oven at 105 °C for 2 hours. Then, all crucibles were kept in a desiccator to cool to room temperature before the addition of lignin. Following TAPPI (Technical Association of Pulp and Paper Industry) T 211 om-93[95]/ASTM (American Society for Testing Materials) D1102,[96] 2 g of oven-dried lignin was added to each crucible and placed in a muffle furnace and heated with a 5 °C/min ramp to 525 °C with a 4-hour dwell time. At least five replicates were performed for each sample. The percent ash content of lignin samples was determined based on initial lignin and residual ash weights.

2.3.2 Elemental Analysis

Samples were dried overnight at 100-105 ^{o}C, ground with a Wiley Mill, and passed through a number 10 sieve (2 mm). All samples were prepared following AOAC (Associate of Official Analytical Chemists) Official Methods 922.02 and 980.03.[97] Afterward, the lignin samples were digested in an open vessel microwave (CEM, MARS 5) procedure following the SW846-3051A. About 0.2 g of lignin was added to 2 mL of nitric acid (68-70 wt.%), placed in the microwave, and the temperature was ramped up to 90 °C with a 90 second dwell time. The samples were then

cooled below 50 ºC before adding 1 mL of hydrogen peroxide (30 wt.%). The samples were microwaved again with a ramp to 105 ºC with a 10-minute dwell. After cooling to room temperature, distilled water was added to the solution to a final volume of 25 mL (1:125 dilution). Mixed samples were analyzed with a Thermo iCAP 6500 Duo instrument. A blank along with several multi-element standards obtained from Inorganic Ventures (aluminum, copper, iron, manganese, zinc, boron, sodium, calcium, magnesium, potassium) was run with the lignin samples as external calibration standard solutions according to Around 1.5 mL of standard or sample was injected in an inductively coupled plasma (ICP)-atomic (or optical) emission spectrometer, Thermo Scientific iCAP 6000 series 6500 Duo, in which 1 mL of sample was used to rinse out the sample loop and 0.5 mL of solution was used for analysis.

Table 2. Around 1.5 mL of standard or sample was injected in an inductively coupled plasma (ICP)-atomic (or optical) emission spectrometer, Thermo Scientific iCAP 6000 series 6500 Duo, in which 1 mL of sample was used to rinse out the sample loop and 0.5 mL of solution was used for analysis.

Table 2. Mineral concentrations in standard solutions

Mineral	High	Medium	Low	Control Solution
Manganese (ppm)	2	1	0.1	0.5
Iron (ppm)	5	2.5	0.25	1.25
Phosphorus (%)	0.01	0.005	0.005	0.0025
Copper (ppm)	0.5	0.25	0.025	0.125
Zinc (ppm)	2	1	0.1	0.5
Boron (ppm)	0.5	0.25	0.025	0.125
Aluminum (ppm)	10	5	0.5	2.5
Calcium (%)	0.05	0.025	0.0025	0.0125
Potassium (%)	0.1	0.05	0.005	0.025
Magnesium (%)	0.01	0.005	0.0005	0.0025
Sodium (%)	0.001	0.0005	0.00005	0.00025
Sulfur (%)	0.01	0.005	0.0005	0.0025

2.3.3 ^{31}P NMR (Phosphorus 31-Nuclear Magnetic Resonance Spectroscopy)

The hydroxyl contents of the lignin samples were measured using ^{31}P NMR, according to a slightly modified method from the previously published procedure by Asgari et al.[98] by adding DMF as a co-solvent to improve the solubility of lignin. About 40 mg (precisely measured using microbalance) of oven-dried lignin sample was dissolved in 325 μL of anhydrous pyridine/ deuterated chloroform mixture (1.6:1, v/v), 8 mL of pyridine and 5 mL of deuterated chloroform, and 300 μL of anhydrous DMF, in which DMF was utilized to fully dissolve the lignin samples. Sequentially, 22 mg of cyclohexanol (precisely measured using a microbalance) was dissolved in 1 mL anhydrous pyridine and deuterated chloroform (1.6:1, v/v). Then 100 μL of the cyclohexanol solution (22 mg/mL) was added as an internal standard, and 50 μL of chromium (III) acetylacetonate solution (5.6 mg/mL) in anhydrous pyridine and deuterated chloroform (1.6:1, v/v) was added as a relaxation reagent. In addition, 100 μL of the phosphitylation reagent (2-chloro-4,4,5,5-tetramethyl-1,3,2-dioxaphospholane, TMDP) was added to the mixture to react and label hydroxyl and carboxylic acid groups of lignin. Finally, 600 μL of the resulting mixture was transferred to a 5 mm NMR tube, and 31P NMR was conducted using an Agilent DDR2 500 MHz NMR spectrometer equipped with 7600AS, running VnmrJ 3.2A, with a relaxation delay of 5 s, and 128 scans were collected. To prevent decomposition of internal standard, samples were tested within 1 hour of preparation.

TMDP is the most common phosphitylation agent for measuring the hydroxyl content of lignin,[99] tannins,[100, 101] and biobased oils.[102-104] When hydroxyl groups in lignin react with TMDP, HCl is released that can decompose phosphitylated compounds. To avoid this, pyridine was used to neutralize HCl by forming pyridine-HCl salt. Deuterated chloroform was used for three purposes: 1) increasing the solubility of lignin, 2) avoiding the precipitation of the pyridine-HCl salt, and 3)

locking NMR signals.[91] Chromium(III) acetylacetonate was added as a relaxation agent to reduce the spin-lattice relaxation time of the phosphorous nuclei.[99, 105] Cyclohexanol was used as an internal standard because it has a sharp and distinguishable chemical shift to avoid overlapping with other chemical shifts of lignin.[99]

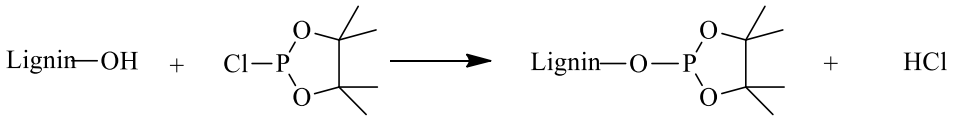

Scheme 4. Proposed reaction of lignin with 2-chloro-4,4,5,5-tetramethyl-1,3,2-dioxaphospholane (TMDP)

All spectra were analyzed by MestReNova software (version: 14.1.2-25024) in the following steps: each .fid file was opened and focused on the region between 150-132 ppm and "fit to highest intensity" in the View tab was selected. Next, a manual correction was chosen under "Phase Correction", and "Biggest" was selected. Then two sides of the internal standard were properly aligned. By selecting "Auto Baseline Correction" and selecting "Ablative Point 5-10," we eliminated variation caused by multiple users performing manual base-line correction, thereby improving the reproducibility of the analyzed data. To use the internal standard as a reference, "Reference" was selected, and 145.1 ppm was entered as the chemical shift. To ensure a sufficient phosphitylation agent was used to react with all hydroxyl groups in the lignin, the peak at 175 ppm must be checked to be present, which corresponds to unreacted phosphitylation agent, ensuring that there was excess phosphitylation reagent than needed for reaction with lignin.[106] The hydroxyl content of each lignin sample was calculated based on the ratio of the internal standard peak area (cyclohexanol) to integrated areas over the following spectral regions (using "Manual Integration" in the Analysis tab): aliphatic hydroxyls (149.1-145.4 ppm), cyclohexanol (145.3-144.9 ppm), condensed phenolic units (144.6-143.3; and 142.0-141.2 ppm), syringyl phenolic units (143.3-

142.0 ppm), guaiacyl phenolic hydroxyls (140.5-138.6 ppm), *p*-hydroxyphenyl phenolic units (138.5-137.3 ppm), and carboxylic acids (135.9-134.0 ppm). For softwood lignin, the entire region of (144.6-138.6 ppm) was considered as condensed phenolic since softwoods do not have any syringyl units. The following equation was used to calculate the internal standard peak area:

$$\text{Internal standard area } \left(\frac{mmol}{g}\right) = \left[\frac{\left(\frac{IS}{100.158}\right)/10}{m}\right] \times 1000$$

where IS the weight of internal standard (mg), the value 100.158 g/mol is the molecular weight of the internal standard, and m is the weight of the lignin sample used (mg).

2.3.4 FTIR (Fourier Transform Infrared Spectroscopy)

The spectrum of each oven-dried lignin sample was recorded on A Perkin Elmer Spectrum II in attenuated total reflectance (ATR) mode with a wavenumber range of 4000-400 cm^{-1} with a resolution of 4 cm^{-1} and 32 scans.

2.3.5 GPC (Gel Permeation Chromatography)

Gel permeation chromatography technique was used to determine the number average molecular weight, weight average molecular weight, and polydispersity index (PDI) of lignin samples. First, acetylation of lignin was conducted to improve the solubility of lignin in tetrahydrofuran (THF), which was used as the mobile phase.[107] To acetylate lignin, 1 g of lignin was dissolved in 40 mL solution comprising pyridine and acetic anhydride (50-50 v/v%) and mixed at room temperature for 24 hours (600 rpm). Then, 150 mL of hydrochloric acid (0.1 N) was used to precipitate acetylated lignin. The precipitates were then vacuum filtered, and the residual solids were washed with 0.05 N hydrochloric acid solution (3 times) and deionized water (3 times). Acetylated lignin samples were then dried in a vacuum oven (Across International) at a temperature of 40 °C for 24

hours. Next, the samples were dissolved in THF (HPLC grade) at a concentration of 5 mg/mL and filtered using a syringe filter (PTFE, 0.45 μm); the filtrate samples were used for GPC analysis. A Waters GPC system (Waters e2695 Separation Module) was then used to analyze the filtrate at a flow rate of 1mL/min, using three 300 mm × 7.8 mm Waters columns in series including 1- Styragel HR 4, 5 μm, THF (5k-600kÅ), 2- Styragel HR 3, 5 μm, THF (500-30k Å) and 3- Ultrastyragel THF, 5 μm, (100-10k Å). Polystyrene standards of specific molecular weights (162, 370, 580, 945, 1440, 1920, 3090, 4730, 6320, 9590, 10400, 16700, and 42400 Da) were used as external calibration standards (R2 = 0.99996). The filtrate solution (25 μL) was injected into the system and was detected using a 2414 RI Detector, which was constantly maintained at the same temperature as the columns (35 °C) during the analysis. Data were collected and analyzed using Empower GPC Software.

2.3.6 DSC (Differential Scanning Calorimetry)

Glass transition temperatures of different lignins were measured using a Q100 Differential Scanning Calorimeter (TA Instrument). Briefly, 8 mg of oven-dried sample was placed in an aluminum standard pan. One hole was made in the lid by needle with a diameter of 0.45 mm to avoid increasing pressure in the sealed pan caused by evaporation or chaining the volume of the sample upon heating.[89, 108] The sample was heated from room temperature to 120 °C at a heating rate of 20 °C/min, then was cooled down to room temperature and kept isothermally for 10 min prior to reheating again to 200 °C under a nitrogen flow of 70 mL/min. The recommended temperature of the first heating cycle of 120 °C was designed for kraft lignins based on the Canadian standard. If there is still noise in the second heating graph, which intends to get rid of the thermal history of polymer, then the sample can be rerun this time using a higher temperature of up to 160 °C, which would be below lignin degradation temperature. The TGA analysis can

help with choosing the best temperature for the first cycle. The second heating cycle was used to calculate the Tg of the lignin sample using TRIOS software.

2.3.7 TGA (Thermogravimetric Analysis)

Thermal property/stability of lignins were monitored through a thermal gravimetric analyzer (TA Instrument, Q50). Briefly, 8 mg of oven-dried lignin sample was placed in a platinum pan and heated from 25 to 105 °C with a constant heating rate of 10 ^{o}C/ min. The temperature was held isothermally at 105 °C for 20 min to evaporate possible hygroscopic water [109] and then continued to ramp up to 800 °C with the same heating rate under a nitrogen flow of 60 mL/min (for thermal stability) and an airflow of 60 mL/min (for oxidation) with a nitrogen flow of 40 mL/min for the balance.

2.4 Results and Discussion

2.4.1 Lignin Composition

2.4.1.1 Ash Content and Elemental Analysis

Ash content is usually defined as total inorganic compounds in lignin and categorized as acid-soluble, acid-insoluble ashes, and silicates,[110] known to interfere with lignin valorization.[86] Ash content of lignin has a broad range (0.5-8%) and strongly depends on the source and isolation process of lignin.[86, 111]

Table 3 presents the ash contents and elemental analysis results of fifteen commercial lignin samples. Generally, ash and mineral contents of lignin samples are ranked based on their isolation methods are in order of sulfite > kraft > soda > organosolv. Ash contents of all kraft lignins, regardless of their sources, are in a range of 0.5-4.3%. Sulfite lignin (16-SW-L) had extremely high ash content (11.4%) and high sulfur content (5.80%) due to sulfonate groups grafted to lignin

phenolic or non-phenolic units. [112] For kraft and soda lignins, the relatively high ash contents are related to the remaining residual of sodium hydroxide and sodium sulfite (only for kraft), which are used during the pulping process, and also sulfuric acid used to precipitate lignin from pulping liquor.[113] The variation in ash contents of different kraft lignins could be attributed to lignin isolation methods from black liquor (Lignoboost or Lignoforce) and the washing steps. Organosolv lignins, in contrast, have lower ash content compared to other isolation processes as expected, ranging from 0.1-3.3 %. In the organosolv process, a mixture of solvents (such as ethanol, acetic acid, and formic acid are used). [114] Although the organosolv process is typically sulfur-free, sometimes sulfuric acid is used as catalysts to improve the isolation process;[115] therefore, yielding organosolv lignins with a sulfur content ranging from 0.02-1.07%.

Organosolv lignins isolated from woody biomass (lignins 15, 13, 14, and 2) had the lowest ash content and inorganic impurities; in contrast, lignins from non-wood species, including wheat straw, corn stover, and peanut shell, had relatively higher ash contents (1.0-3.3%) than woody lignins. This is probably due to fertilizers use and nutrient uptake by plants from soil which is explicitly attributed to high nitrogen and phosphorus content.[111, 116, 117] Similarly, fertilizers and usage of potassium hydroxide during the soda cooking process explain relatively high potassium content in lignins 15 ± 1.13% and 14 ± 0.14%.[118]

Table 3. Ash contents and elemental results of lignin samples, Mean (s.d.), n=3

Sample ID*	Ash content (%)	S (%)	P (ppm)	K (ppm)	Mg (ppm)	Ca (ppm)	Na (ppm)	B (ppm)	Zn (ppm)	Mn (ppm)	Fe (ppm)	Cu (ppm)	Al (ppm)
1-SW-K	4.34 (0.2)	1.97 (0.05)	16 (4)	1160 (200)	142 (7)	430 (17)	6890 (870)	21 (1.2)	17 (0.7)	41 (2.4)	45 (1)	1 (0.4)	153 (11)
2-SW-K	1.88 (0.1)	3.00 (0.25)	10	1160 (730)	23	100	8530 (320)	23 (6.8)	130 (70)	23 (5.3)	125 (20)	208 (84)	165 (2)
3-SW-K	0.61 (0.05)	1.85 (0.10)	17 (4)	277 (10)	153 (9)	107 (9)	1450 (38)	28 (1.4)	11 (0.8)	39 (1.2)	60 (4)	3 (2.6)	56 (12)
4-SW-K	0.54 (0.02)	1.93 (0.35)	10	135 (15)	200 (10)	265 (25)	1100 (80)	9 (4.0)	4 (1.2)	24 (4.5)	30 (7)	3 (0.5)	62 (14)
5-SW-K	0.74 (0.13)	1.51 (0.21)	10	170 (20)	30 (5)	100	1700 (30)	27 (6.2)	8 (1.4)	12 (1.7)	30 (6)	1	39 (5)
6-SW-K	0.76 (0.02)	1.800 (0.03)	10	250	110	106	2030 (86)	19 (1.5)	4	42 (1)	20 (5)	2 (0.43)	22 (1)
7-SW-K	0.93 (0.07)	1.60 (0.09)	150 (20)	610 (15)	150 (10)	155	3800 (300)	17 (1.1)	4.3 (0.17)	29 (1.4)	73 (3)	3 (0.63)	87 (7)
8-HW-K	1.05 (0.01)	2.12 (0.06)	200 (5)	570 (10)	100 (7)	630 (3)	1800 (60)	25 (1.2)	4 (0.4)	28 (0.4)	171 (11)	3 (0.5)	137 (11)
9-HW-K	1.45 (0.07)	0.33 (0.01)	10	200 (20)	10	100	4300 (300)	1	1	1	32 (4)	5 (0.9)	17 (7)
10-SW-O	0.34 (0.01)	0.12 (0.07)	10	130 (10)	10	120 (20)	100	7 (4.2)	4 (0.5)	8 (0.5)	240 (15)	2 (0.5)	18 (8)
11-HW-O	0.13 (0.01)	0.02 (0.001)	100 (1)	100 (10)	10	160 (20)	100	3 (1.7)	4 (0.5)	7 (0.5)	25 (3)	1 (0.0)	4 (3)
12-HW-O	0.43 (0.04)	0.25 (0.003)	60	300 (10)	0	100	40 (3)	3 (1.7)	3 (0.5)	7 (0.5)	238 (10)	1 (0.5)	8 (1)
13-WS-O	1.40 (0.02)	0.18 (0.004)	210 (5)	300 (10)	10	1370 (10)	100	21 (0.9)	8 (0.5)	4 (1.2)	2380 (300)	65 (0.9)	130 (3)
14-PS-O	0.98 (0.11)	1.07 (0.01)	300 (20)	1430 (200)	10 (0.5)	120 (8)	90 (2)	11 (1.2)	42 (0.9)	21 (0.8)	1950 (180)	21 (1.2)	13 (8)
15-CS-O	3.31 (0.04)	0.97 (0.02)	700 (20)	11300 (100)	930 (30)	1950 (70)	20 (9)	7 (1.3)	48 (0.4)	22 (0.8)	540 (7)	95 (3.3)	32 (23)
16-SW-L	11.45 (0.03)	5.80 (0.13)	900 (5)	2250 (10)	1640 (50)	39340 (900)	1600 (300)	6 (0.5)	11 (0.5)	138 (7.7)	60 (1)	6 (3.6)	45 (16)
17-WS-S	1.76 (0.11)	0.72 (0.01)	20	550 (10)	1100	4830 (100)	1100	15 (1.4)	3 (0.5)	7 (0.5)	80 (4)	10 (0.8)	99 (5)

*K: kraft, O: organosolv, L: lignosulfonate, S: soda, SW: softwood, HW: hardwood, WS: wheat straw, PS: peanut shell, and CS: corn stover

2.4.2 Chemical Structure Analysis

2.4.2.1 ^{31}P NMR (Phosphorus 31-Nuclear Magnetic Resonance Spectroscopy)

^{31}P NMR spectroscopy is widely used to quantify different types of hydroxyl groups in lignin, including aliphatic OH, phenolic 5-substituted OH, syringyl OH, guaiacyl OH, and carboxylic acid after phosphitylation.[91] Cholesterol,[105] bisphenol,[119] benzoic acid,[120] and cyclohexanol[99] have been used as internal standards in ^{31}P NMR analysis of lignin. Some may overlap with the resonance of lignin moieties, thus causing underestimating the OH content of lignin. N-hydroxy-5-norbornene-2,3-dicarboximide (NHND) [121] was introduced as an internal standard to avoid potential overlapping; however, Meng et al. [91] reported that NHND forms a derivative that is not stable, and the prepared sample must be analyzed immediately, which is not always possible for most labs and would result in non-reproducible and overestimated results. Therefore, cyclohexanol was employed as an internal standard in our analyses that has much longer stability than NHND. The amounts of hydroxyl groups of different lignin samples calculated by ^{31}P NMR are presented in Figure 1. For each lignin, three replicates were run, the measurements demonstrated very good reproducibility as evident by the low standard deviation values.

The distribution of S/G/H moieties is correlated with the source of biomass. Softwood, hardwood, and herbaceous lignins were rich in guaiacyl, syringyl, and hydroxyphenyl units, respectively, as expected.[7, 122] Aliphatic hydroxyl groups in lignin and carbohydrate appear underneath a broadband (145.5-149.5 ppm), and unfortunately, ^{31}P NMR cannot distinguish them due to overlapping.[5] Therefore, compositional analysis of lignin samples that shows high aliphatic OH content should be cautiously considered to track the origin and source of hydroxyl groups (either lignin or carbohydrate). According to Figure 1, the carboxylic acid amount in herbaceous lignins (samples 18, 7, and 9) is higher than softwood and hardwood lignin, possibly due to the presence

of hydroxycinnamic acids such as *p*-coumaric acid and ferulic acid, which are linked to lignin via easter and ether bonds.[123, 124]

The isolation process has a significant impact on the hydroxyl content of lignin. It is clear that most of the lignin isolated by the kraft process had higher phenolic (average 3.57 mmol/g) and total hydroxyl contents (average 6.07 mmol/g) than lignins isolated from other processes (average 1.99 and 3.82 mmol/g phenolic and total hydroxyl contents, respectively). We surmise that in the kraft process, various types of reactions such as cleavage of lignin-carbohydrate linkages, recondensation, and depolymerization have occurred.[111] As illustrated in Scheme 5 quinone methides, the intermediates formed during the isolation process, acted as electrophiles to react with high nucleophilic hydrosulphide ions to form benzylthiol structures. Sequentially, the aryl ether attached to the β carbon was displaced, forming phenolic hydroxyl groups, which eventually increased lignin solubility in an alkali medium.[90, 125] Cleavage of phenolic ether linkages and recondensation as a result in kraft cooking can be seen by relatively high phenolic hydroxyl to aliphatic hydroxyl ratio. In addition, a high amount of 5-substituted OH (condensed) confirms recondensation via new-formed and C-C units.[126]

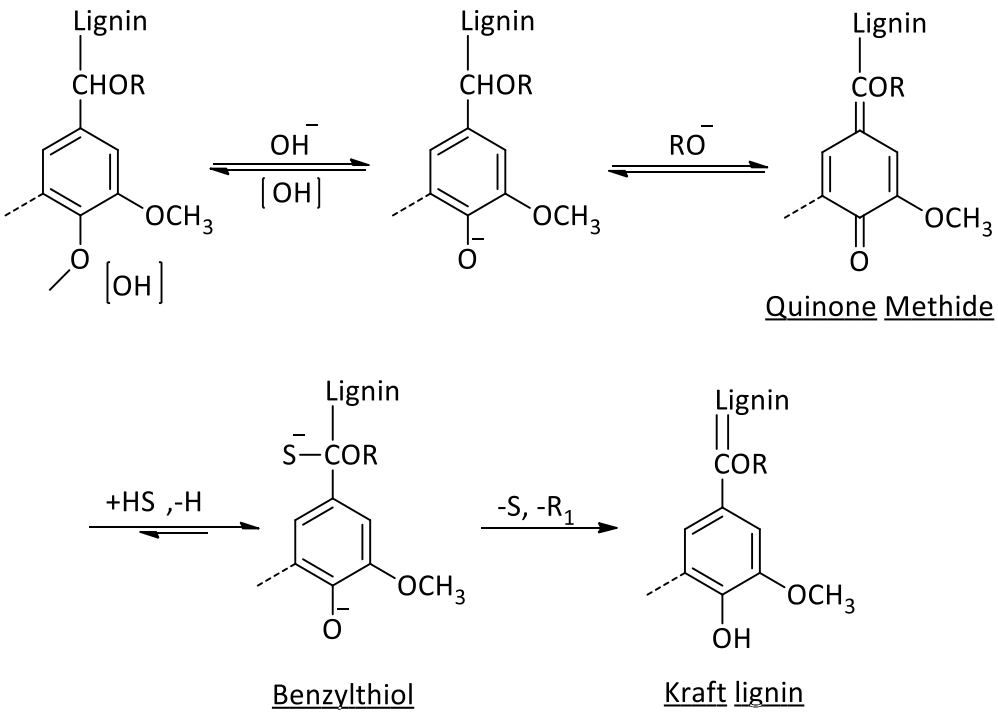

Scheme 5. Potential reactions occurred during the kraft process [111]

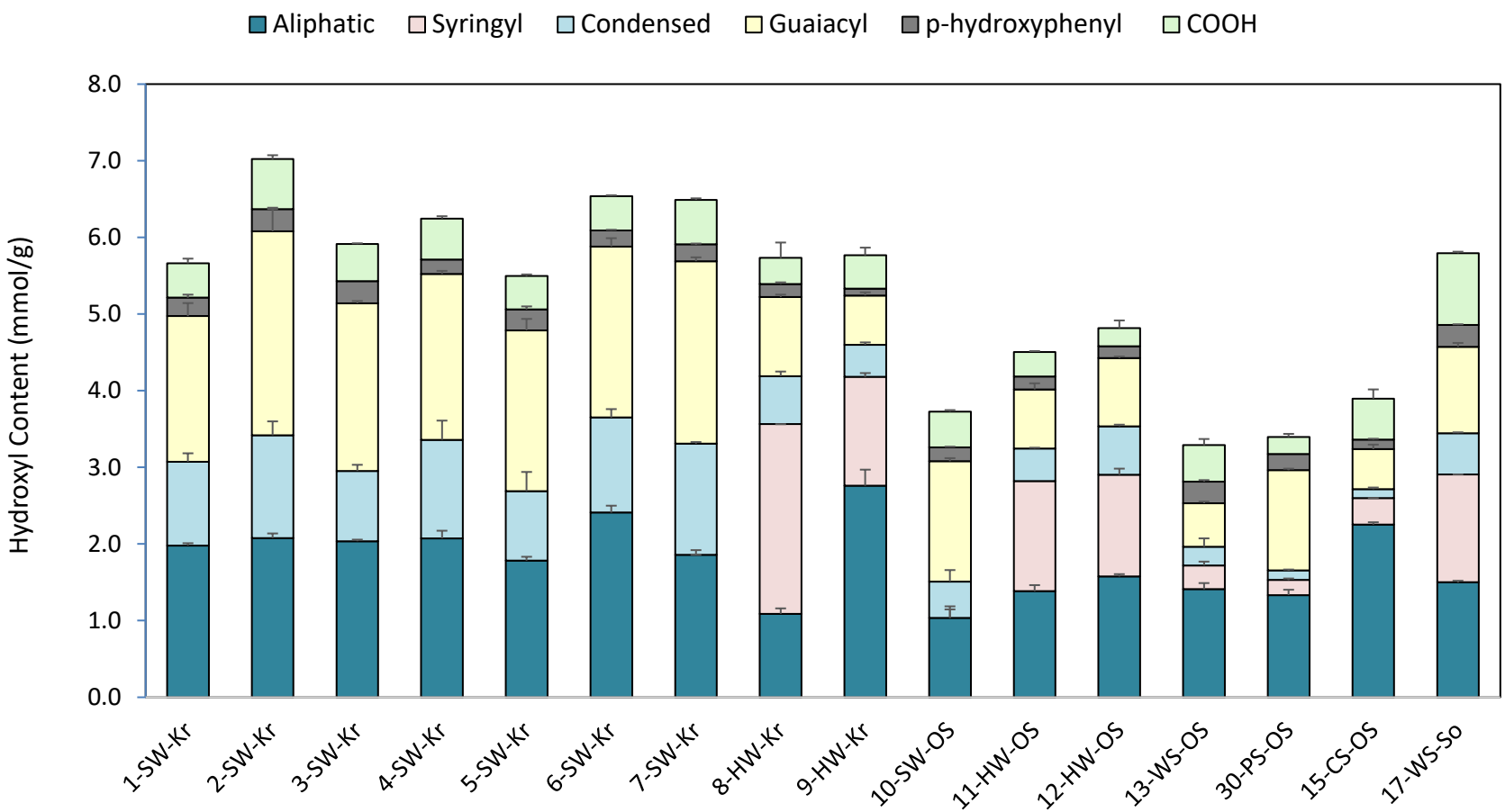

Figure 1. Hydroxyl contents (mmol/g) of lignins quantified by ^{31}P NMR

*K: kraft, O: organosolv, and S: soda, SW: softwood, HW: hardwood, WS: wheat straw, PS: peanut shell, and CS: corn stover

** Sample 16-SW-L was not soluble in NMR solution (CDCl3, pyridine, and DMF)

Isolated lignins with the organosolv process had lower hydroxyl content than kraft lignin due to less harsh conditions (lower temperature and pressure).[127] Soda cooking method is usually used with herbaceous plants, which isolates lignin based on the cleavage of α and β aryl ether bonds, resulting in relatively less modified lignin.[111, 117] In this process, depolymerization mainly takes place on non-phenolic β aryl moieties, giving more aliphatic hydroxyl groups.[125]

2.4.2.2 FTIR (Fourier Transform Infrared Spectroscopy)

FTIR spectroscopy can be used to classify different types of lignins based on their sources, namely hardwood, softwood, and herbaceous feedstocks, due to different distributions in aromatic units (G, S, and H). Table 4 presents the band assignments for O-H, C-H, C=O, aromatic skeletal, and C-O groups in lignins based on their lignin sources which are in accordance with previous studies.[128-131] Syringyl units showed two characteristic bands at 1326 and 1112 cm^{-1} related to C-O stretching of syringyl rings and in-plane deformation Syringyl C-H, respectively. In contrast, three peaks were detected for guaiacyl units at 1266, 851, and 812 cm^{-1}, which were correspondingly assigned to C-O stretching of guaiacyl ring, C-H out of plane deformation of guaiacyl. In addition, one characteristic peak at 983 cm^{-1} was found in herbaceous lignin.[128] Although most peaks in FTIR spectra for various lignin sources overlap, specific assignments could be applied to identify the feedstock source of lignin.

Table 4. Band assignments in mid-infrared region for softwood, hardwood, and herbaceous lignins

No	Band Origin	Wavenumber (cm^{-1})		
		Softwood	Hardwood	Grass
1	O-H stretching	3410	3458	3430
2	C-H stretching in methyl and methylene groups	3000	3000	3002
		2931	2937	2040
		2880	2880	2889
		2833	2833	2835
3	C=O stretching in unconjugated ketones, carbonyls, and esters	1708	1710	1705
4	C=O stretching in conjugated ketones, carbonyls, and esters	1663	1658	-
5	Aromatic skeletal vibration, C=O stretching	1595	1593	1600
6	Aromatic skeletal vibration	1510	1512	1513
7	C-H deformation (asymmetric) in methyl and methylene groups	1455	1458	1460
8	Aromatic skeletal vibrations combined with C-H in-plane deformation	1422	1426	1423
9	Aliphatic C-H stretching in CH3 and phenolic OH	1365	1365	-
10	C-O stretching of syringyl ring	-	1326	1318
11	C-O of syringyl ring	-	1315	-
12	C-O stretching of guaiacyl ring	1266	1267	1266
13	C-O stretching of syringyl ring and guaiacyl	1213	1213	1212
14	C-O stretching of syringyl ring and guaiacyl	1150	1151	1153
15	C-O of syringyl and guaiacyl ring, C-H bond in guaiacyl ring	1027	1030	1032
16	In-plane deformation syringyl C-H	-	1112	1113
17	C-H out of plane deformation of guaiacyl	851, 812	912	983
18	C-H out of plane deformation of syringyl	-	830	832
19	C-H out of plane deformation of guaiacyl	812	-	-

2.4.3 Molar Mass Distribution

Gel permeation chromatography (GPC), also known as size exclusion chromatography (SEC), is a common method to determine the molar mass distribution of lignin samples.[132, 133] Multiple benefits, including short processing time (0.25-2 hours per sample), ability to analyze sample even in milligram scale and wide range of molecular weight detection, make SEC an attractive technique for lignin characterization. Generally, the experimental setup is inclusive of a column, eluent, standards for calibration, and calibration method significantly affect the molar mass determination.[134-136] In this study, all lignin samples were acetylated prior to eluting in THF using three commercial columns (5k-600 kÅ, 500-30 kÅ, and 100-10 kÅ).[110, 137] It should be mentioned that it was difficult to solubilize and acetylate the sulfite lignin (16-SW-Su), making the THF column not suitable to measure its molecular weight.

Table 5. Molecular weight data of lignin samples

Sample ID*	M_n	M_w	M_z	PDI
1-SW-K	1990	6580	15590	3.3
2-SW-K	2080	6920	16910	3.3
3-SW-K	1770	6070	15400	3.4
4-SW-K	2030	8090	19670	4.0
5-SW-K	1740	5510	13410	3.2
6-SW-K	1750	9310	44990	5.3
7-SW-K	1640	7440	44860	4.5
8-HW-K	1270	2830	7360	2.2
9-HW-K	2590	10390	23018	4.0
10-SW-O	1440	4970	13420	3.5
11-HW-O	1290	3440	10700	2.7
12-HW-O	1490	4250	12830	2.9
13-WS-O	1960	15530	26790	7.9
14-PS-O	1640	9080	21400	5.5
15-CS-O	1750	6240	14160	3.6
16-SW-L	-	-	-	-
17-WS-S	1480	4330	14210	2.2

*K: kraft, O: organosolv, L: lignosulfonate, S: soda, SW: softwood, HW: hardwood, WS: wheat straw, PS: peanut shell, and CS: corn stover

2.4.4 Thermal Characterization

Glass transition temperature (T_g) of lignin, a critical physical property that can be measured by differential scanning calorimetry (DSC),[138, 139] generally vary widely between different lignins and

range from 64 -176°C. This is due to numerous factors, including the pretreatment strategy, isolation methods, and cross-linking extent during the cooking process. Utilizing DSC, in this study, we found that all the kraft lignin, regardless of their sources, exhibited glass transition temperatures ranging from 119 - 131°C with a concomitant second T_g ranging from 140 - 165°C, illustrating a higher dispersity of these lignins. This is consistent with the fact that harsh conditions, *i.e.*, high temperature or concentrated alkaline treatment, usually yield the resulting lignin in a more heterogeneous form. Organosolv lignins, in contrast, usually exhibit only one T_g (generally lower than that of kraft lignins), associated with the well-preserved inherent backbone of lignin. It is noticeable that peanut shell lignin (14-PS-OS) had the lowest T_g of 72°C, which was significantly lower than other lignins analyzed in this study. Also, organosolv lignin from hardwood (12-HW-OS) showed the low T_g - around 93°C, very likely caused by the high methoxy group content, which are known to increase the heat capacity of lignin, thus lowering its T_g.[140, 141] The low T_g of 14-PS-OS and 12-HW-OS lignin makes them good candidates for developing lignin-based polyurethane coatings, flexible foams, and elastomers.

Thermostability, one of the most important factors[10] that is highly impacted by different process methods and affecting lignin's application, was also examined in this work. We examined the lignin's thermo-degradation behavior under both anaerobic (N_2 atmosphere) and aerobic (O_2 atmosphere) conditions, attempting to reveal the performance of lignin in further application. Lignin pyrolysis often involves multiple stages, comprising various types of reactions over a broad temperature range. As shown in Table 6, kraft lignin's are more thermally stable than other types of lignin, reflected by the higher decomposition onset temperatures (referred to as $T_{5\%}$ and $T_{10\%}$, temperatures corresponding to 5% and 10% of weight loss, respectively) in the range of approximately 190 to 230°C, regardless under N_2 or O_2 atmosphere. Cross-linking or condensation

reactions and formation of 5-5 biphenyls during the kraft process likely contributed to the higher decomposition starting temperature.[142] Weight loss at this early stage is usually correlated with dehydration, loss of the side chains, and other fragments.[142] Noticeably, organosolv hardwood lignin's (11-HW-OS and 12-HW-OS) showed similar $T_{5\%}$ and $T_{10\%}$ as those of kraft lignins.

All types of lignin exhibit similar T_{max} (temperature corresponding to maximum weight loss) in the range of 350 - 370°C under N_2 and 400 - 500°C under O_2, respectively, attributed to the decomposition of the aromatic rings. In addition, all lignin samples used in this study had similar solid residue char at the end of thermal analysis, ranging approximately ~ 30 - 40% under N_2 atmosphere and an only trace amount of residual (< 5%) left under O_2 atmosphere.

Table 6. Thermal characterization of 17 commercial lignin

Sample ID	T_g (°C)		TGA (under N_2)				TGA (under O_2)			
	T_g-1	T_g-2	$T_{5\%}$ (°C)	$T_{10\%}$ (°C)	T_{max} (°C)	Residue (%)	$T_{5\%}$ (°C)	$T_{10\%}$ (°C)	T_{max} (°C)	Residue (%)
1-SW-K	127	148	189	275	352	38	211	257	425	1.2
2-SW-K	131	153	190	260	373	41	207	262	418	2.9
3-SW-K	131	145	222	270	364	42	221	269	459	5.7
4-SW-K	119)	162	223	267	350	40	223	268	487	5.4
5-SW-K	120	153	233	279	372	37	233	280	470	5.0
6-SW-K	125	145	227	268	381	36	235	271	456	5.2
7-SW-K	121	155	231	271	383	38	234	269	469	5.4
8-HW-K	120	140	228	271	364	30	242	288	477	0
9-HW-K	119	165	217	267	349	34	227	262	432	0.8
10-SW-O	64	130	184	229	376	39	185	229	449	0
11-HW-O	100	-	231	267	351	37	239	281	525	0
12-HW-O	93	-	213	247	372	35	210	247	471	0
13-WS-O	119	176	194	236	356	35	206	241	398	6.5
14-PS-O	72	-	174	203	367	35	169	199	508	0
15-CS-O	65	120	165	207	217	32	185	209	523	2.5
16-SW-L	138	175	191	255	363	35	208	258	518	0
17-WS-S	120	150	182	213	293	19	170	206	509	6.9

*K: kraft, O: organosolv, L: lignosulfonate, S: soda, SW: softwood, HW: hardwood, WS: wheat straw, PS: peanut shell, and CS: corn stover

CHAPTER 3 (Lignin-Based Epoxy Resins)[143]

3.1 Introduction

Hydroxyl groups of lignin (mainly phenolic hydroxyl groups) can undergo epoxidation via two possible mechanisms: SN2 and ring-opening (two steps epoxidation). In the SN2 reaction, an epoxidized product is obtained (also called direct epoxidation). In the ring-opening reaction, first a chlorinated intermediate is formed, then an intermolecular SN2 reaction with an aqueous solution of NaOH will create the epoxide ring.[38] The general reaction mechanisms are illustrated in Scheme 6.

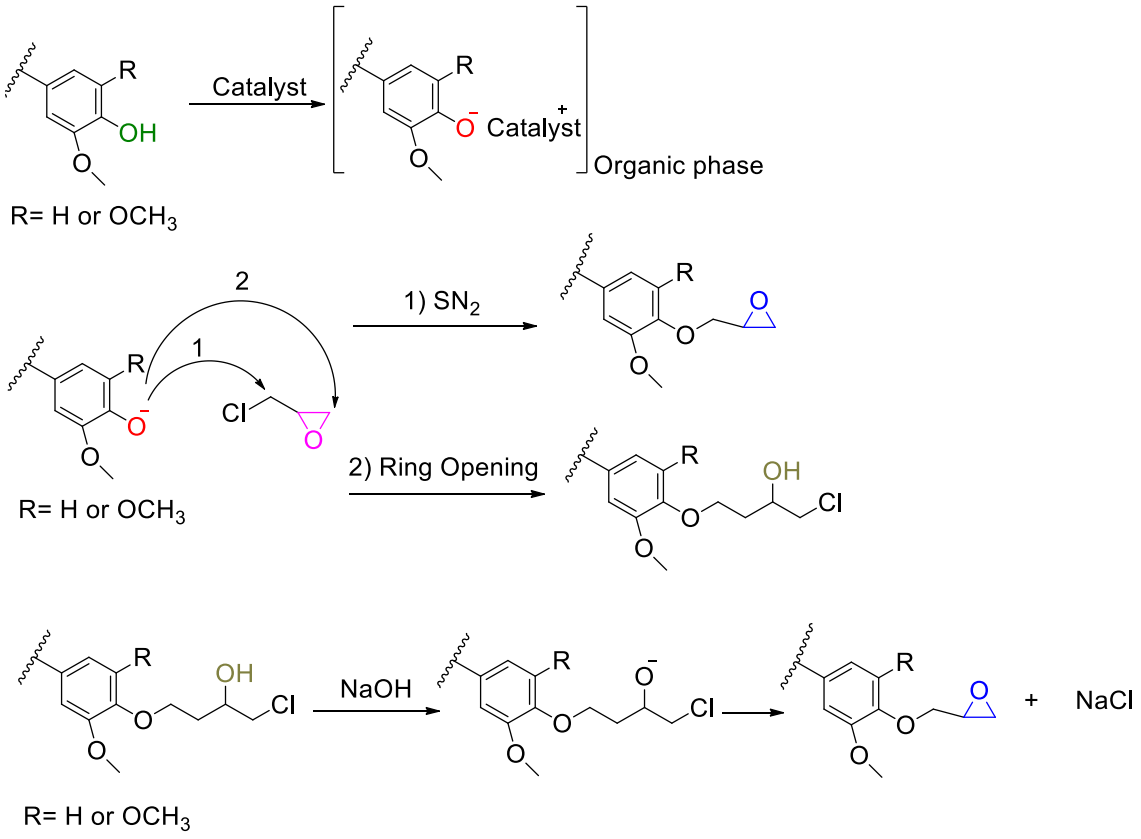

Scheme 6. Phenol epoxidation mechanisms in lignin

The epoxidation reaction of unmodified lignin depends on several factors, including the type of catalyst, amount of ECH, co-solvent, and type of lignin. Two types of catalysts are commonly used for lignin epoxidation, alkaline and phase transfer catalysts. An alkaline catalyst like NaOH and KOH deprotonates the hydroxyl groups of lignin and forms a phenolate ion (the conjugate base of phenol obtained by deprotonation of the OH group) to react with ECH.[58] While, phase transfer catalysts such as tetrabutylammonium bromide (TBAB) and triethyl benzyl ammonium chloride (TEBAC) allows phenolate ion to transfer in organic solution and react with ECH by facilitating the migration of phenolate ion to the organic phase.[75, 76] Usually, the alkaline catalyst is added in a significantly higher amount (0.5-2.5 eq of total hydroxyl groups of lignin). The equivalent amount is calculated based on the total hydroxyl content of lignin obtained from phosphorus-31 nuclear magnetic resonance (^{31}P NMR) analysis result according to the following equation: Total OH content (mmol/g) × number of equivalent × molar mass of catalyst) compared to quaternary ammonium salts as catalyst (0.05-0.26 eq of total hydroxyl groups in lignin) because the alkaline catalyst is consumed during the reaction (by neutralizing released hydrochloric acid) and formed NaCl salt.

Most lignin samples from different sources and isolation methods are soluble in ECH at elevated temperatures. However, co-solvent is necessary to keep the epoxidized lignin soluble since the solubility of epoxidized-lignin drastically decreases during epoxidation reaction.[143] Dimethyl sulfoxide (DMSO) was used as co-solvents for lignin epoxidation. It was shown that not only using co-solvents decrease the side reactions, it also increases the epoxy content of epoxidized lignin.[58] In addition, a higher amount of ECH is always used (10-20 eq of total hydroxyl groups) to increase the epoxy content of epoxidized lignin and reduce the side reactions.[38]

Table 7 summarizes the published papers which used unmodified lignins from different isolation processes (kraft, soda, organosolv, steam explosion) and various biomass sources (softwood, hardwood, herbaceous plants) for epoxy resin applications.[57-60, 144] Although several studies used lignins from different isolation processes and sources for epoxidation reaction, the factors affecting the suitability of lignin in epoxidation reaction have not been evaluated. On the other hand, only two studies fully replace BPA with unmodified, non-technical lignins (bamboo steam exploded and enzymatic hydrolysis corncob). Therefore, it is critical to developing a new method to epoxidize unmodified technical lignins and find the most important lignin properties affecting their suitability for epoxidation.

Table 7. Summary of the previously published paper focused on epoxidation of unmodified lignins

NO	Lignin Type*	Catalyst	Co-solvent	Epoxy equivalent weight (EEW)	BPA replacement (wt.%)	Ref
1	Bamboo steam exploded	TBAB	-	333	0-100	[57]
2	Kraft softwood		DMSO	309-1075	2-10	[58]
3	Enzymatic hydrolysis corncob	TBAB	-	294	0-100	[59]
4	Organosolv hardwood	TBAB/KOH	-	312	0-42	[60]
5	Alkali Sal leaves	NaOH	-	-	5-20	[61]
6	Alkaline lignin	NaOH	-	-	0-20	[62]

In this chapter, first, the reactivity of thirteen unmodified lignins toward epichlorohydrin was measured to identify the most important factors affecting lignin epoxidation. Next, two technical

hardwood and softwood lignins from kraft processes were epoxidized and their crosslinking behaviors and thermomechanical properties were investigated.

3.2 Measuring Reactivity of Different Lignins Toward ECH

3.2.1 Experimental (Reactivity Measurement)

3.2.1.1 Materials

Thirteen commercially available lignin samples from different plant sources and isolation processes were provided by Advanced Biochemical (Thailand) Co., Ltd. Other chemicals used in this study were: N, N Dimethylformamide (DMF; 99.8 %, extra dried, Acroseal, Acros Organics); tetrabutylammonium bromide (TBAB; Tokyo Chemical Industry Co., LTD, Purity >98 %); biobased ECH (Advanced Biochemical Thailand Co., Ltd, 99.9 %). GX-3090 and DGEBA (EPON 828) were obtained from Cardolite and E. V. Roberts, respectively. Additional reagents were purchased from Fisher Scientific, Alfa Aesar, Sigma-Aldrich, and Acros Organics and were used as received.

3.2.1.2 Methods

First, 4 g of each lignin sample was dissolved in 20 g dimethylformamide (DMF) and stirred for 10 min at room temperature (DMF was used as co-solvent since all lignin samples were completely soluble in DMF). Then 0.4 g tetrabutylammonium bromide (TBAB) and 40 g biobased ECH were added to the lignin/DMF solution and stirred for 3 h at 60 °C under reflux conditions (Scheme 1). The mixture was then cooled down to room temperature, and 50 mL of 2% w/w NaOH solution containing 1.2% w/w TBAB was gradually added to the mixture dropwise (one drop every 5 s). Then, the reaction was continued at room temperature for 8 h while stirring at 500 rpm using a magnetic stirrer. After that, 1000 mL deionized (DI) water was added to the solution to precipitate

epoxidized lignin. The epoxidized lignin was collected by vacuum filtration and washed several times with DI water to remove formed salt and unreacted ECH. Finally, a vacuum oven was used to dry the epoxidized lignin samples at 40 °C, 76 kPa for 48 h.[145]

3.2.1.3 Curing of Epoxy Resins

The two epoxidized lignin samples (4-O-CS and 11-K-HW) with the highest epoxy contents and a commercial DGEBA epoxy resin were cured with a biobased diamine (GX-3090) (Scheme 7). The epoxy equivalent weight (EEW) of epoxidized lignin was calculated by the following equation [146]:

$$\text{EEW}=\frac{4300}{\%\ Epoxy\ Content}$$

Each hydrogen of the amine group could react with one epoxy group based on active hydrogen equivalent weight (AHEW), then the stoichiometric ratio between the hardener epoxy resins can be calculated as AHEW/EEW. First, epoxidized lignin samples were dissolved in acetonitrile, then a specific amount of GX-3090 was added and mixed according to Table 8. To evaporate the solvent, epoxidized lignin systems were heated at 50 °C for 1 h. All samples were cured at 130 °C for 2 hrs and post-cured at 150 °C for 1 h (as recommended by the supplier of hardener).

Table 8. Formulation of different epoxy samples

Sample ID	EEW	Mass Ratio (epoxy resin/hardener)
4-O-CS/GX-3090	346.8	1/0.21
11-K-HW/GX-3090	354.2	1/0.20
DGEBA/GX-3090	185	1/0.37

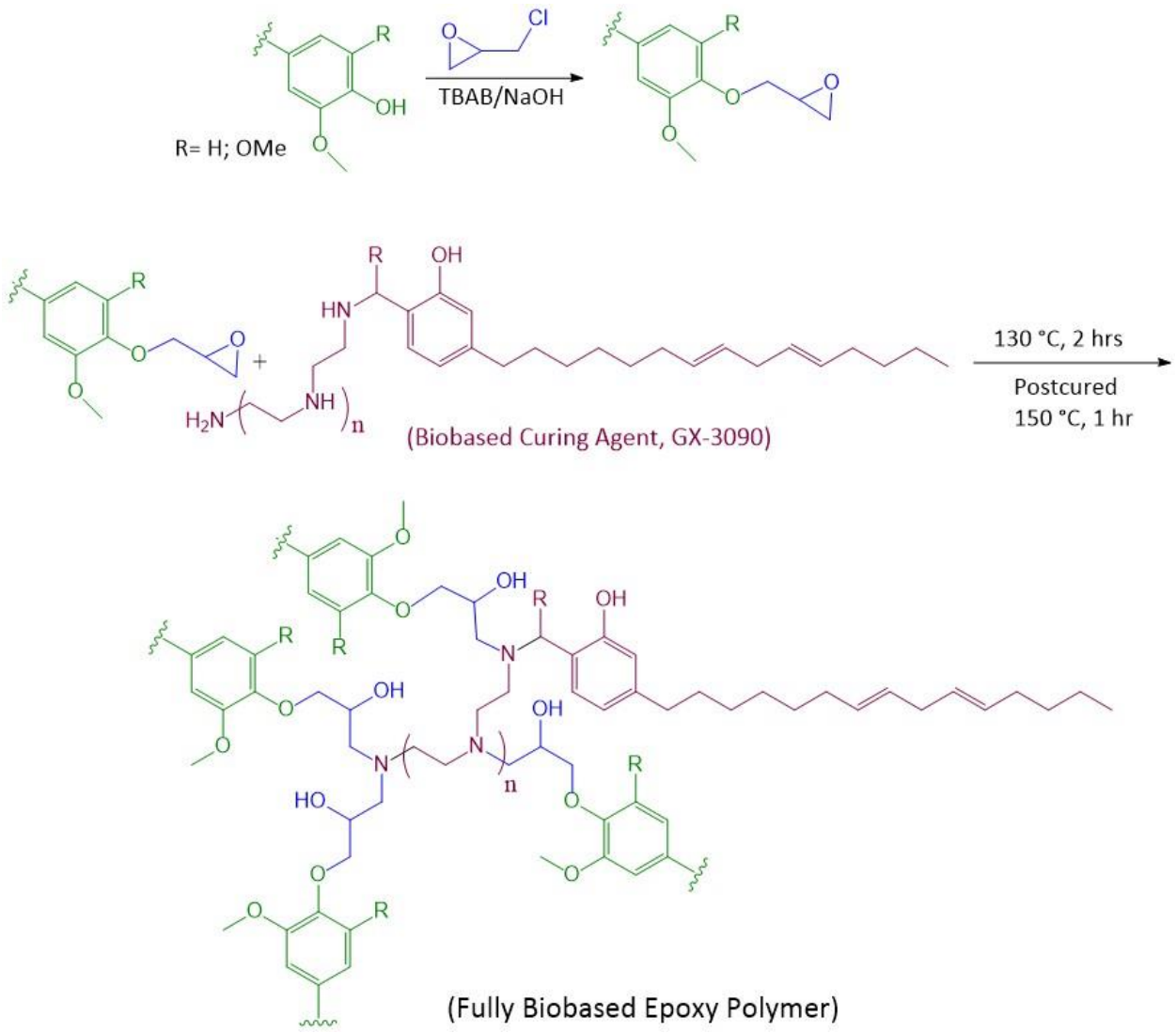

Scheme 7. Synthesis and curing reaction of epoxidized lignin

3.2.2 Characterization (Reactivity Measurement)

All lignin properties were measured according to characterization methods explained in Chapter 2.

3.2.2.1 Characterization of Epoxidized Lignins

3.2.2.1.1 Epoxy Content Measurement (Auto-Titration)

The epoxy content of epoxidized lignin was measured according to a modified version of ASTM D1652-11 using an auto-titrator (Metrohm, 916 Ti-touch Swiss Mode). Due to the dark color of lignin, it was impossible to use a color-changing indicator; instead, the electric potential was measured to determine the endpoint of the titration. Briefly, 0.2-0.3 g epoxidized lignin was dissolved in 30 mL dichloromethane and 15 mL of a prepared tetraethylammonium bromide reagent (100 g of tetraethylammonium bromide in 400 mL of glacial acetic acid). The resulting solution was stirred for 5 min to ensure the epoxidized lignin was entirely dissolved in the solution. The titration is based on the in-situ formation of hydrobromic acid by the reaction of perchloric acid with excess tetraethylammonium bromide. Initially, the produced hydrobromic acid (HBr) immediately reacts with epoxy rings; thus, there is no change in potential. After all epoxy rings are consumed, the formed HBr drops the pH and increases the potential of the solution, which is used as the endpoint. The auto-titrator was used to titrate the solution with 0.1 N perchloric acid reagent until the endpoint (Figure 2).

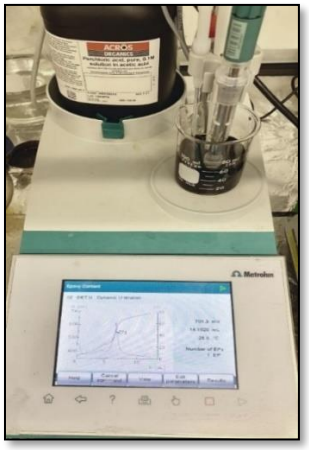

Figure 2. Auto-titrator used to measure epoxy content of epoxidized lignin

3.2.2.1.2 Epoxy Content Measurements (Proton Nuclear Magnetic Resonance-^{1}H NMR)

Epoxy contents of epoxidized lignin samples were measured by ^{1}H NMR according to a previously published report.[147] Around 50 mg of each epoxidized lignin sample was dissolved in 700 µl of deuterated dimethyl sulfoxide (d-DMSO). Then approximately 20 mg internal standard (1,1,2,2 tetrachloroethane) was added. NMR analysis was performed using an Agilent DDR2 500 MHz NMR spectrometer equipped with 7600AS, running VnmrJ 3.2A, with a 10 s relaxation delay, and 64 scans. The epoxy content of each epoxidized lignin was calculated based on the ratio of the following peaks δ [ppm, DMSO-d_6]: 2.77 (m, 1H); 2.92 (m, 2H); 3.41 (m, 1H), 4.32 (dd, 1H), and 4.64 (m, 1H); these peaks are assigned to the epoxy ring chemical shifts and peaks of internal standard (6.89 ppm, S, 1H). In addition, the average number of epoxy groups in each macromolecule was calculated according to the following equation:

$$\bar{n} = \text{epoxy group (mol/g)} \times M_n$$

3.2.2.2 Chemometric Modeling

UMetric Simca 16.0.2 software was used to model the correlation between lignin properties and their reactivity toward ECH. The partial least square regression (PLS-R) modeling method was used, as it can tolerate highly correlated variables (lignin properties).[20] To build the model, the properties of lignin such as ash content, elemental analysis, hydroxyl content, and molecular weight of lignin samples were considered as inputs (X-variables). The epoxy content (measured reactivity of lignins with ECH, using both titration and ^{1}H NMR techniques) were considered as responses or Y-variables.

3.2.2.3 Thermomechanical Properties of Cured Epoxy Systems (DMA Analysis)

The thermomechanical properties of two cured epoxidized lignin samples and a cured DGEBA-based sample were analyzed using a dynamic mechanical analyzer (DMA). A TA Instrument Q800 with a single cantilever under airflow, and a heating rate of 3.0 °C/min from room temperature to 250 °C, with a constant deformation frequency of 1 Hz was used to analyze the properties of cured epoxy systems. All samples were cured at 130 °C for 2 hours and post-cured at 150 °C for 1 hour in Teflon molds measuring 35 mm (length) by 12 mm (width) by 3 mm (depth). Samples were polished (by different sandpaper grits 1500, 2000, 2500, 3000, 5000, and 7000) to have smooth surfaces before analysis.

3.2.2.4 Thermal Stability of Cured Epoxy Systems (TGA Analysis)

Thermogravimetric analysis (TGA, TA Analysis, Q100) was carried out to compare the thermal stability of cured lignin-based epoxy samples with a DGEBA-based sample as a reference. Briefly, 5-10 mg of each sample was placed on a platinum pan and heated from 30 to 700 °C, with a constant heating rate of 20 °C, under an airflow of 25 mL/min for the sample and 10 mL/min for balance.

3.2.3 Results and Discussion (Reactivity Measurement)

3.2.3.1 Lignin Characterization

Table 9 shows the physicochemical properties of thirteen lignin used.

Table 9. Measured lignin properties (epoxy)

Sample ID*	Ash Content (%)	C (%)	H (%)	N (%)	S (%)	M_n (Da)	M_w (Da)	PDI	T_g (°C)
1-K-SW	0.52 (0.10)	62.9	5.9	0.1	1.7	1800	7000	3.9	144
2-K-HW	1.39 (0.14)	60.	5.8	0.2	0.3	2700	12400	4.6	164
3-S-HW	4.84 (0.11)	58.5	5.8	0.8	1.9	1900	6400	3.4	158
4-O-CS	0.50 (0.20)	63.7	5.7	0.5	0.1	1900	5380	2.8	174
5-O-Ba	3.37 (0.04)	61.1	5.5	0.7	0.1	2300	11500	5.0	130
6-O-PS	0.88 (0.02)	63.9	6.6	1.8	1.1	1750	9300	5.3	83
7-O-HW	0.47 (0.02)	62.9	6.0	0.2	0.2	1800	8200	4.6	79
8-K-SW	0.54 (0.02)	62.7	6.0	0.1	1.4	2000	8700	4.4	159
9-K-SW	0.65 (0.01)	62.9	6.0	0.1	1.3	1900	7200	3.8	150
10-K-HW	5.19 (0.01)	58.7	5.7	0.1	1.9	1600	4000	2.5	167
11-K-HW	1.62 (0.01)	60.9	5.8	0.1	2.3	1400	3200	2.3	146
12-O-WS	1.73 (0.06)	58.1	5.8	2.1	0.2	3100	15300	4.9	123
13-K-SW	0.75 (0.02)	63.7	6.0	0.1	1.8	2000	9300	4.7	143

*K: kraft, S: soda, O: organosolv, SW: softwood, HW: hardwood, CS: corn stover, Ba: bagasse, PS: peanut shell, and WS: wheat straw, PDI= Polydispersity index

Figure 3. Hydroxyl contents (mmol g^{-1}) of different lignin samples obtained by ^{31}P NMR

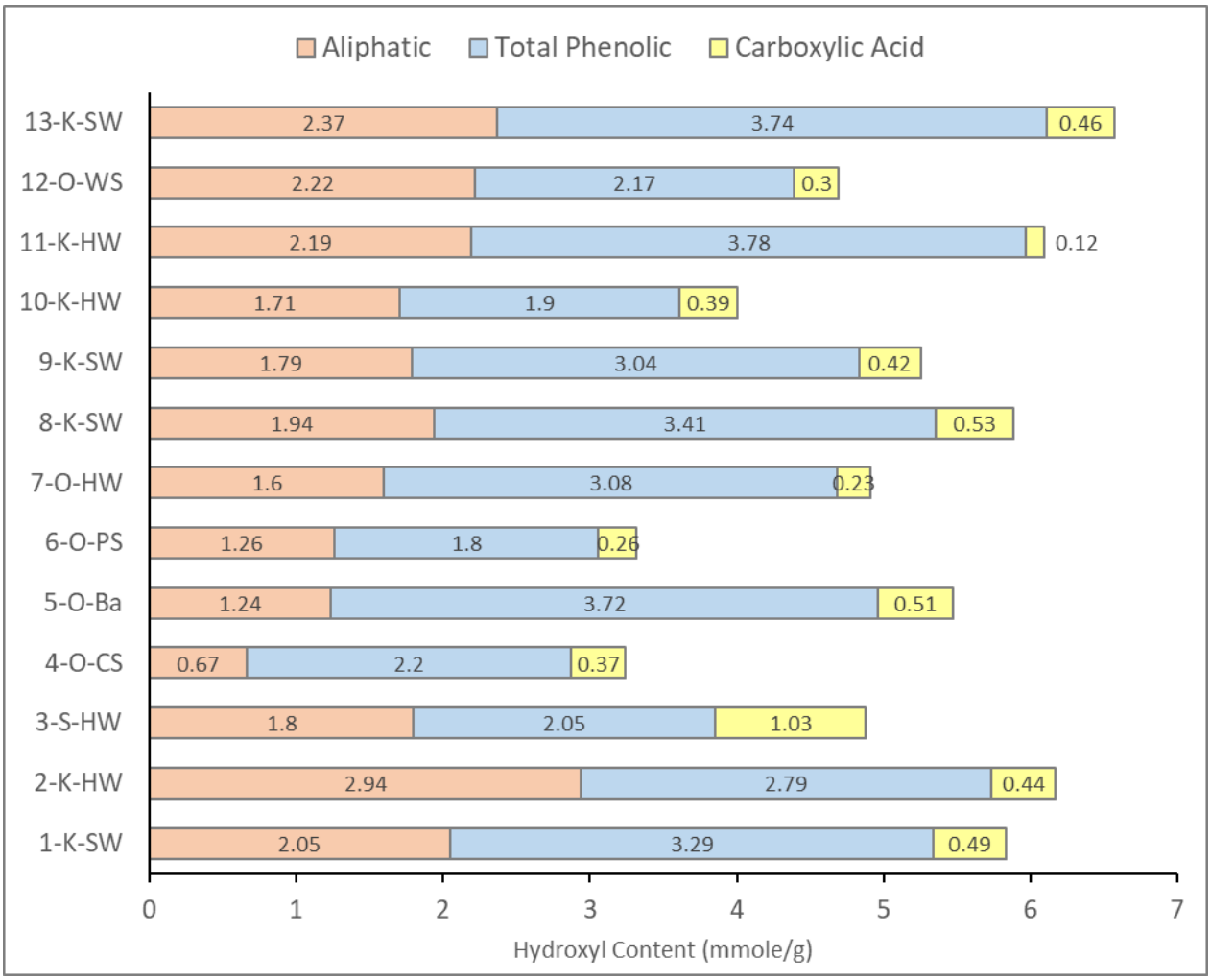

3.2.3.2 Lignin Epoxidation

The epoxy contents of different epoxidized lignin were measured by titration and ^{1}H NMR methods. Figure 4 shows the ^{1}H NMR spectrum of epoxidized lignin (1-K-SW). The results of these tests on all lignin samples, based on epoxy content and epoxy equivalent weight (EEW), are reported in Table 10. Epoxy contents measured by titration are based on three replicates, while epoxy contents based on ^{1}H NMR are based on one replicate. As shown, there were no significant differences (p-value: 0.671) between the results of the two methods, which confirms both are

reliable methods for measuring the epoxy content of epoxidized lignin samples. Samples 4-O-CS and 10-K-SW had the highest yield (89.9% and 66.9%, respectively). In addition, the average number of epoxy groups ($\bar{n}$) in each macromolecule [epoxy group (mol/g) × Mn] are presented in Table 10.

The results showed that the reactivities of hydroxyl (OH) functional groups in lignin toward ECH, in decreasing order, are phenolic-OH > carboxylic acid > aliphatic-OH.[148] It has been reported that the phenol epoxidation mechanism has three steps.[149] During the epoxidation reaction, a phase transfer catalyst (TBAB) transfers the phenolate ion into the organic solution. In the second step, deprotonated lignin (phenolate ion) reacts with ECH via two mechanisms: 1) SN2, and 2) ring-opening reactions. In the third step, the chlorinated intermediate is closed in the presence of NaOH to form the epoxy ring. It was found that the hydroxyl groups of lignin could only partially react with ECH. The reaction was also incompletely quenched due to side reactions between lignin's OH groups, ECH, and epoxidized lignin.[149] This may lead to the formation of ether bonds between epoxidized lignin functional groups and ECH. In addition, unreacted hydroxyl groups could potentially react with epoxy groups and form crosslinked products.[150] The formation of crosslinked epoxidized lignin reduces its solubility in organic solvents, negatively affecting the curing reaction of epoxidized lignin with a hardener.

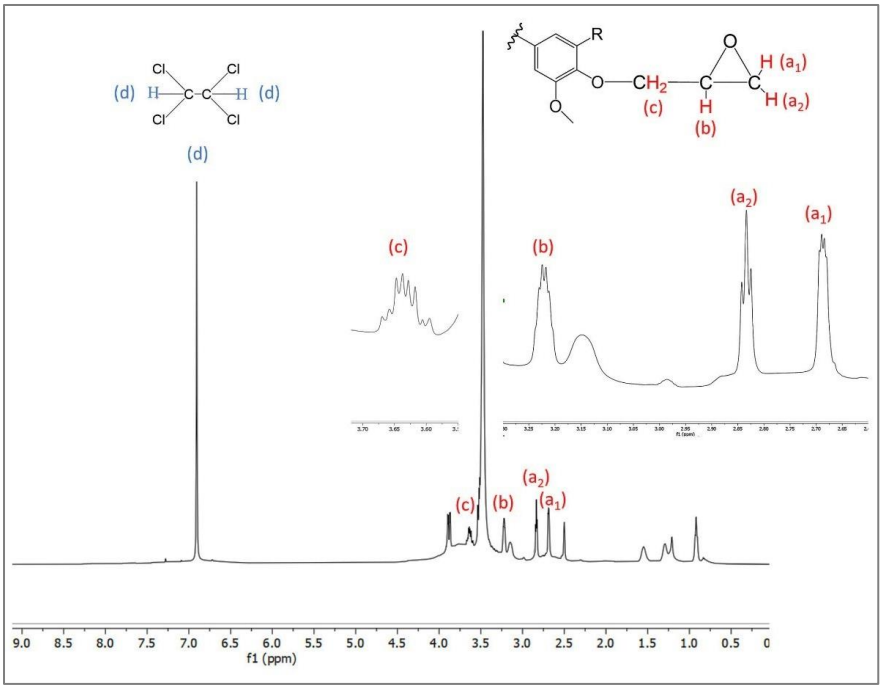

Figure 4. ^{1}H NMR spectrum of epoxidized lignin (1-K-SW)

Table 10. Properties of epoxidized lignins, including epoxy content and the epoxy equivalent weight measured by titration and ^{1}H NMR methods, yield (%) based on total hydroxyl content, and average number of epoxy groups in each lignin macromolecule

Sample ID*	% Epoxy Content (Titration)	EEW (Titration)	% Epoxy Content (^{1}H NMR)	EEW (^{1}H NMR)	Yield %	$\bar{n}$
1-K-SW	9.56 ± 0.26	450	9.72	442	39	4.0
2-K-HW	6.79 ± 0.12	633	7.00	614	26	4.4
3-S-HW	8.59 ± 0.35	501	8.21	524	39	3.5
4-O-CS	12.40 ± 0.31	347	12.53	343	90	5.6
5-O-Ba	5.93 ± 0.13	725	5.87	732	25	3.1
6-O-PS	5.18 ± 0.12	830	4.93	872	35	2.0
7-O-HW	8.75 ± 0.19	491	8.93	481	42	3.7
8-K-SW	7.97 ± 0.15	539	7.88	546	31	3.8
9-K-SW	10.01 ± 0.24	430	9.81	438	44	4.2
10-K-HW	11.27 ± 0.28	381	11.50	374	67	4.1
11-K-HW	12.14 ± 0.15	354	11.98	359	46	3.7
12-O-WS	4.35 ± 0.08	988	3.81	1129	19	2.5
13-K-SW	8.63 ± 0.18	498	8.98	479	32	4.1

*K: kraft, S: soda, O: organosolv, SW: softwood, HW: hardwood, CS: corn stover, Ba: bagasse, PS: peanut shell, and WS: Wheat straw

Samples 2-K-HW, 4-O-CS, 9-K-SW, 10-K-HW, and 13-K-SW had higher $\bar{n}$ compared to other lignin samples. The higher $\bar{n}$ indicates that the crosslinking density of the cured sample is higher. The weight of epoxidized lignin after the reaction was precisely measured for 11-K-HW to be 4.8 g. Although lignins 4-O-CS, 10-K-HW, and 11-K-HW all have high epoxy contents, based on the

overall data, the organosolv corn stover lignin (4-O-CS) seems to be a better lignin for epoxy resin applications due to its low ash content, low molecular weight, and low polydispersity index. In addition, this lignin has low carboxylic acid content, which will reduce potential hydrolysis and increase the service life of epoxy systems after crosslinking with a hardener.[151]

3.2.3.3 Modeling

Partial least-square regression modeling was used to find correlations between different lignin properties and their epoxy contents after epoxidation (reaction with ECH). The PLS model was developed with two PLS components, which had 92% fitting accuracy (R2Y=the explained variation) and 90% prediction ability (Q2Y=the predicted variation) based on a cross-validation method. Two PLS components were shown to be optimal for the model. Figure 5 plots the components' contributions; light blue-colored bars represent R2 as an indicator of how well the model fits the measured data for each performance criterion, and the dark blue-colored bars show Q2 as an indicator of how well the model can predict the epoxy content of a new lignin sample based on its measured properties.

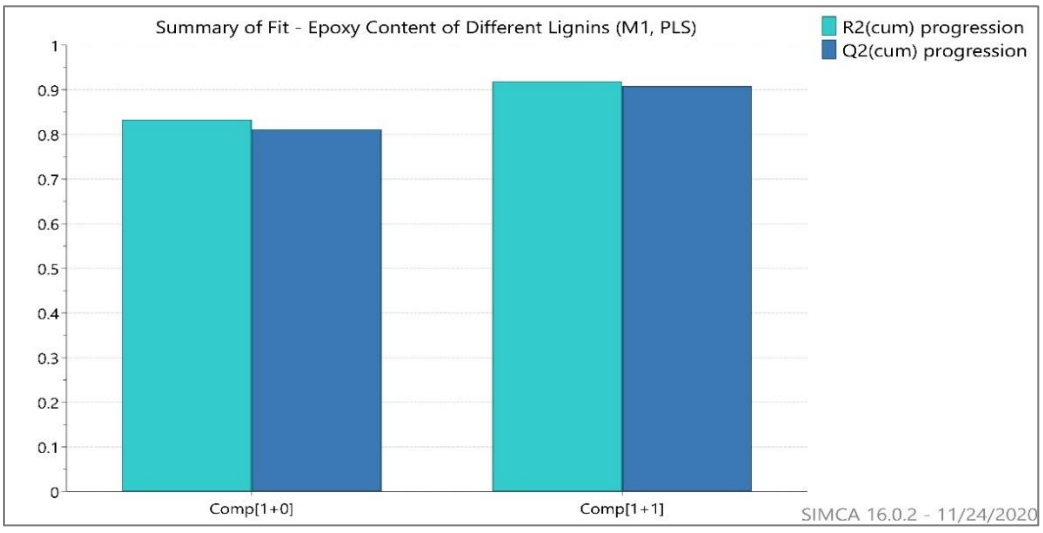

Figure 5. Component contribution plot for the response variable (epoxy content) measured both by titration and ^{1}H NMR methods.

According to the loading plot (Figure 6), M_n, M_w, PDI, and nitrogen content have strong negative (opposite side) correlations with epoxy content. In contrast, phenolic hydroxyl content has strong positive correlation (same side) with the epoxy content of lignin. In other words, lignins with lower molecular weights, molecular numbers, PDI, nitrogen, and higher phenolic hydroxy contents are more suitable for replacing BPA in epoxy resin formulation. We believe the reason that higher nitrogen content seems to have a very high negative effect on epoxy content is because there is a strong negative correlation (r=-73%) between the nitrogen content of the lignin samples used in this study with their total phenolic hydroxyl groups. Rather than higher nitrogen content being a fact that contribute to the reaction of lignin and ECH. It simply indicates that among the lignins used in this study, most of them that had nitrogen content (mainly from annual crops) had relatively lower phenolic hydroxyl content, which resulted in lower epoxy content.

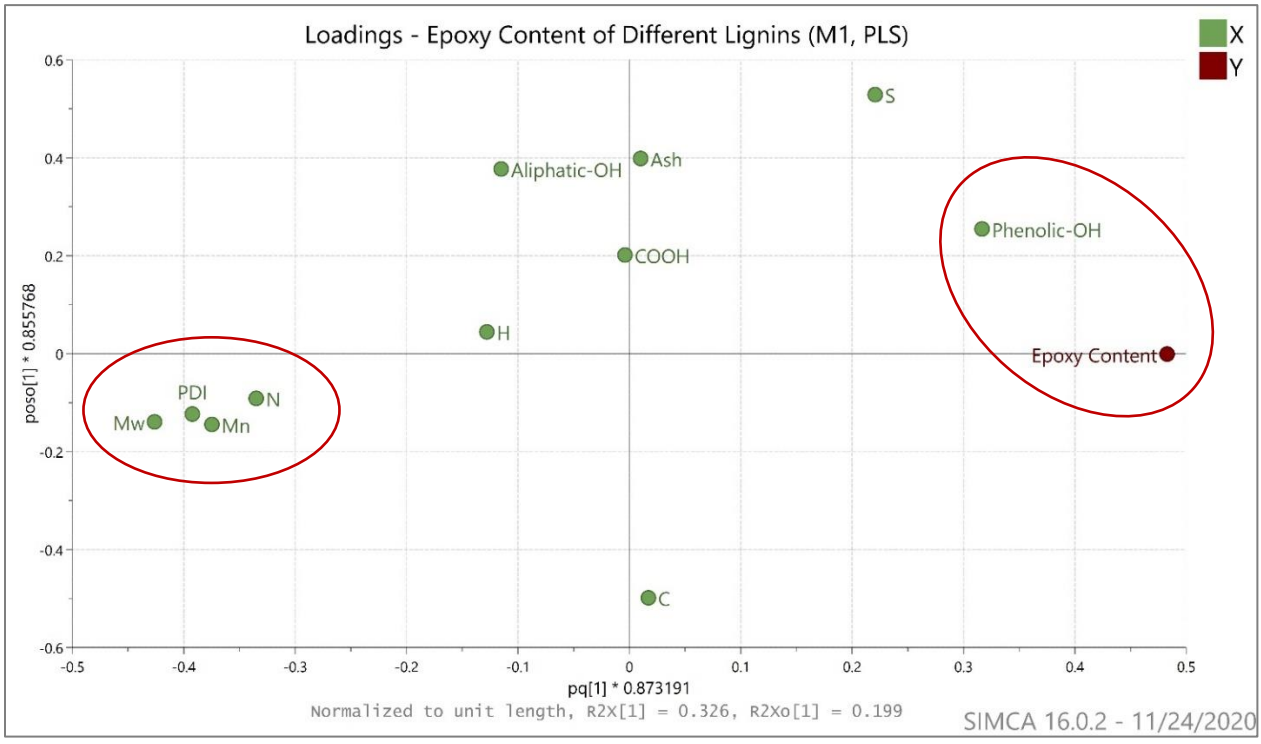

Figure 6. Loadings plot of PLS-R modeling of epoxy content based on lignin properties

3.2.3.4 DMA Analysis of Cured Samples (Thermodynamic Performance)

Thermodynamic performances of lignin-based epoxy and DGEBA-based thermosets cured by GX-3090 (biobased hardener) were studied by DMA using a single cantilever mode. Figure 7 shows storage modulus, tan δ, and loss modulus as a function of temperature; these parameters are summarized in Table 11. The storage modulus (E′) and loss modulus (E″) represent the elastic and viscoelastic response of a material, respectively. The ratio of loss modulus to storage modulus is tan δ. The peak temperatures of tan δ and loss modulus are usually reported as glass transition temperature, where a network transits from a glassy state to a rubbery state.

The storage moduli (E′) of all cured samples ranged between 1.3 to 1.6 GPa at 25 °C. The storage moduli of lignin-based epoxy networks (1.3-1.4 GPa) were lower than the DGEBA system (1.6 GPa), which could be related to the lower epoxy content of the epoxidized lignins compared to DGEBA resin. This shows that the lignin-based epoxy system had a lower crosslinking density than the petroleum-based epoxy system (DGEBA) prepared using bisphenol A. The organosolv corn stover lignin (4-O-CS) had a much higher storage modulus than kraft hardwood (11-K-HW). This could be due to the higher average number of epoxy groups ($\bar{n}$) and lower molecular weight of 4-O-CS compared to 11-K-HW. At the higher temperature (100 °C), the storage moduli of 4-O-CS and 11-K-HW samples were higher than that of DGEBA, possibly due to the higher glass transition temperature of cured lignin-based epoxy systems. The loss moduli (E″) of 4-O-CS and 11-K-HW thermosets were also higher than that of the DGEBA sample at higher temperatures (120-200 °C), which shows they can better dissipate deformation energy at higher temperatures.[152]

The tan δ peak gives valuable information regarding cured epoxy networks; generally, higher tan δ peaks correspond to better fracture toughness and higher T_g.[94] The width of tan δ represents sample homogeneity, with broader peaks indicating less homogeneous samples.[94] Both lignin-based epoxy thermosets showed significantly broader tan δ peaks, meaning that they are less homogeneous than the DGEBA system, as expected due to the high polydispersity index of lignin compared to BPA. Side reactions at different temperatures [152] as well as multiple functionalities [94] in the system could also result in observing broader tan δ peaks. Also, the glass transition temperatures (T_g) (recorded from tan δ profile) of epoxidized lignin samples (181 °C and 173 °C) were significantly higher than the T_g of the DGEBA system (106 °C), which indicates that lignin-based epoxy systems have higher toughness.[56]

Table 11. DMA performance of epoxidized lignins (4-O-CS and 11-K-HW) and DGEBA cured by biobased hardener (GX-3090)

Sample ID	E´ (GPa, 25 °C)	E´ (GPa, 100 °C)	Tan δ
4-O-CS/GX-3090	1396	701	181
11-K-HW/GX-3090	1275	613	173
DGEBA/GX-3090	1557	331	106

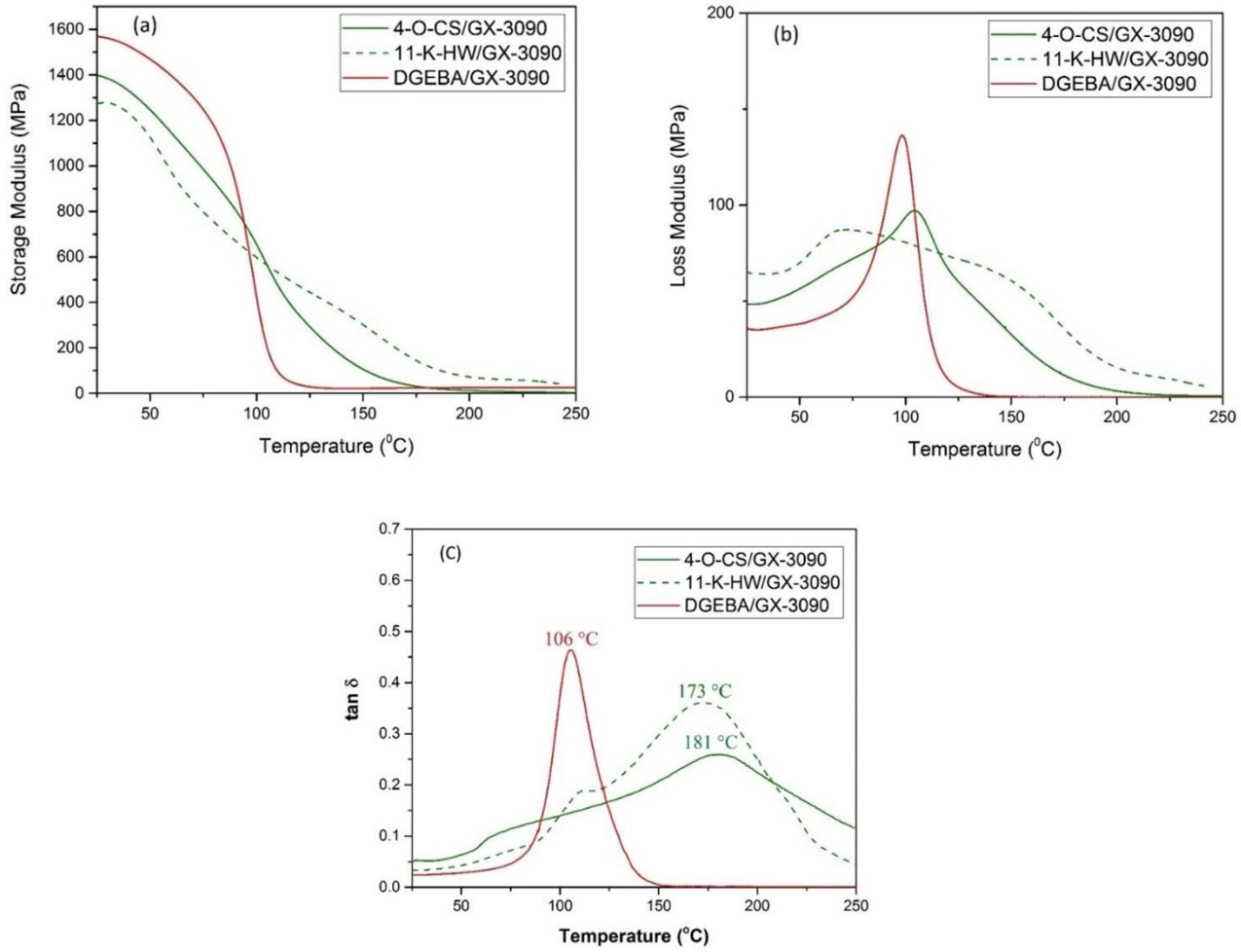

Figure 7. Storage modulus (a), loss modulus (b), and tan δ (c) of cured epoxidized lignin samples (4-O-CS and 11-K-HW) and DGEBA with GX-3090.

3.2.3.5 TGA Analysis of Cured Samples (Thermal Stability)

Thermal stabilities of cured lignin-based and DGEBA thermosets were evaluated (Figure 8) using thermal gravimetric analysis (TGA). The temperatures at 5% ($T_{d5\%}$), 30% ($T_{d30\%}$), weight loss, maximum weight loss (T_{max}), and the statistic heat-resistance index temperature (T_s) for different samples were summarized in Table 12. T_s was calculated from $T_{d5\%}$ and $T_{d30\%}$ according to equation 1, which represents the thermal stability of the crosslinked polymers.[68, 153]

$$T_s = 0.49 [T_{d5\%} + 0.6 (T_{d30\%} - T_{d5\%})]$$

All epoxy thermosets showed two-step degradation profiles, including a considerable weight-loss stage around 400 °C and another weight-loss stage at above 500 °C. The first stage of degradation is primarily due to the breaking of aliphatic chains and releasing small molecules like CO, CO_2, and water.[154] The second stage of degradation is most likely associated with the degradation of aromatic rings and oxidation of C-C linkages and different functional groups such as methoxy, phenol, and carbonyl.[155] Although the degradation of lignin-based thermosets was started at lower temperatures (241-245 °C) compared to the DGEBA thermoset (350 °C), the difference was smaller at higher temperatures. According to TGA analysis results (Table 12), the $T_{d30\%}$ of lignin-based thermosets were 40-50 °C lower than the DEGBA thermoset. Also, the degradation temperatures of both lignin-based thermosets are remarkably higher than their T_g, indicating that they can be used for applications that do not require high-temperature stability.[156] The statistical heat resistant-indices (T_s) of cured lignin-based samples were about 33-36 °C lower than T_s of cured DGEBA, showing their lower heat tolerance.[155] The epoxy system made with organosolv lignin (4-O-CS) had higher thermal stability than the epoxy made with kraft hardwood (11-K-HW). This can be explained by higher $\bar{n}$ of 4-O-CS thermoset, which resulted in an epoxy system with higher crosslinking density. The lower thermal stability of lignin-based thermosets is probably due to the lower crosslinking density of epoxidized lignin and lignin's lower thermal stability.[157]

Table 12. Thermal stability of cured epoxidized lignin and DGEBA networks

Sample ID	$T_{d5\%}$ (°C)	$T_{d30\%}$ (°C)	T_s (°C)
4-O-CS/GX-3090	241	345	149
11-K-HW/GX-3090	245	334	146
DGEBA/GX-3090	350	385	182

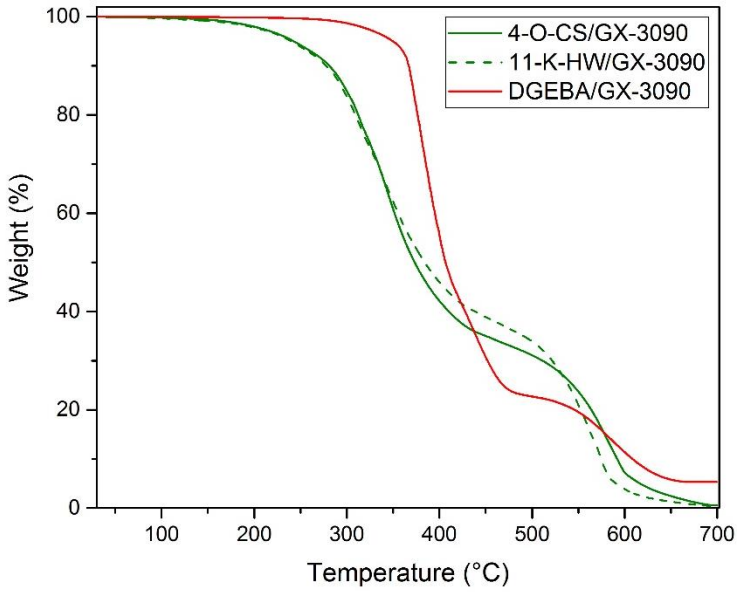

Figure 8. TGA profiles of different cured lignin-based and DGEBA epoxy thermosets

3.3 Crosslinking Behavior of Epoxy Resins

3.3.1 Materials and Methodology (Crosslinking Behavior)

Two commercially available lignins (hardwood kraft (HW-K) and softwood kraft (SW-K) were provided by Suzano, and West Fraser. Ethyl lactate was purchased from Scientific Fisher Co.

3.3.1.1 Modified Epoxidation Method of Lignin

Some parameters of the previous procedure of lignin epoxidation were changed, resulting shorter reaction time (3 hrs total), and replacing DMF with a biobased solvent (ethyl lactate). First, 4 g of

lignin was dissolved in 20 g ethyl lactate and mixed for 10 min at room temperature. Then, biobased ECH (20 eq) and TBAB (0.1 eq), based on the total hydroxyl content of lignin, were added to the mixture and stirred for 2 h at 80 °C under reflux conditions. Next, the mixture was cooled down to 10-15 °C, and 20 wt.% NaOH solution (2 eq of total hydroxyl OH) containing 20 wt.% TBAB was slowly added to the mixture. The mixture was stirred for 1 h. After that, the lignin was precipitated by adding 1000 mL deionized (DI) water. Epoxidized lignin was separated using vacuum filtration and washed multiple times to remove salt, unreacted ECH, and ethyl lactate. Lastly, the epoxidized lignin was freeze-dried (Labconco, FreeZone 4.5) at -52 °C for 6 h.

3.3.1.2 Curing of Epoxy Resins

Table 13 shows the compositions of different epoxy systems. Epoxidized lignin was dissolved in ethyl lactate (40 wt.%). The stoichiometrically determined amount of curing agent was then added to the mixture, followed by mixing for 2-3 min. To slowly evaporate ethyl lactate, prepared samples were kept at a regular oven at 40 °C for 8 h, then heated at 80 °C for 1 h, cured at 130 °C for 2 h, followed post-cured at 150 °C for 1 h. The same method was used for Epon (EP) systems (with and without solvent).

Table 13. Composition of different epoxy systems

Sample ID	EEW	Mass ratio (epoxy resin/curing agent)	Ethyl lactate (wt.%)
HW-K/GX-3090	320.9	1: 0.22	40
SW-K/GX-3090	364.4	1: 0.19	40
EP-EL/GX3090	185	1: 0.37	40
EP/GX3090	185	1: 0.37	0

The physiochemical properties of two lignins were measured according to explained methods in Chapter 1. Also, the epoxy contents of epoxidized lignins were measured according to methods discussed in sections 3.2.2.2.1 and 3.2.2.2.2.

3.3.2 Characterization of Epoxidized Lignin (Crosslinking Behavior)

The epoxy contents of epoxidized lignins were measured according to methods discussed in sections 3.2.2.2.1 and 3.2.2.2.2.

3.3.2.1 Rheology (Crosslinking Behavior)

Viscosity measurements and curing studies were carried out on a TA Instrument DHR-1. The viscosity of uncured epoxy systems was measured in scanning mode (0.02-1000 1/s). Isothermal curing studies were measured using a parallel plate geometry (25 mm diameter, 1 mm gap) at 40, 45, 50, 55, 60, 65, and 70 °C. Before running the sample, the linear viscoelastic region of cured epoxy systems was determined by running a strain sweep experiment.

3.3.2.2 Gel Fraction and Swelling Ratio

The gel fraction and swelling ratio of cured thermosets were measured according to a previously published method by Tellers et al.[158] All samples were vacuum dried, and 200 mg of each sample was placed in a 20 mL vial, and 5 mL THF was added. Vials were kept at room temperature for 7 days while the lids were closed. After that, samples were removed from the vials and immediately dried with a paper towel before weighing the swollen samples. Then, samples were placed in a vacuum oven until their weight stabilized. The gel fraction and swelling ratio were obtained according to the following equations:

$$\text{Gel fraction} = \left(\frac{m_d}{m_i}\right) \times 100$$

$$\text{Swelling ratio} = \left(\frac{m_s - m_i}{m_i}\right) \times 100$$

Where m_i, m_d, and m_s are initial mass, dry mass, and swollen mass, respectively.

3.3.3 Results and Discussion (Crosslinking Behavior)

3.3.3.1 Characterization of Technical Lignins (Crosslinking Behavior)

Two kraft lignins derived from different sources (hardwood and softwood) were chosen since kraft lignin is widely available (265,000 tons produced annually),[15] and the effect of their different monolignol compositions can be investigated on the epoxidation reaction. The measured properties of the two kraft lignin samples are presented in Table 14. HW had higher ash content than SW, which might be related to the different methods (Lignoboost Vs. Lignoforce) or various parameters (pH, temperature, time, and acid concentration) used to isolate these lignins from black liquor or severity of the final washing steps. GPC data showed that SW had a higher molecular weight than HW, as expected. This could be due to the high amount of sinapyl alcohol in HW, which has two methoxy groups and limits the formation of 5–5 and dibenzodioxins linkages in the hardwood lignin.[159] Therefore, HW has a more linear structure with a lower molecular weight compared to SW. In addition, SW had a significantly higher PDI than HW, which could be related to the isolation process conditions (such as temperature and time), which resulted in breaking the intermolecular linkages and potential repolymerization of lignin chains.[94] The hydroxyl contents of lignin samples were measured by ^{31}P NMR (Figures S1 and S2). The HW lignin had significantly higher phenolic hydroxyl content (4.88 mmol/g) than SW (2.38 mmol/g) used in this study. Generally, high phenolic and total hydroxyl contents of kraft lignins is due to cleavage of lignin-carbohydrate linkages, recondensation, and depolymerization.[111]

Table 14. Ash content, molecular weight, glass transition temperature, and hydroxyl content of lignin samples

Properties	HW-K*	SW-K*
Ash %	0.34 (0.01)	1.62 (0.01)
Mn (Da)	1370	2250
Mw (Da)	3160	12100
PDI	2.3	5.4
Aliphatic OH (mmol/g)	1.37	1.65
Condensed phenolic OH (mmol/g)	0.77	0.57
Syringyl (mmol/g)	2.78	-
Guaiacyl (mmol/g)	1.14	1.62
Hydroxyphenyl (mmol/g)	0.19	0.19
Carboxylic acid (mmol/g)	0.34	0.61
Total phenolic (mmol/g)	4.88	2.38
Total OH (mmol/g)	6.59	4.64

*HW: hardwood, SW: softwood, and K: kraft

^{13}C ^{1}H HSQC was used to further study lignin intermolecular linkages and skeletal structure. The HSQC spectra of SW and HW are shown in Figure 9 and Figure 10. Several linkages including β-O-4, β-5, and β-β are present in the structure of native lignin. Still, due to the harsh conditions during the kraft isolation process, the amount of these linkages are significantly reduced in technical lignin.[160, 161] For example, phenolic ether linkages are cleaved and recondensed, resulting in a high amount of phenolic hydroxyl groups in kraft lignins.[90, 125] Table 15 presents the corresponding abundances of inter-unit linkages for the hardwood and softwood kraft lignin samples. Based on HSQC spectra, the methoxy groups are dominant in both lignin samples. The residual carbohydrates were observed in both lignins (black spots). The S/G ratio of lignin samples are correlated with the sources of lignin. Also, the abundance of β-5 and β-O-4 linkages was higher

in SW than HW, while HW had higher β-β linkages than SW. Lignin interunit are illustrated in Figure 11.

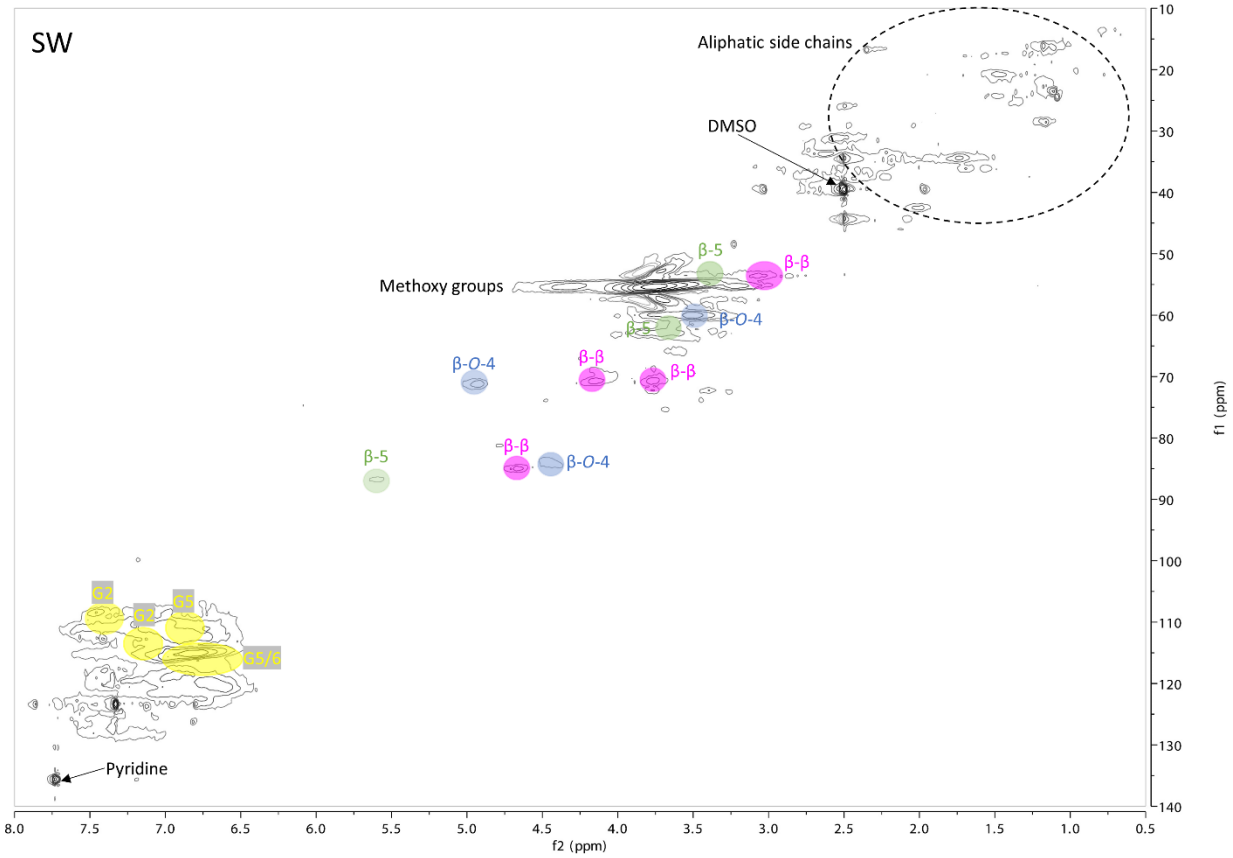

Figure 9**.** HSQC spectrum of softwood lignin (SW)

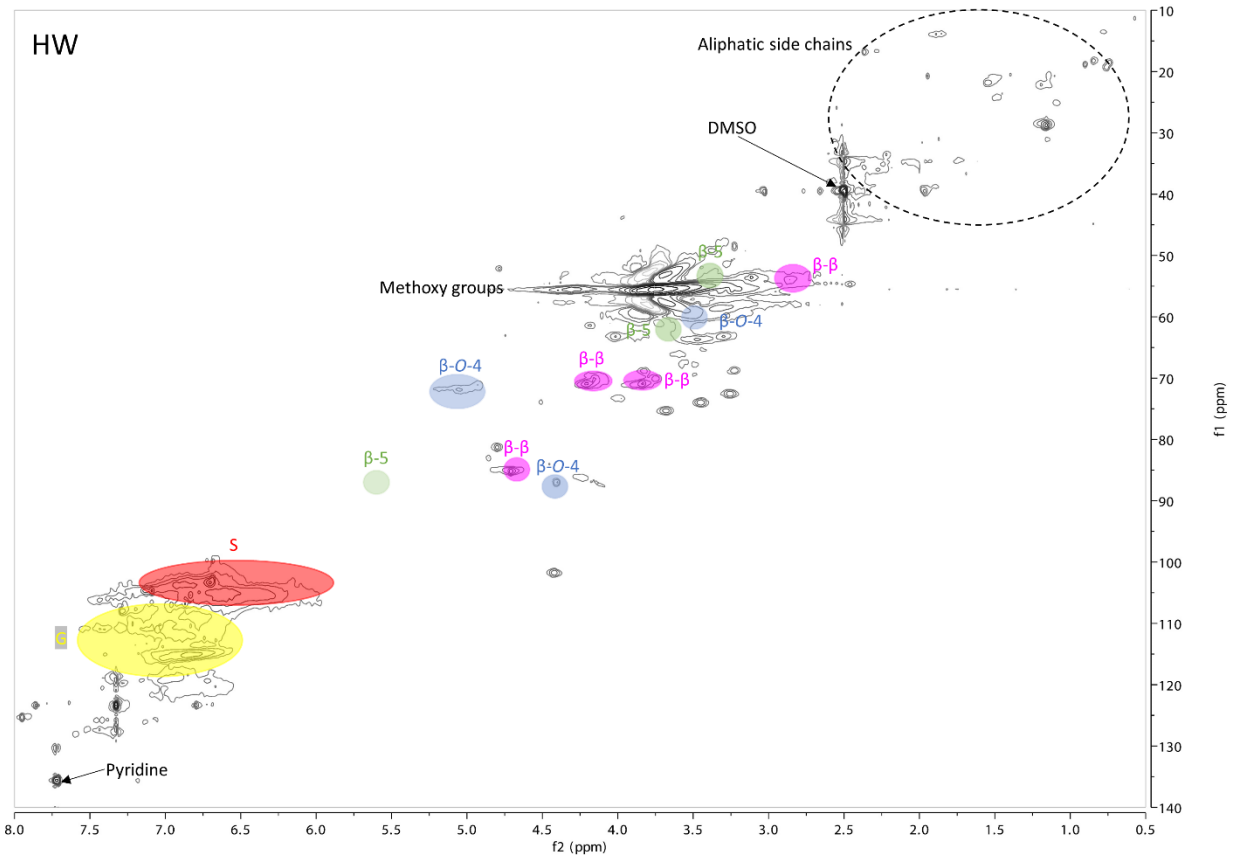

Figure 10. HSQC spectrum of hardwood lignin (HW)

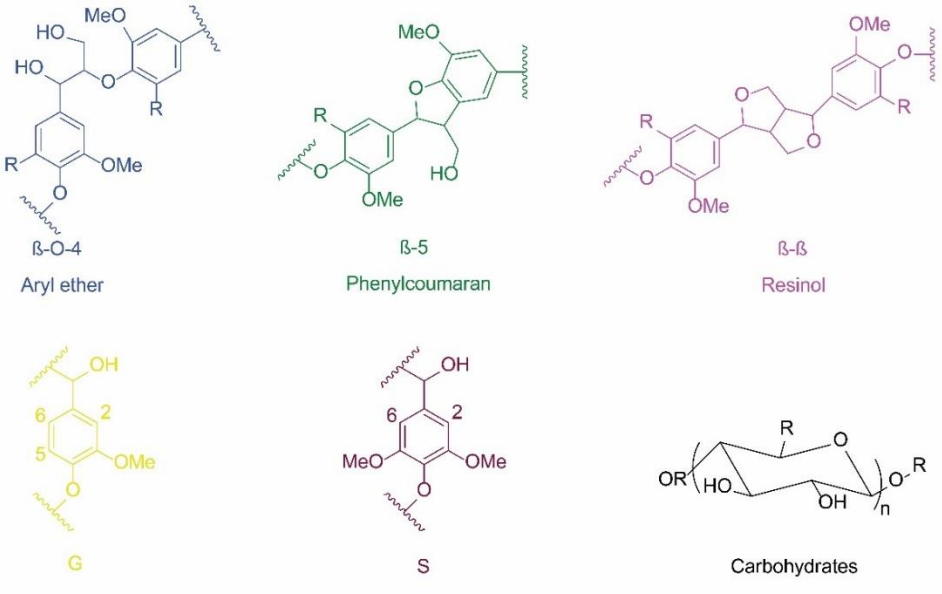

Figure 11. Lignin interunit presented in original lignins

Table 15. Semi-quantification of inter-unit linkages and aromatic units detected in lignin samples

Sample ID*	S/G	B5%	BO4 %	BB%	MeO/Aro
HW-K	3.1	6.2	53.5	40.2	1.7
SW-K	0	15.9	59.2	23.5	1.4

*HW: hardwood, SW: softwood, and K: kraft

3.3.3.2 Characterization of Epoxidized Lignins

Epoxy functional groups were selectively introduced on two lignin samples by reacting ECH in ethyl lactate solvent under mild conditions for a relatively short time (only 3 h reaction time). HW and SW kraft lignins were modified by epoxidation (EHW and ESW). ^{31}P NMR analysis confirmed that only phenolic hydroxyl groups and carboxylic acid groups in lignin had undergone epoxidation, while aliphatic hydroxyl groups were left unreacted, which confirms the optimized conditions of the reaction.

HSQC analysis of epoxidized lignin (Figure 12 and Figure 13) identified several peaks (70/4.4, 7-/3.8, 50/3.3, and 45/2.4 ppm), assigned to introduced epoxy rings in lignin.[162, 163] Besides epoxidation, no other major structural changes were observed, indicating that the epoxidation reaction was run with a mild condition that maintained the structural integrity of the lignin skeleton.

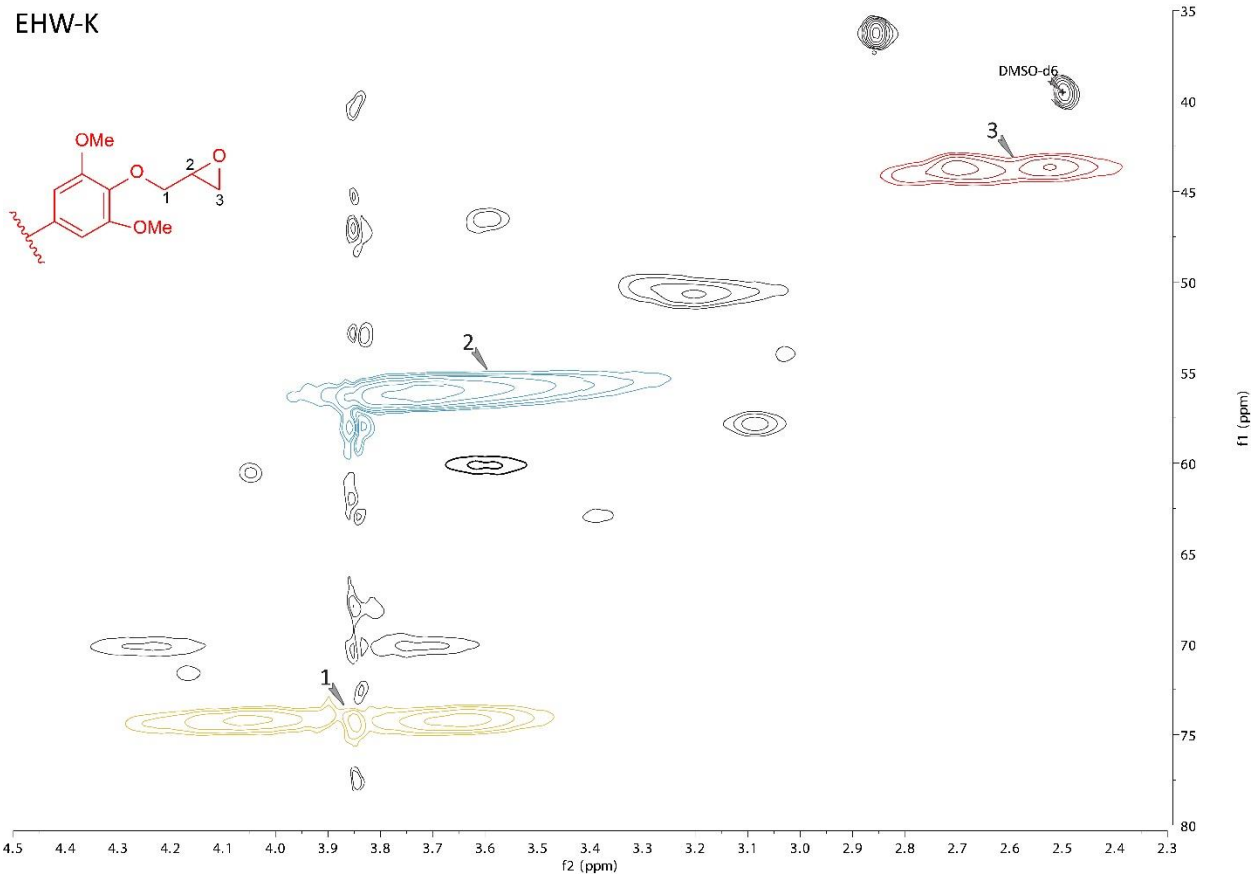

Figure 12. HSQC spectrum of epoxidized hardwood kraft lignin (EHW-K)

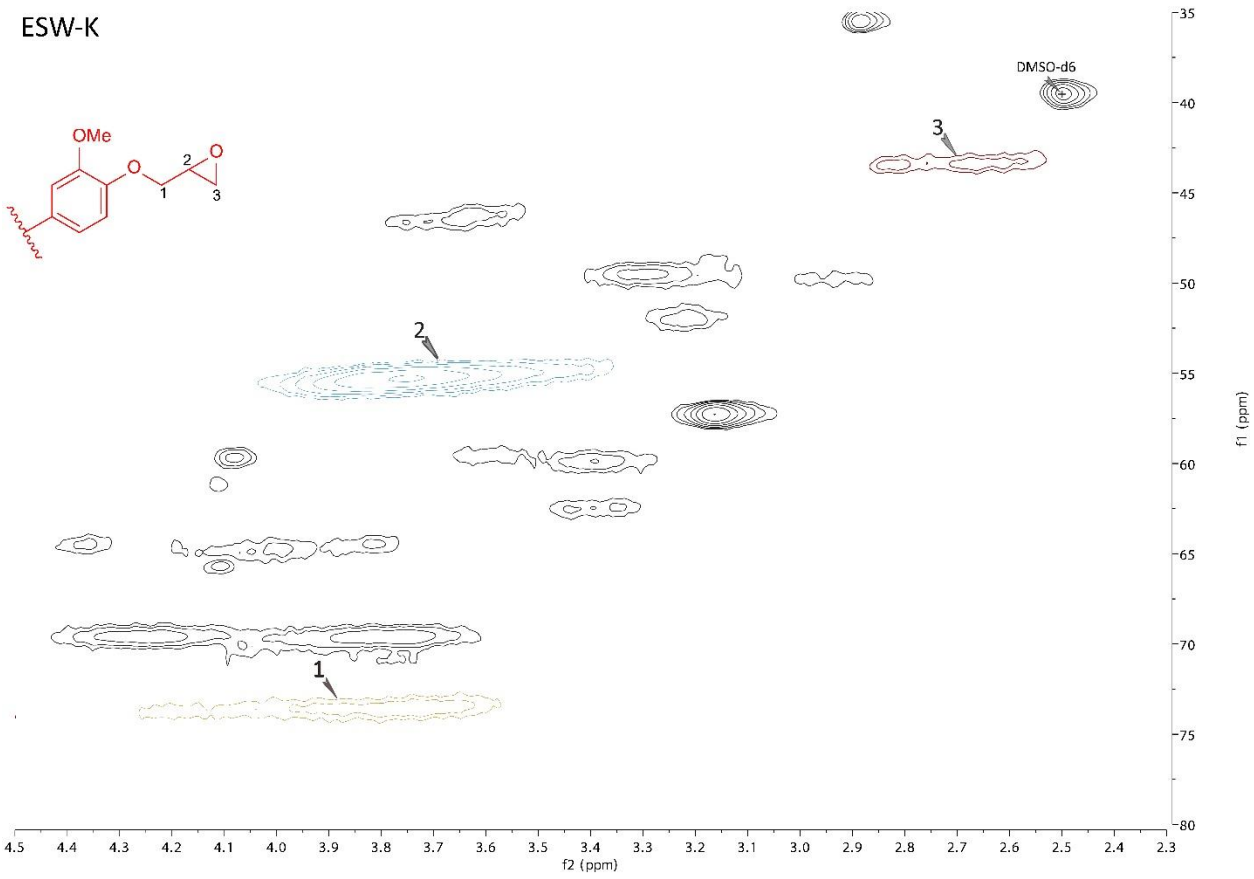

Figure 13. HSQC spectrum of epoxidized softwood kraft lignin (ESW-K)

The epoxy contents of two epoxidized lignins measured by titration and ^{1}H NMR methods are presented in Table 16. The epoxy content for HW-K lignin was higher than SW-K (13.4% and 11.8%, respectively). In a previous study, we showed that lignin with lower molecular weight and higher phenolic hydroxyl content is more reactive toward ECH and resulted in higher epoxy content after epoxidation reaction.[143] In addition, the average number of epoxy groups in each lignin macromolecule ($\bar{n}$) was calculated according to the following equation:

$$\bar{n} = \text{epoxy content (mmol/g)} \times \text{Mn},$$

The $\bar{n}$ of EHW-K and ESW-K were 4.3 and 5.7, respectively, while DGEBA resin has only 2 epoxy groups per molecule. In this case, ESW-K provides a higher number of reacting sides compared with EHW due to the higher number average molecular weight (Mn) of SW lignin.

Table 16. Properties of epoxidized lignin samples

Sample ID	Epoxy content (%) by titration	Epoxy content (%) by ^{1}H NMR	Average number of epoxy groups $\bar{n}$ [a]
EHW-K	13.4 (0.1)	13.2	4.3
ESW-K	10.8 (0.2)	10.5	5.7

a) $\bar{n}$= epoxy content (mmol/g) × Mn

3.3.3.2.1 FTIR spectroscopy

The FTIR spectra of epoxidized lignin samples (Figure 14) confirmed the epoxidation by forming new peaks of oxirane ring at 760, 840, 908, and 3000 cm^{-1}.[58] Complete epoxidations was confirmed by the disappearance of phenolic OH peaks at 1365 cm^{-1}. The intensity of non-phenolic OH groups at 3500 cm^{-1} was not changed after epoxidation, which means those hydroxyl groups were not converted during the epoxidation reaction.[56, 144]

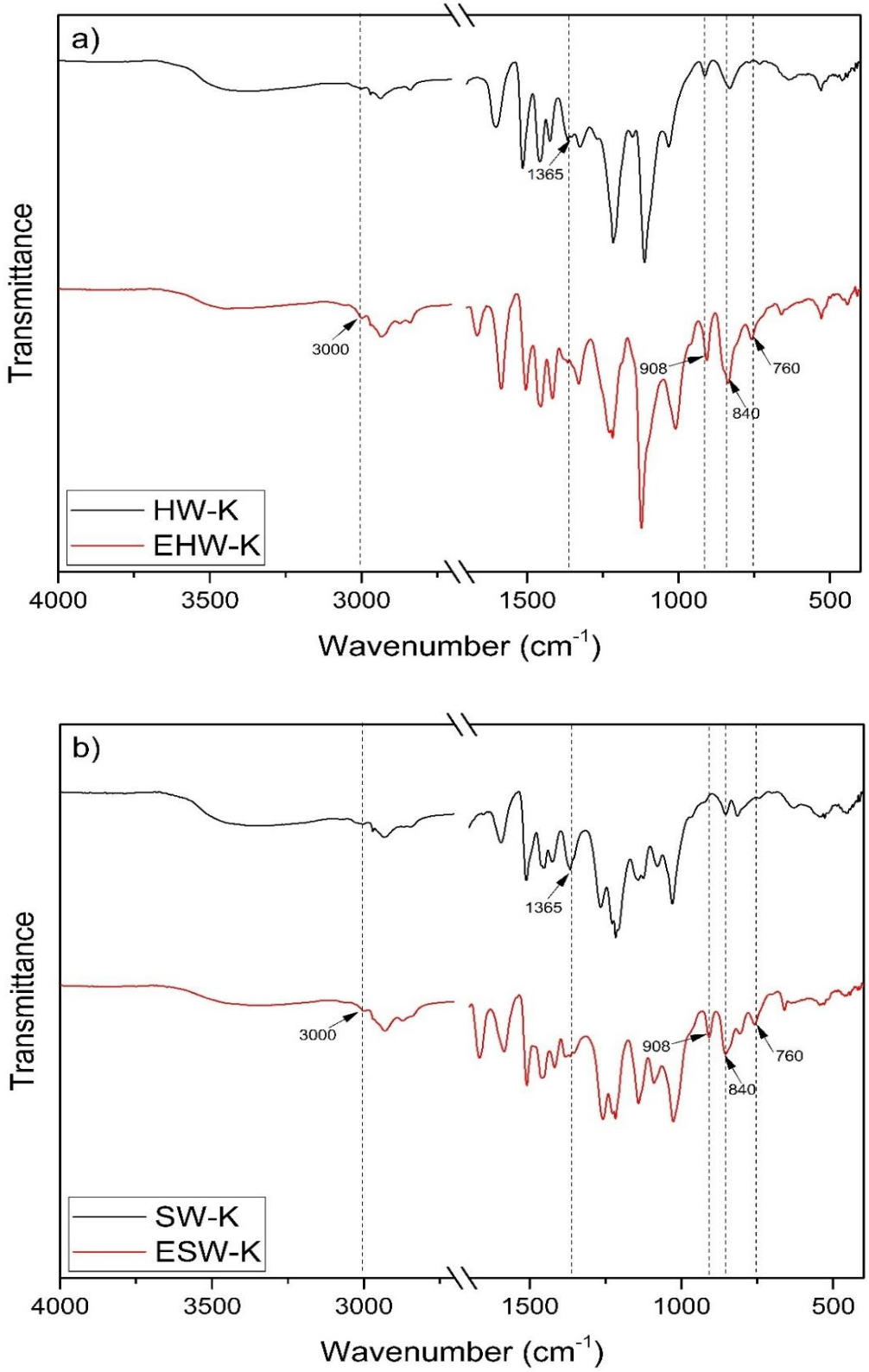

Figure 14. FTIR spectra of original and epoxidized a) HW-K and b) SW-K lignins

3.3.3.2.2 Ethyl Lactate (EL)

Ethyl lactate was used as a solvent to dissolve epoxidized lignins to cure with a curing agent. It is an environmentally friendly compound (in accordance with at least eight of twelve principles of Green Chemistry). Ethyl lactate can be generated from renewable raw materials (synthesized by the esterification reaction between lactic acid and ethanol)[164] and due to its high polarity and boiling point (151-155 °C),[165] it is a good solvent to replace high boiling point solvents such as dimethyl sulfoxide (DMSO) and dimethylformamide (DMF). It was shown that ethyl lactate is fully biodegradable, recyclable, non-corrosive, non-carcinogenic, and non-ozone depleting.[166] Hence, the United States Food and Drug Administration (FDA) approved its use in food products.[166]

3.3.3.2.3 Viscosity

The viscosity of lignin-based epoxy sample dissolved in 40 wt.% ethyl lactate as well as Epon system without and with 40 wt.% ethyl lactate before curing was measured at a constant shear rate (Table 17). It was observed that the viscosity of lignin-based epoxy systems (including ethyl lactate and curing agent) are significantly higher than the viscosity of the Epon system containing 40 wt.% solvents, while their viscosities are much lower than the Epon system without solvent. Between the two lignin-based epoxy systems, the EHW-K system had a lower viscosity than ESW-K. It is due to the higher amount of liquid curing agent used in the EHW-K system (more liquid curing agent was used because EHW-K has a higher epoxy content than ESW-K). In addition, the higher molecular weight of SW-K lignin may increase viscosity.

Table 17. The viscosity of lignin-based and DGEBA-based systems measured at two shear rates (100 and 1000 1/s)

Sample ID	Viscosity cP (100 1/s)	Viscosity cP (1000 1/s)
EP/GX-3090 (no solvent)	4810	3485
EP-EL/GX-3090	286	264
EHW-K/GX-3090	545	520
ESW-K)/GX-3090	602	548

In addition, all epoxy systems displayed shear-thinning flow behavior (reducing viscosity with increasing shear rate).

3.3.3.2.4 Rheology

Chemical composition, curing time, and curing temperatures are among the processing parameters that greatly influence the performance of epoxy systems. Different thermal and mechanical techniques such as differential scanning calorimetry (DSC), dynamic mechanical analysis (DMA), rheological analysis, and thermogravimetric analysis (TGA) were employed to investigate the curing process of epoxy systems.[167-170] Although DSC is widely used to study the epoxy curing process and provides valuable information about the degree of conversion and heat capacity changes, it does not reveal the rate of the curing process (gelation).[171] This information can be obtained from rheological analysis by measuring viscoelastic properties such as storage modulus (G'), loss modulus (G''), and damping factor (tan δ) throughout the curing process.

Curing studies of lignin-based epoxy and Epon systems were carried out under isothermal conditions at different temperatures (40, 45, 50, 55, and 60 °C). Higher temperatures were not tested to avoid evaporation of ethyl lactate. To obtain a good signal-to-noise ratio close to the gel

point, a 25 mm diameter geometry was used to stay within the linear viscoelastic region of the cured sample and avoid overloading the instrument torque while a small strain was applied.

The applied strains for all experiments were determined to be in the viscoelastic region of each sample. This was achieved by using a strain sweep on a fully cured sample and selecting the lowest strain that either resulted in a non-linear stress-strain relationship or reduced the storage modulus by 5% (Figure 15). A non-iterative sampling feature was activated on the rheometer to automatically adjust the strain through the experiment. This mode is important and applicable for thermoset resins where rapid measurements over accurate strain control is required. In addition, the axial force was controlled within 0 ± 0.1N to compensate generated forces due to sample shrinkage during the curing process as well as to monitor possible solvent evaporation.

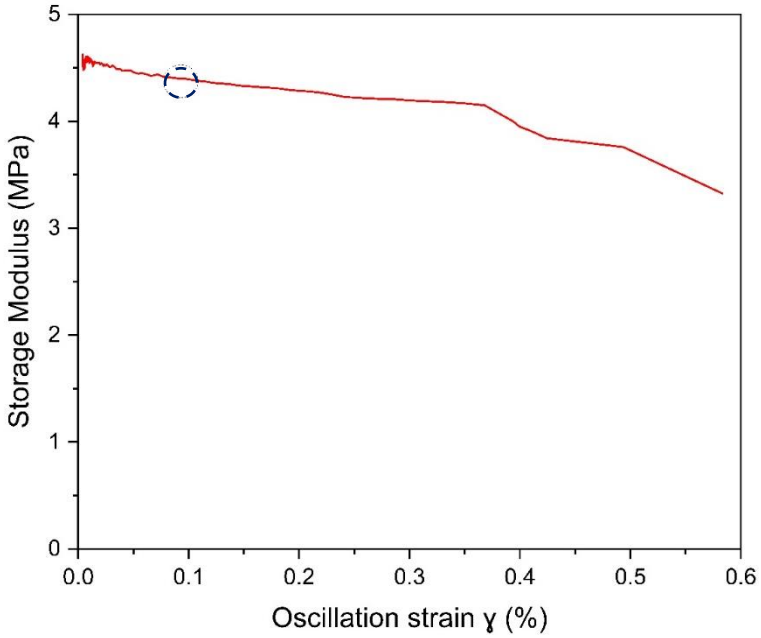

Figure 15. Oscillation strain on cured sample to determine the linear viscoelastic region

One of the most important characteristics of thermoset curing systems is the gel point, which is the boundary between the polymerization and crosslinking step; in simpler terms, it losses

flowability (dramatic increase in the viscosity of the curing resin) where the crosslinking density reaches infinity.[172] It is defined as the time or temperature point where G’ and G’’ intercept and the damping factor (tan δ) is equal to 1. The gel point is frequency-dependent. It was shown that using the G'/G" crossover to measure gel point is accurate if the stress relaxation in gel point follows a power law of G(t)=t -1/2. To overcome this issue and design a more accurate method, Winter et al. [172] proposed to use the intersection of tan (δ) cures obtained at multiple frequencies to determine the gel point. The rheological multi-wave test was used to avoid several sample preparations and save time by applying multiple frequencies in sequence (1, 10, and 50 Hz). All three curves of tan (δ) were overlapped, and the true gel point which is independent of frequency was obtained (Figure 16).

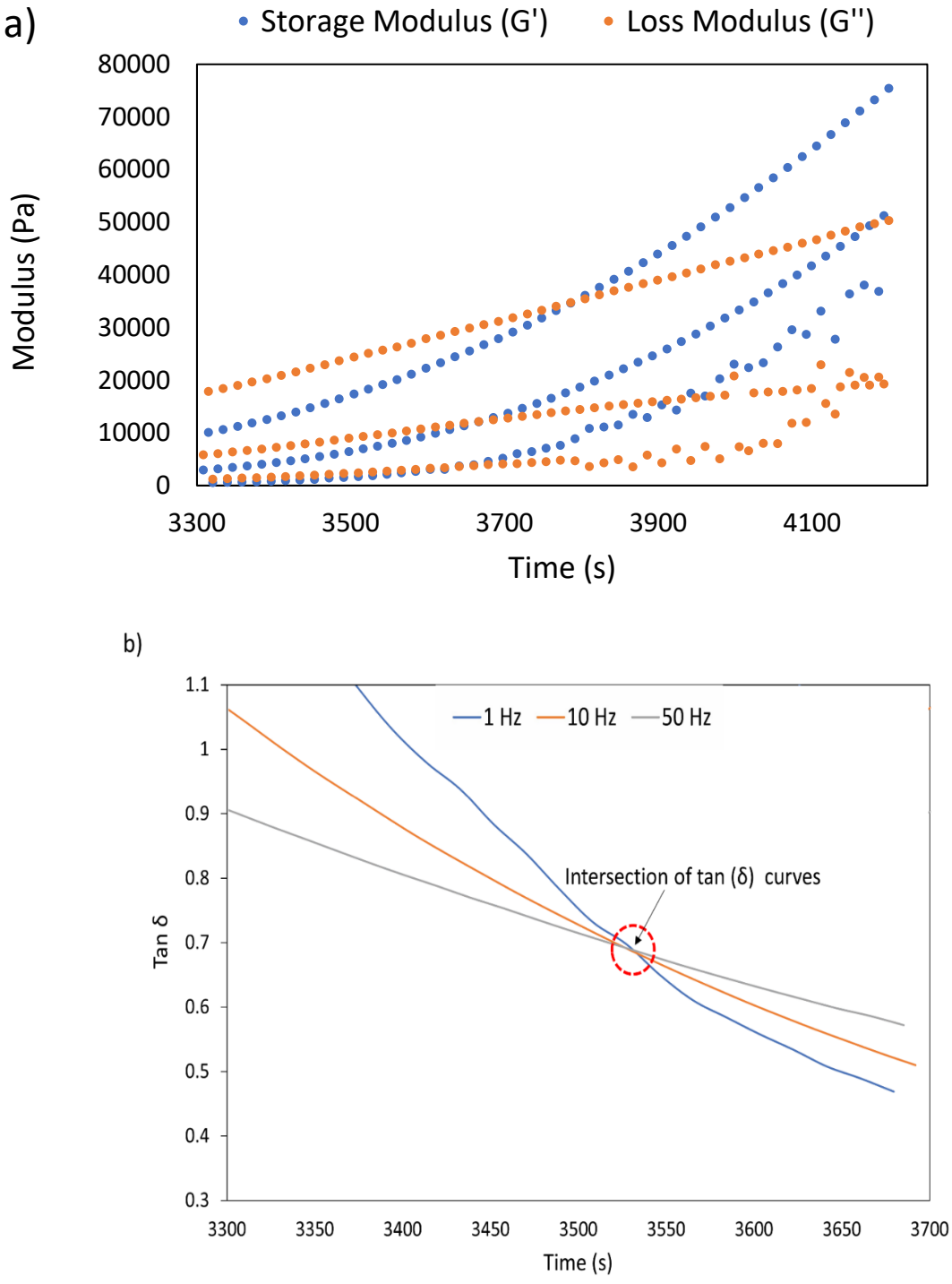

Figure 16. a) Multi-wave experiment at 1, 10, 50 Hz, b) Plot of tan δ to identify true gel point

The gel point (t_α gel) always occurs at the same conversion for the same material, regardless of temperature. Therefore, the activation energy (E_A) of gelation based on this iso-conversional phenomenon can be measured using the following equation.[173-175]

$$ln(t_{\alpha,gel}) = C + \frac{E_A}{RT_i}$$

Where C is a polymer constant, R is the gas constant, and T is the temperature. The measured activation energy for each system obtained at different temperatures is shown in Figure 17. Interestingly, both lignin-based systems showed significantly lower activation energies compared to EP systems (with and without solvent). Two reasons could explain this behavior. According to statistical approaches by Flory [176] and Stockmeyer [177], monomer functionality is inversely related to the critical extent of reaction; this means the system will reach the gel point at a lower extent of reaction. On the other hand, the system is gelled faster. The functionalities of lignin-based epoxy systems were 2-3 times higher than EP system; therefore, the gel point is achieved at a lower conversion, according to the following equation.

$$P_c = \frac{1}{[r + r\rho(f-2)]^{1/2}}$$

Where Pc is the gel point, r is the ratio of two different monomers (ratio of epoxy groups and amine groups in this case), ρ is the fraction of multifunctional groups to all functional groups in the mixture, and f is the functionality of a multifunctional monomer.

In addition, it was shown that hydroxyl functional groups accelerate the curing reaction of epoxy/amine systems, but they only serve as a catalyst and do not compete with the reaction between amines and epoxy groups.[178, 179]

When solvent was added to the epoxy resin (EP-EL), the gel point and the activation energy increased. Wu et al.[180] reported that the presence of solvent in epoxy resin results in a lower reaction rate and reaction order. Thus, adding solvent could decrease the curing rate and increase the activation energy, possibly due to a decrease in the interaction of functional groups.

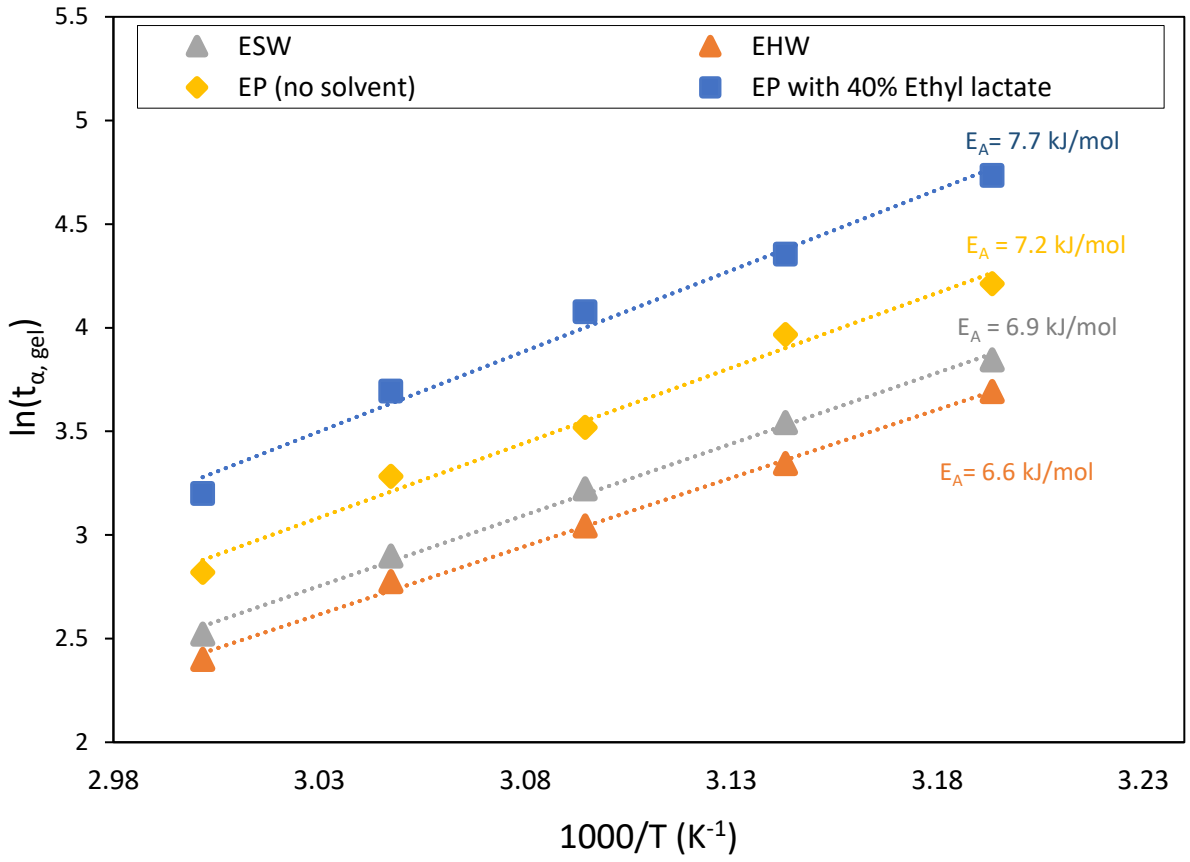

Figure 17. The plot of obtained activation energy of epoxy resins

E-SW: epoxidized softwood

E-HW: epoxidized softwood

Ep: Epon 828 (DGEBA)

3.3.3.2.5 Gel Fraction and Swelling Ratio

The gel fraction and swelling ratio of cured samples were measured to obtain further information regarding their network density. Sample swelling and dry states are presented in Figure 19, following immersion of samples in THF for 24 h. The EP sample without EL showed the highest gel fraction and lowest swelling ratios. In the EP-EL system, the gel fraction decreased, which indicates the solvent (EL) was partially washed out because it was not incorporated into the network. For lignin-based epoxy systems, both cured samples (EHW and ESW) showed higher gel fractions, which might be related to a 3D crosslink network that retained more EL solvent than the EP-EL system. Sample EHW-K had a higher gel fraction than ESW-K, probably due to its higher epoxy content, which provides a higher crosslinking density.

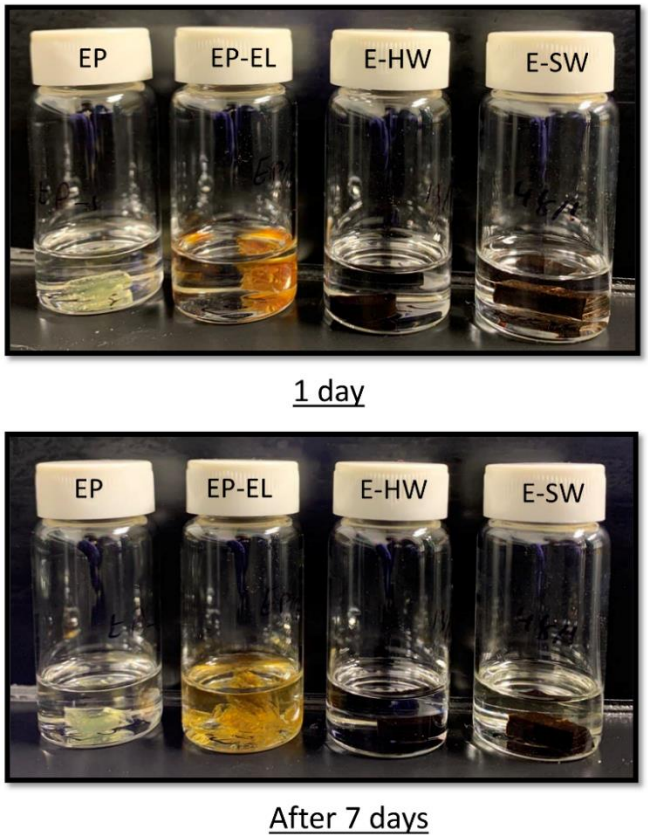

Figure 18. Immersed epoxy thermosets in THF

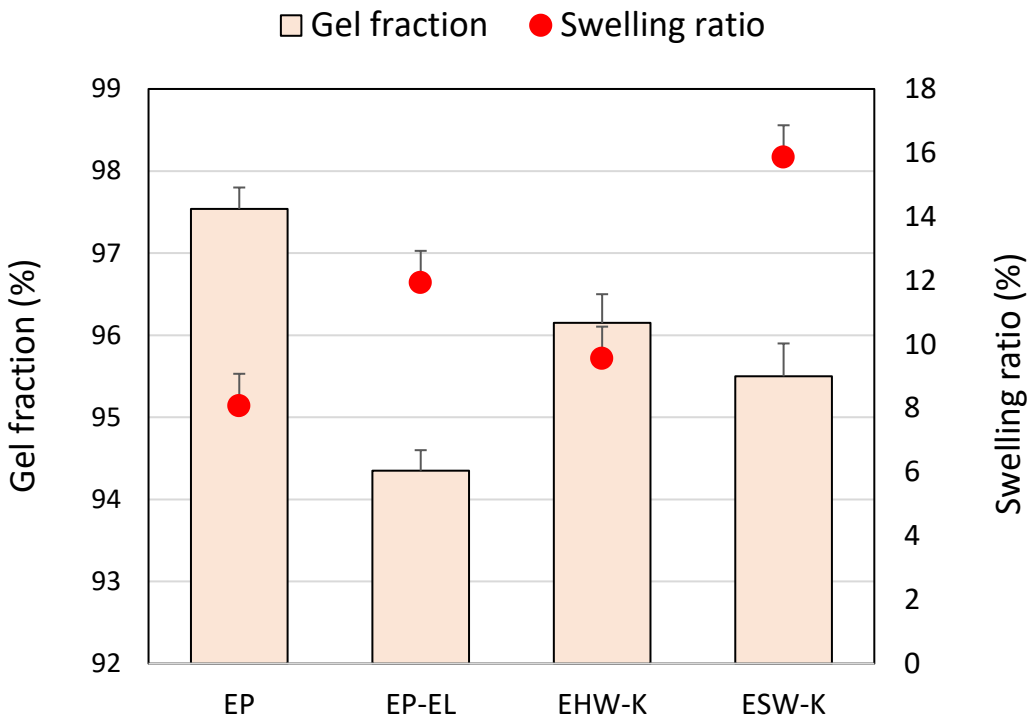

Figure 19. Measured gel fractions and swelling ratios of the cured samples

CHAPTER 4 (Lignin-Based PUD)

4.1 Introduction

4.1.1 Incorporation of Lignin in Polyurethane Formulations

Lignins derived from different sources and isolation methods, including wheat straw,[181] organosolv,[182] and kraft lignin [183] have been used to partially (40- 80 wt.%) replace polyol in PU resin formulations used for coating applications. Different modification approaches such as solvent fractionation,[184] depolymerizations,[185] and functionalization[186] have been used to improve the suitability of lignin as polyol replacement in polyurethane formulations.

Although several studies successfully replaced petroleum-based polyol with unmodified lignin, all formulated resins were designed for solvent-borne systems, which require a high amount of organic solvents (2-3 times the weight ratio of lignin) to dissolve lignin. Previous studies dissolved lignin first in tetrahydrofuran (THF) or DMF before PU formulation, which caused the final resin to contain about 40-60 wt.% volatile organic compound (VOC).[184, 187] Reducing VOC emissions is the goal of most industries, resulting in most resins and coating producers shifting from solvent-borne to waterborne systems.[188] Thus, it is crucial to develop lignin-based polyurethane systems that meet the requirement of green chemistry in formulating zero or low VOC waterborne resins.

4.1.2 Waterborne Polyurethane Formulations (PUDs)

Waterborne polyurethane dispersions (PUD) are widely used as coatings for wood, plastic, metallic, and mineral substrate. PUD is a polyurethane polymer resin dispersed in water rather than solvent due to its hydrophilic functional groups.[189] PUD has attracted great interest in coating applications due to its excellent flexibility, impact and abrasion resistance, and low or even zero VOC content.[189]

Based on the synthesis method, PUDs are classified into two groups:

1. PUDs are first synthesized in a water-miscible organic solution, then water is added to the resin
2. PUDs synthesized in the presence of water

In both groups, a medium molecular weight isocyanate-terminated prepolymer (polymer chains containing active isocyanate functional groups in the structure) is formed by a reacting di- or poly-ols and an excess of di- or poly-isocyanates. In this way, the formed prepolymer is chemically active for further reactions. The main differences between the two methods in PUD systems are how the prepolymer chain is extended. In the first method, the water-solubilizing/dispersing groups from the internal emulsifier are functionalized (neutralized) in the prepolymer before chain extension. Then, the water is added to the polymer, and stable small particle dispersions are obtained without using an external surfactant. Later on, the solvent is removed to obtain the desired PUD system. This PUD system is not chemically active and can be directly applied on substrate.[189]

In the second method, the PUD is synthesized by adding di or polyamines in the aqueous phase to the isocyanate-terminated PU prepolymer for chain extension. Chain extension with amine is possible because amine groups in polyamine are more reactive towards isocyanates than water. It is essential to keep the water temperature low enough to maintain this reactivity preference.[189]

Several biobased PUD systems have been developed using castor oil,[190] linseed oil,[191] canola oil,[192] tung oil,[193] and, cardanol [194], which all are edible feedstock and not desirable by the industry as they compete with food sources. In one study,[195] unmodified alkali lignin dissolved in DMF to replace 25-33 wt.% of petroleum-based polyol to synthesize PUD resin. It was found that

introducing alkaline lignin in PUD formulation improved the thermal stability and tensile strength of PUD films.

4.2 Experimental

In the present study, lignin-based PUD formulations were prepared. Two approaches were utilized to modify and improve the PUD formulations. Tartaric acid (TA) was used as an emulsifier to replace DMPA and increase the percentage of biobased reagent in PUD formulation. In addition, a soy-based polyol with a low OH value was added to the formulation to increase the flexibility and elongation of lignin-based PUD.

4.2.1 Materials

Hardwood lignin isolated from alkaline pre-extraction pretreatment was used. Isophorone diisocyanate (IPDI), hexamethylene diisocyanate (HDI), dimethylol propionic acid (DMPA), tartaric acid (TA), methyl ethyl ketone (MEK), and triethylene amine (TEA) were purchased from Fisher Scientific. Hydrazine monohydrate (HZ), and cyrene were supplied from Sigma Aldrich. Cargill kindly provided the soy-based polyol with OH value of 40 mg KOH/g.

4.2.2 Synthesis Lignin-Based PUD Resins

First, 5g dried alkaline pre-extraction lignin was dissolved in 25 g cyrene and 80 g MEK. Then, different formulations were prepared according to Table 18. The mixture of lignin, emulsifier, and isocyanate was mixed under reflux and a nitrogen atmosphere at 70 °C for 4 hours. Then, it was cooled to 50 °C, and TEA was added as a neutralizing agent and mixed for 1 hour. Next, an equivalent amount of HZ was gradually added at room temperature to react with the remaining NCO groups to complete the polymerization step. Finally, 40 g DI water was added to the mixture at a high shear rate (2000 rpm) to disperse formed PUD particles. A rotary evaporator at 50 °C

was employed to remove MEK from the solution. Commercial PUD resin from WIL was used as a reference for comparison with lignin-based formulations.

Table 18. Components of tested PUD formulations

Sample ID	Lignin (g)	Soy-polyol (g)	Tartaric acid (g)	Triethylene amine (g)	Isocyanate (g)
Pre-ex IPID-PUD	5	-	1	1.3	IPDI*- 4.4
Pre-ext HDI-PUD	5	-	1	1.3	HDI**- 3.3
Pre-ext 10% soy HDI-PUD	4.5	0.5	1	1.3	HDI**- 3.1
Pre-ext 20% soy HDI-PUD	4	1	1	1.3	HDI**- 2.6
Pre-ext 30% soy HDI-PUD	3.5	1.5	1	1.3	HDI**- 2.4

*Isophorone diisocyanate

**Hexamethylene diisocyanate

4.3 Characterization of Lignin-Based PUDs

Solid contents of all resins were measured according to the ASTM D4426-01. First, aluminum pans were placed in a furnace at 270 °C for 1-2 min to burn off any contaminations. Then they were cooled to room temperature in a desiccator and weighted. Then, around 1 g of resin was added to a pan and placed in an oven for 105 min at 125 °C. Later, samples were moved to a desiccator to reach the room temperature and then weighted. The solid content of resins was calculated according to the following equation:

$$\text{Solid Content (\%)} = \frac{\text{Weight of dried resin (g)}}{\text{Weight of initial resin (g)}} \times 100$$

The pH of all resins was measured using a calibrated Mettler Toledo S220 pH meter at room temperature. The viscosity measurement was performed using a Discovery HR-1 hybrid rheometer (TA instrument) at room temperature and a constant shear rate (100 1/s).

PUD resins were added to a silicon mold and dried at room temperature for 72 hrs. Then, the formed films were taken out and subjected to a micro-tensile test, using an Instron universal testing machine, to measure the tensile strength and elongation at break. The sample dimensions were 25×5×1 mm, and the elongation rate was 500 mm/min.

4.4 Results and Discussion

Cyrene, also called dihydrolevoglucosenone, is a heterocyclic cycloalkanone that is made either by hydrogenation,[196] or enzymatic reduction of levoglucosenone.[197] It is a biobased solvent and is considered a green alternative for toxic aprotic solvents such as dimethylformamide (DMF) and N-methyl-2-pyrrolidone (NMP); it has recently been commercially available.[198] It is widely used in different applications such as synthesis chemistry, pharmaceutical products, and polymers.[199-202] DMF is known as a good solvent for lignin due to their relatively low Hansen relative energy difference (RED), which is 0.77. Because of similar aprotic dipolar properties to DMF, the RED of lignin and cyrene is 0.89, indicating that cyrene can be a great solvent for lignin.[203] Therefore, cyrene was used to dissolve lignin for further reaction in PUD formulations. Table 19 shows the properties of prepared PUD resins.

Table 19. Properties of PUD resins

Sample ID	Solid Content (%)[a]	pH	Viscosity (cP)[b]
Pre-extraction PUD	33.7 (0.5)	8.0	228
Cu-AHP (1.2% H_2O_2+O_2) PUD	31.8 (0.4)	8.2	211

Cu-AHP (4% H_2O_2+O_2) PUD	34.2 (0.3)	7.9	234
Commercial PUD	34.9 (0.2)	8.1	240

a) Dried at 125 °C, according to ASTM D4426-01

b) 25 °C, constant shear rate 100.0 (1/s)

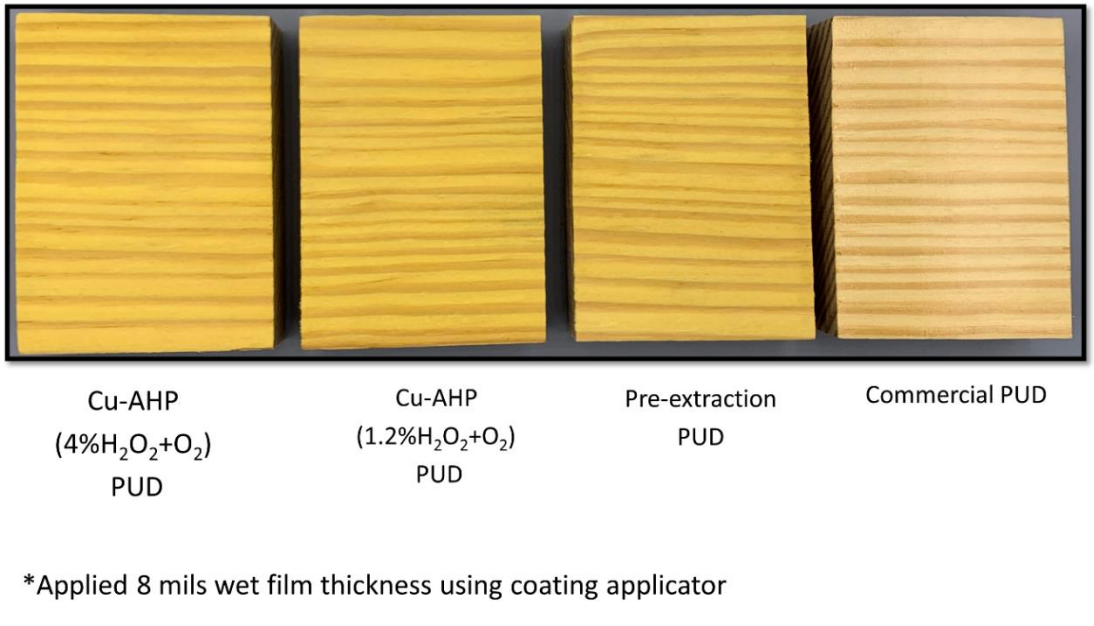

Figure 20. Wood coated samples with PUD resins

The mechanical testing results of the formulations are illustrated in Figure 21. The sample prepared with IPDI showed low tensile strength and significantly lower elongation at break than the commercial PUD. HDI was used as an isocyanate reagent to improve the elongation at the break of PUD films since it has a linear structure. It was found that replacing IPDI with HDI did not substantially improve the tensile properties of PUD film. Therefore, soy-polyol with a low hydroxyl value partially replaced the lignin (10, 20, and 30 wt.%) to provide flexibility. By adding 10 wt.% soy-polyol, the elongation at break and tensile strength increased by 160% and 116%, respectively, compared with lignin-based PUD formulated with HDI. Both tensile strength and elongation at break continued to increase with higher incorporation of soy-polyol, but the increase

rate plateaued from 20wt.% to 30 wt.% soy-polyol. The lignin-based PUD formulation with 20% soy-polyol displayed a tensile strength that was 88% of the commercial PUD's tensile strength; similarly, its elongation to break was 68% of the commercial PUD's corresponding value.

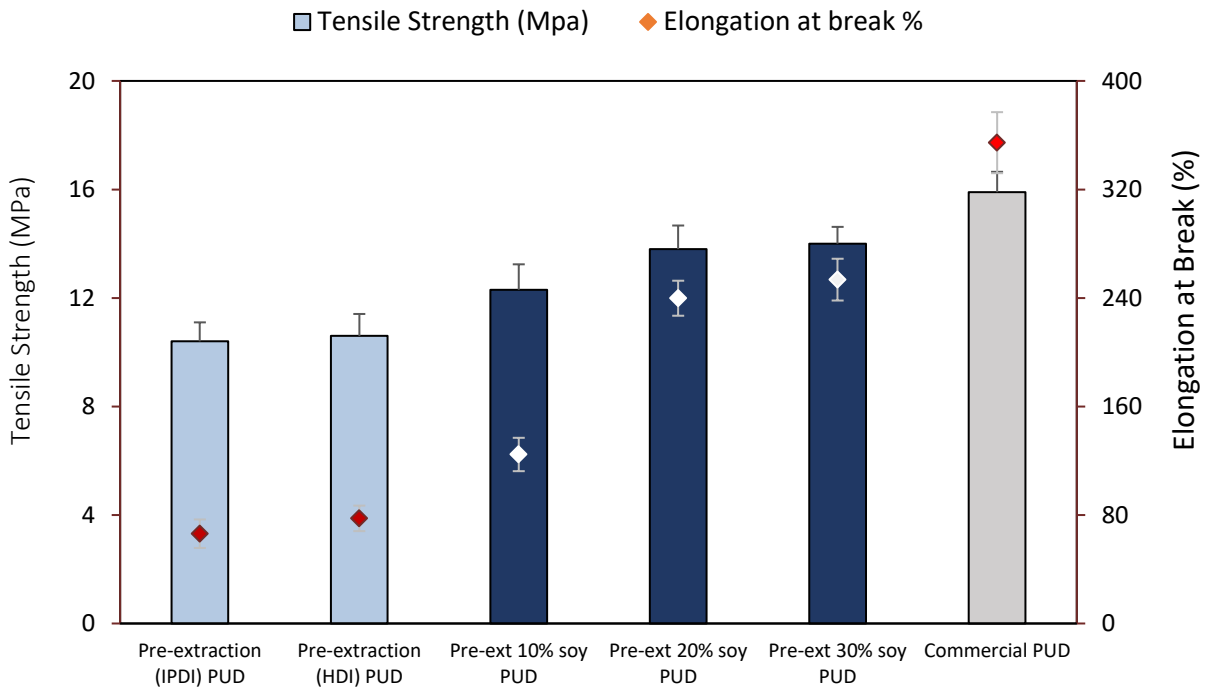

Figure 21. Tensile properties of different PUD resins

CHAPTER 5 (Conclusions and Future Recommendations)

5.1 Conclusions

Lignin, the most abundant renewable aromatic polymer, is recovered as a by-product of pulp and paper and bioethanol production. It is currently burned to provide energy for pulp and paper plants, while lignin has excellent potential to be used for synthesis of different value-added products. The structural complexity of lignin varies among biomass sources and isolation processes. Comprehensive characterization is required to find the most suitable applications for a particular lignin. To achieve this, seventeen commercially available lignins covering softwood, hardwood, and herbaceous sources, isolated by four common methods including kraft, organosolv, sulfite, and soda, were thoroughly characterized.

5.1.1 Insight into the Composition and Structure of Commercial Lignins

According to results obtained by multi-techniques characterization, hardwood lignins generally had more linear structures and lower molecular weights. Furthermore, kraft lignins on average had higher aliphatic and phenolic hydroxyl contents because of the cleavage of phenolic ether linkages (β-O-4, α-O-4, and 4-O-5), which provide more hydroxyl groups for further reactions. Also, lignin isolated through the organosolv process had lower hydroxyl content due to milder conditions (lower temperatures and concentrated alkaline pretreatment) used in that process. In summary, the molecular weight, impurity, and chemical structure of lignin should be all taken into consideration when choosing a specific lignin for valorization.

5.1.2 Entirely Replacing Bisphenol A with Unmodified Lignin in Epoxy Resin

The efficacy of a wide range of commercially available unmodified lignins in replacing 100 % of bisphenol A in epoxy resin formulation was investigated. According to our developed method,

molecular weight and phenolic hydroxyl content had the most significant impact on lignin suitability in replacing BPA in epoxy resin. It was found that lignins which had lower molecular weights (Mw) and higher phenolic hydroxy contents, had higher reactivities towards biobased epichlorohydrin. Dynamic mechanical analysis (DMA) proved that the fully biobased cured systems containing epoxidized lignin and biobased diamine (from cashew nutshell) as a hardener had comparable thermomechanical properties to the petroleum-based epoxy system (diglycidyl ether bisphenol A) but had lower thermal stability based on TGA results. This is an important step forward in establishing the possibility of formulating a fully biobased epoxy resin using unmodified technical lignins, biobased ECH, and biobased hardener with comparable performance to petroleum-based resins for coating, adhesive and composite applications.

5.1.3 Formulating Lignin-Based Waterborne Polyurethane Resins

The high aliphatic hydroxyl contents of lignins (3-5 mmol/g) isolated through an MSU patented technology (pre-extraction and enzymatic hydrolysis) indicated that these lignins are excellent candidates to formulate polyurethane waterborne resins due to the high reactivity of aliphatic hydroxyl groups toward isocyanates. In this study, several lignin-based waterborne polyurethane dispersion (PUD) resins with zero volatile organic compounds were developed for the first time by entirely replacing petroleum-based polyols with unmodified lignins. Additionally, the petroleum-based emulsifier in PUD formulations was successfully substituted with a biobased compound (tartaric acid). Then to improve the flexibility of developed lignin-based PUD resin, 20 wt.% of lignin was replaced with soy-polyol, which enhanced tensile strength and elongation of the resin. The promising results of this study can potentially expand the application of biorefinery lignin and soy-polyol in formulating low VOC, high biobased content PUD resins.

5.2 Future Recommendation

This study was focused on developing lignin-based epoxy and PUD resins using unmodified lignins from different isolation processes and sources. For considering these resins for coating applications (mainly wood coatings), it is recommended to evaluate the performance of formulated coatings made with the developed lignin-based PUD resins when applied on different substrates. In addition, to consider the feasibility of producing lignin-based epoxy and PUD resins on commercial scales, it is helpful to conduct a comprehensive techno-economic analysis (TEA) for both processes.

APPENDICES

6.1 APPENDIX A (UV Degradation of Lignin)

Evaluating Efficacy of Different UV-Stabilizers/Absorbers in Reducing UV-Degradation of Lignin

Abstract

Susceptibility of wood to UV degradation decreases the service life of wood products used outdoors. Organic UV absorbers and hindered amine light stabilizers (HALS), as well as inorganic UV absorbers, are added to coatings to improve the UV stability of coated wood products. Although about 85% of UV radiation is absorbed by lignin in the wood, it is unclear which UV stabilizers can minimize lignin degradation. In this study, the photodegradation of softwood organosolv lignin was monitored over 35 days of UV exposure. Changes in lignin properties were assessed using Fourier transform infrared spectroscopy (FTIR), differential scanning calorimetry (DSC), gel permeation chromatography (GPC), and phosphorus nuclear magnetic spectroscopy (^{31}P NMR). It was found that the aromatic rings of lignin underwent significant degradation, resulting in increased glass transition temperature and molecular weight of lignin. Subsequently, eighteen different additives were mixed with lignin and exposed to UV irradiation. The analysis of samples before and after UV exposure with FTIR revealed that inorganic UV absorbers (cerium oxide and zinc oxide) and a mixture of organic UV absorbers and HALSs (T-479/T-292, T-5248, and T-5333) were the most effective additives in reducing lignin degradation. This study can help coating scientists to formulate more durable transparent exterior wood coatings.

Keywords: Lignin; Photodegradation; UV Absorber; UV Stabilizer

Introduction

Wood products used outdoors are susceptible to photodegradation,[204] which usually causes yellowing, discoloration, loss of gloss, increased roughness, and diminished mechanical and physical properties.[205-207] Wood is mainly composed of three compounds: cellulose, hemicellulose, and lignin; these compounds have different sensitivities to UV light during photodegradation. Lignin is a macromolecule in wood that acts as a binder in holding cellulosic fibers;[208] it is composed of various arrangements of three monolignols: guaiacyl, syringyl, and *p*-hydroxyphenyl units.[209]

Cellulose and hemicellulose only absorb 5-20% of UV light, while lignin absorbs about 80-95% of the UV light due to the presence of chromophores and aromatic rings, making it more prone to decomposition by photooxidation reactions.[208, 210] During UV irradiation, three chemical reactions occur in lignin, 1) dehydrogenation, 2) dehydroxymethylation, and 3) demethoxylation.[211] The formation of free radicals triggers the UV degradation process, followed by the oxidation of phenolic hydroxyl groups in lignin.[212, 213] Free phenolic radicals are generated immediately under UV irradiation. This way, the radicals delocalization favors the formation of *o*- and *p*-quinonoid structures after demethylation and cleavage of the side chain.[214] As shown in Scheme 8, the newly formed carbonyl groups in *o*- and *p*-quinonoid are considered chromophoric groups that cause significant color changes on the wood surface.[214]

In addition to lignin, extractives are also susceptible to UV degradation. Extractives types and contents significantly affect the color, odor, and biological durability of the wood.[215] Similar to lignin, extractives will also undergo structural changes after UV exposure contributing to wood discoloration.[216-219]

UV radiation (295-400 nm) provides sufficient energy to dissociate lignin moieties that have carbonyl, biphenyl, or ring-conjugated structures. It was shown that violet light (380- 430 nm) extends photodegradation into the wood beyond the area affected by UV light since larger wavelengths penetrate deeper into the wood than UV light.[220]

In addition to UV light, water also plays a vital role during the photodegradation, of wood, including carrying the radicals formed on the wood surface to deeper layers in the wood, forming hydroperoxide that can initiate chain scission reactions in polymeric wood compounds. Kalnins [221] reported that oxygen is necessary for free radical initiation, and phenoxy radicals are formed during lignin photodegradation can react with oxygen to form *O*-quinoid structures after demethylation. Hon also stated that the reaction of oxygen to form hydroperoxide is an essential part of the photodegradation process.[222]

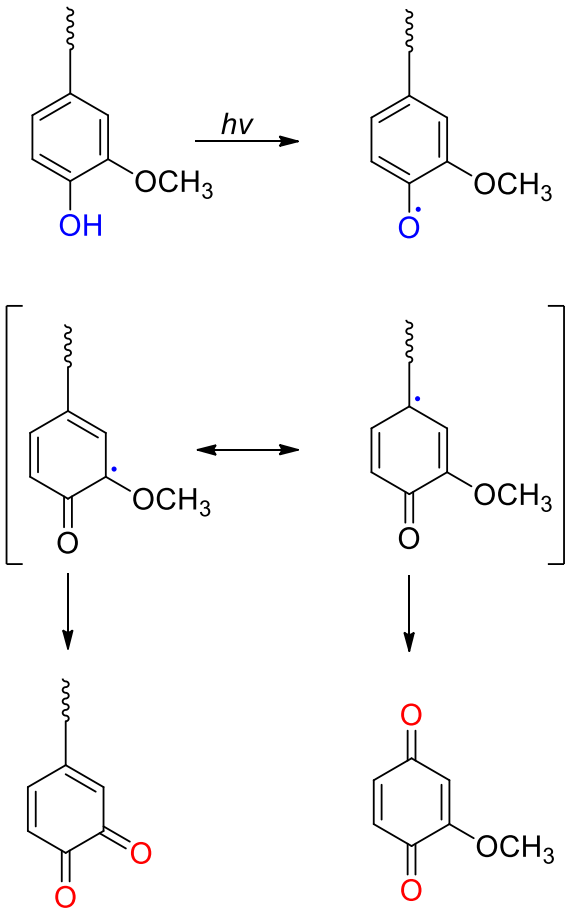

Scheme 8. Formation of *o*- and *p*-quinonoid structures resulting from UV degradation of lignin [223]

Researchers have explored many ways to improve weathering performance of wood. Treating wood surfaces with chromic acid is a well-known method that stabilizes wood by oxidizing phenolic sub-units at the surface, making them more resistant to photodegradation.[224, 225] However, concern about chromium compounds' potential adverse health effects limited the commercialization of chromic acid treatment for wood.[226] Chemical modification has also been widely used to enhance the weathering stability of wood. Chemically treated wood with butylenes, butylene oxide, and methyl isocyanate, benzoyl chloride, as well as acetylation showed better weathering performance.[227-230] Additionally, 1,3-dimethylol-4,5-dihydroxyethyleneurea (mDMDHEU) was used to treat scots pine wood and reported to significantly improved the

weathering stability of the wood.[231] One of the most common ways to increase the photostability of wood while maintaining its aesthetic appeal is to use transparent coatings such as epoxy, polyurethane, alkyd, and acrylic, containing UV stabilizers and/or nano-pigments.[232-236]

Organic UV stabilizers are categorized into two groups: 1) UV absorbers (UVAs) and 2) hindered amine light stabilizers (HALSs). UVAs like 2-(2-hydroxyphenyl)-benzotriazoles (BTZ) filter out the vulnerable wavelengths of the light before they reach the wood surface; therefore, decreasing the rate of radical formation due to their high absorbance profile in the UV region (typically 300-350 nm).[237] The most common UVAs have primary photophysical properties, including a high absorbance profile in the UV range and high photochemical stability.[238] HALS (a common derivative of 2,2,6,6-tetramethylpiperidine), also known as a radical scavenger, inhibiting the photo-oxidative degradation of polymers.[239] It was shown that a combination of organic UV absorber and HALS improved the transparent wood coating performance.[240]

On the other hand, inorganic UV absorbers are based on metal oxide particles like ZnO or TiO_2, which are applied to scatter or absorb light. Using nanosized pigments can protect both coating and the substrate (wood) while preserving transparency in the visible spectrum.[241, 242] Pretreatment of wood for dimensional stability and applying the flexible and photostable coating is another way to achieve durable exterior coated wood products.[243, 244] Also, it has been shown that phenol-formaldehyde resins can improve weathering stability of plywood samples.[213, 245]

Although several studies have evaluated the photostability performance of different wood coatings, they were mainly focused on assessing color change as a visual indicator,[246] to the best of our knowledge, there is no published work on examining the interaction between lignin, as the main UV susceptible component of the wood, with a wide range of UV stabilizers. The aim of the present research was to find the most effective additives that can reduce lignin degradation. The

results of this study can help coating formulators or preservative producers choose additives proven to minimize lignin degradation, thus improving the UV performance of wood products in exterior applications.

Experimental

Materials and Methods

Since most exterior wood products (fences and decks) are made of softwood in North America, a high purity softwood organosolv lignin provided by Lignol (Current Suzano) was used. An organosolv lignin was chosen because, among technical (commercially available) lignins, organosolv lignin has the closest structure to the structure of native lignin in the wood due to the mild ethanol biorefinery isolation process.[247] Eighteen different additives (Table 1), including organic UV absorbers (UVA), organic hindered amine light stabilizers (HALS), and inorganic UV absorbers, were kindly supplied by chemical industries. All other chemicals were purchased from Fisher Scientific Co and Sigma Aldrich and used as received.

Sample Preparation

First 4 g of organosolv softwood lignin was dissolved in 15 g of tetrahydrofuran (THF). Next 2 wt.% of individual additives were added to the mixture (lignin and THF). The solution was mixed for 15 min at room temperature (200 rpm) and then was poured into aluminum pans (40 mm diameter, 10 mm height). For some samples, the mixture of both organic UV absorber and HALS was used, as recommended by the additives manufacturers. The mixtures of inorganic UV absorbers in lignin-THF were placed in a sonication bath for 10 min to ensure their homogenous dispersions. Minex, a functional filler made from nepheline syenite, that is used as a performance enhancer for brightness, weathering stability, abrasion, and burnish resistance in coating

formulations, was also added to the lignin as an additive. The control sample (lignin, without any additives) was also dissolved in THF to obtain a uniform and smooth surface similar to other samples. Later, all samples were placed under a fume hood (with lights off for 24 hrs) to let the solvent evaporate (THF). Then the samples were kept in the dark place for one week at room temperature to ensure complete removal of solvent while avoiding any potential exposure to light that might trigger undesirable reactions of photoactive compounds. The names and compositions of all samples are shown in Table 20.

Table 20. Composition of prepared samples

ID	Sample Name	Role	Supplier
1	Tinuvin-1130	Organic UV absorber	BASF
2	Tinuvin-400	Organic UV absorber	BASF
3	Tinuvin-479	Organic UV absorber	BASF
4	Tinuvin-384	Organic UV absorber	BASF
5	Chiguard 5330	Organic UV Absorber	Chitec Technology
6	Tinuvin-292	Organic HALS[1]	BASF
7	Tinuvin-123	Organic HALS	BASF
8	Chiguard 101	Organic HALS	Chitec Technology
9	Tinuvin-5333	Organic UV absorber & HALS	BASF
10	Tinuvin-5248	Organic UV absorber & HALS	BASF
11	Tinuvin-479-123	Organic UV absorber & HALS	BASF
12	Tinuvin-292-1130	Organic UV absorber & HALS	BASF
13	Tinuvin-384-292	Organic UV absorber & HALS	BASF
14	Tinuvin-400-123	Organic UV absorber & HALS	BASF
15	Tinuvin-479-292	Organic UV absorber & HALS	BASF
16	Fe_3O_4[2]	Inorganic UV absorber	US Research Nanomaterials
17	Cerium oxide[2]	Inorganic UV absorber	Strem Chemical, Inc.
18	Zirconium oxide[2]	Inorganic UV absorber	US Research Nanomaterials
19	Zinc Oxide[2, 3]	Inorganic UV absorber	Zochem
20	Titanium oxide[2, 3]	Inorganic UV absorber	NYACOL Nano Technologies Inc.
21	Minex[3]	UV and binder stabilizer	Covia Canada Ltd.
22	Control (pure lignin)	----	Lignol (Current Suzano)

[1]HALS= Hindered amine light stabilizer

[2]Nanosized pigments

[3]Provided by the third-party supplier, and it is assumed were obtained from listed producers

UV Exposure

Photodegradation of the lignin mixtures was studied following the EN 927-6 Standard procedure.[248] The UVA-340 lamp (recommended by EN 927-6 Standard) manufactured by Q-Lab Corporation (Canada) was chosen for this study due to its similar spectrum to sunlight (Table 21). All samples were placed under UV light irradiation at a 5 cm distance from the lamp for 35 days. UV exposure was run in ambient conditions (24 °C, 70-80 RH%, and air atmosphere). There were not any dark periods during the UV exposure, except for brief sample collections. Because powdered lignin was used during the test, the samples were not exposed to water during the photodegradation test.

Table 21. Relative spectral irradiance of UV-A 340 lamp

Wavelength (nm)	Relative Spectra Irradiance %
$290 < \lambda \leq 400$	100
$\lambda \leq 290$	0.0
$290 < \lambda \leq 300$	0.2
$300 < \lambda \leq 320$	6.2 to 8.6
$320 < \lambda \leq 340$	27.1 to 30.7
$340 < \lambda \leq 360$	34.2 to 35.4
$360 < \lambda \leq 380$	19.5 to 23.7
$380 < \lambda \leq 400$	6.6 to 7.8

Lignin Characterization

The pure lignin and mixture of additives and lignin samples were analyzed with Fourier-transform infrared spectroscopy (FTIR) before UV irradiation and then every week during 35 days of UV irradiation. A Jasco FTIR-ATR-6600 equipped with an attenuated total reflection accessory (ATR) was used to monitor potential chemical changes of samples because of the photodegradation

reaction. Spectra were recorded in a wavenumber range between 500 and 4000 cm^{-1} at a resolution of 4 cm^{-1} with 64 scans. All spectra were normalized and baseline-corrected before quantitative analysis using OriginPro 2015 software (version 2.214). The spectra were normalized by selecting the C-H deformation band at 2921 cm^{-1} as a reference since its intensity remained the same during UV exposure. Linear background correction in the absorbance mode was applied to remove any potent background compound. The same procedure was applied for selected bands (aromatic skeleton or carbonyl), which are expected to change during the UV exposure. The lignin and carbonyl indexes were calculated by dividing the absorbance of a specific band (after background correction) by the absorbance of the C-H band (the unchanged band used as reference). The glass transition temperature, molar mass distribution, and hydroxyl content of lignin before and after 35 days UV irradiation were measured according to the procedures discussed in Chapter 2.

Results and Discussion

Lignin Degradation

To confirm that the lignin structure was not changed after dissolving it in THF and solvent was entirely removed, the sample was analyzed with ^{31}P NMR. The analysis showed that the drying method was effective with no residual THF in lignin (based on quantitative data). No change in lignin structure was observed compared with spectra of original lignin before dissolving it in THF. FTIR spectroscopy was used to monitor chemical changes of lignin (with and without additives) before UV irradiation and at weekly intervals over 35 days of UV irradiation. Table 22 shows different assignments of FTIR bands in lignin. The C=C stretching vibrations of aromatic rings, which have an absorption band at 1508 cm^{-1}, were considered as the lignin bands [249]. The carbonyl groups showed an absorption band at 1714 cm^{-1}, which moved to 1735 cm^{-1} after UV exposure that was assigned to formed quinone groups [250]. The wide absorption band around 3400 cm^{-1} was

assigned to hydroxyl groups.[251] The FTIR spectra of pure lignin before and after each week of UV irradiation are shown in Figure 22.

Table 22. Summary of the major FTIR peaks of the organosolv lignin.

Wavenumber (cm^{-1})	Band Assignment
3414	O-H stretching
2925	C-H stretching
2842	C-H stretching
1714	C=O stretching
1508	Aromatic skeletal vibration
1182	Guaiacyl C-H

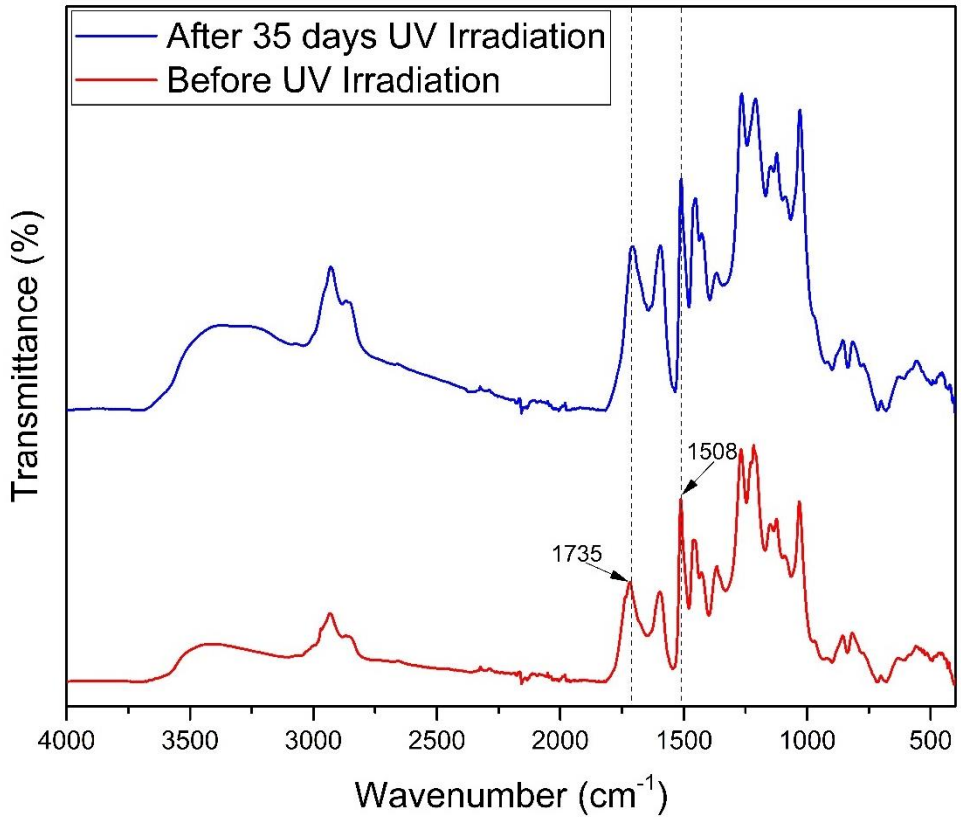

Figure 22. FTIR spectra of pure lignin sample (control) before and after 35 days of UV-irradiation, 1508 cm^{-1}, vibrations of aromatic rings; 1735 cm^{-1}, vibration of carbonyl groups

All spectra were baseline corrected and normalized using the band at 2921 cm^{-1} as reference band, which was not affected by photodegradation.[252] Two parameters were used to monitor potential photodegradation of lignin: I $\frac{1508}{2921}$ and I $\frac{1735}{2921}$, corresponding to lignin and carbonyl indices, respectively, where "I" represents the measured intensity from the top band to the baseline.[252]

$$\text{Lignin index} = \frac{A\,1508}{A2921}$$

$$\text{Carbonyl index} = \frac{A\,1735}{A2921}$$

Different indices of pure lignin at different UV irradiation times are displayed in Figure 23. The lignin content decreased rapidly as a result of photodegradation, which was accompanied by the formation of carbonyl groups.[253] It can be seen that with the increase in exposure time, lignin index (I 1508/2921) decreased as a result of the decreased amount of aromatic rings during the photodegradation phenomenon, as also confirmed by previous studies.[250, 254] On the contrary, carbonyl index (I 1735/2921) increased due to ortho and para-quinoid formation forming as free radicals react with oxygen forming carbonyl and carboxylic groups.[214, 255, 256] The results showed that the rate of carbonyl formation significantly increased after 21 days of UV irradiation.

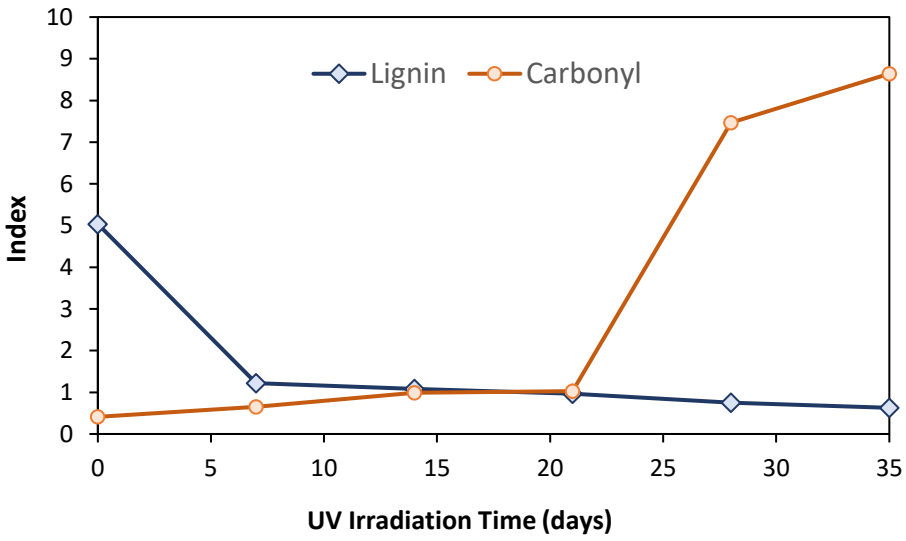

Figure 23. Lignin and carbonyl indices of pure lignin at different UV irradiation times.

Table 23 shows the properties of pure lignin before and after 35 days of UV irradiation. The molecular weight of lignin increased after UV irradiation. This enhancement may be related to radical coupling reactions, causing the formation of higher molecular weight compounds such as condensed phenyl propane structures like 5-5, 4-*O*-5, and *β*-5.[257, 258] Also, the

polydispersity index (PDI) of lignin was increased significantly, which is probably due to depolymerization and repolymerization of lignin polymeric chains under UV light.[259, 260] The T_gs of lignin increased from 93 °C to 122 °C after UV exposure. The increase in T_g is reported to be due to the formation of polar groups, such as carbonyl during UV irradiation, confirmed by FTIR data.[261, 262]

Table 23. Summary of the measured lignin properties before and after 35 days of UV irradiation.

Lignin Properties	Before	After 35 days of UV Irradiation
Mn (Da)	1190	1290
Mw (Da)	5250	7050
PDI	4.4	5.5
T_g (°C)	93 ± 2	122 ± 3
Aliphatic Hydroxyl (mmol/g)	1.31	1.04
Phenolic Hydroxyl (mmol/g)	2.39	1.99
Carboxylic Acid (mmol/g)	0.42	0.68

Figure 24 illustrates the ^{31}P NMR spectra of lignin before and after UV irradiation. The aliphatic and phenolic hydroxyl functional groups of lignin decreased by 21% and 17%, respectively, after UV exposure, while the carboxylic groups increased by 62%. The decrease in aliphatic and phenolic hydroxyl groups could be related to the formation of quinone structures, whereas an increase in carboxylic acid functional groups could be due to the ring-opening of quinone compounds.[263]

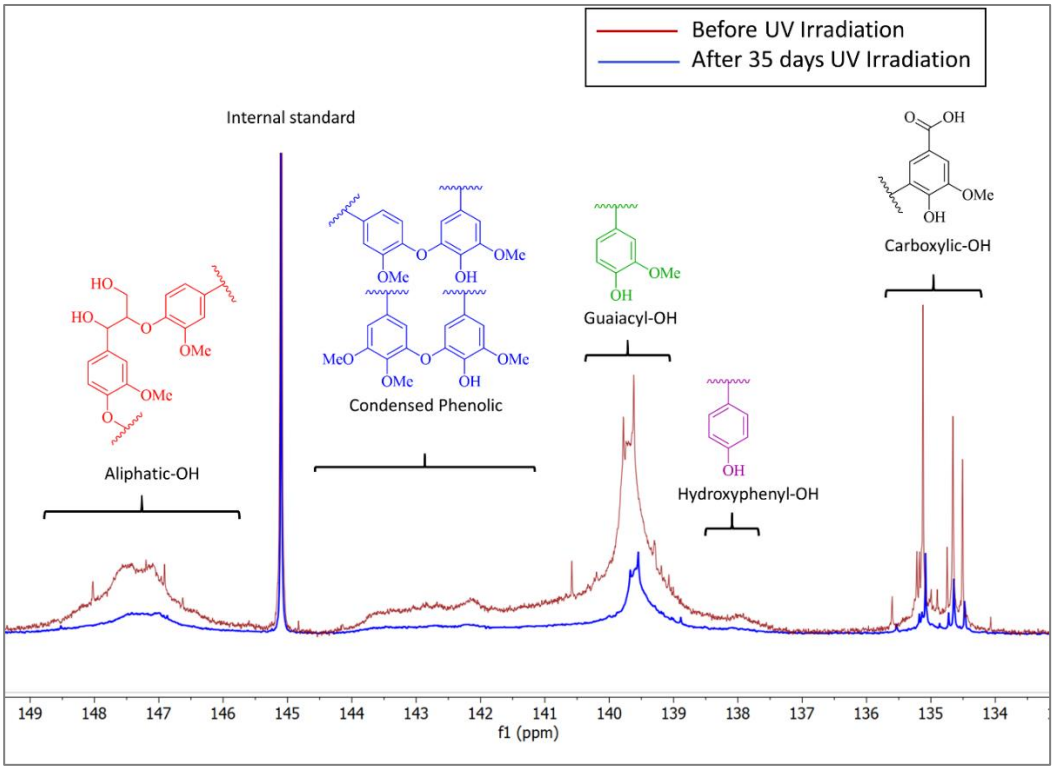

Figure 24. ^{31}P NMR spectra of lignin before(red) and after 35 days of UV irradiation (blue)

Efficacy of Different Additives on Improving UV Stability of Lignin

Figure 25 shows the percent decrease of the lignin index $(\frac{A\ 1508}{A2921})$ as a measure of lignin loss. Pure lignin (control) showed the highest decrease (85%), and the sample containing 2 wt.% cerium oxide had the lowest lignin loss (28%), possibly due to its excellent UV absorption capacity, as also indicated by Dao et al. [264] Additionally, samples containing a mixture of organic UV absorber and HALS (T-479/T-292, T-5248, and T-5333) illustrated lower lignin loss than other additives.

The average lignin loss of organic UV absorbers (65%) was significantly lower than the average lignin loss of HALSs (74%) and other additives (78%). The combination of organic UV absorbers and HALSs showed 58% lignin loss, which is remarkably lower than using them individually. Overall, inorganic UV absorbers (56%) were more effective in reducing lignin loss than a mixture

of organic UV absorbers and HALSs (UV absorbers 65% and HALSs 74%) and other additives (78%). Also, using a mixture of both organic UV absorbers and HALSs were more effective in reducing the photodegradation of lignin (58% lignin loss) than using individual components. When they are used together, UV absorber helps to absorb UV light, and HALS captures any free radicals that form during exposure resulting in reducing the UV degradation of lignin.[265]

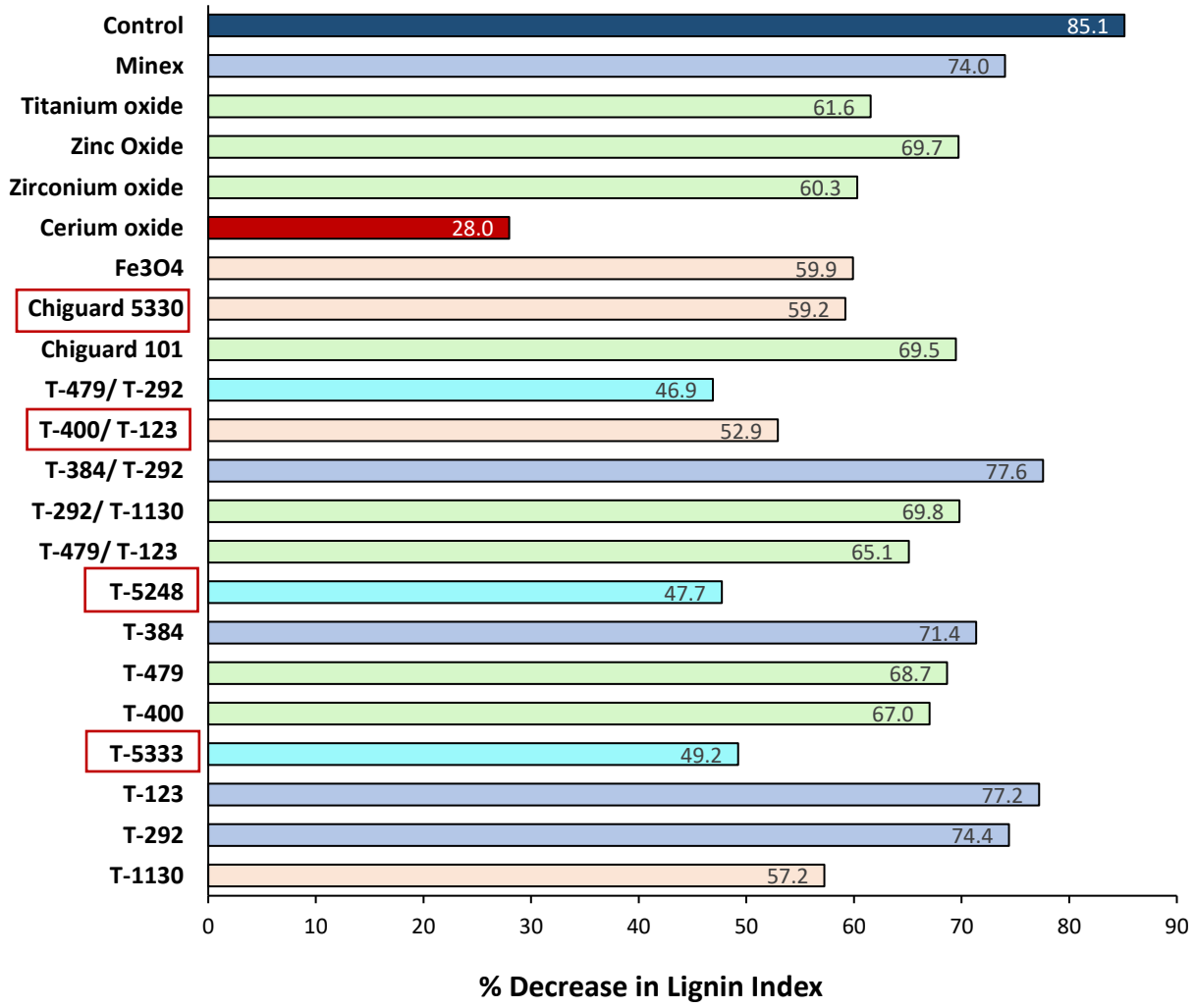

Figure 25. Decrease in lignin index (%) ($\frac{A\ 1508}{A2921}$) of various samples after 35 days of UV irradiation (lower numbers are better), the bars with the same color are not significantly different (α=0.05).

When lignin undergoes photodegradation, quinone groups, which have two carbonyl groups, are formed. Therefore, the photodegradation of lignin will increase the number of carbonyl groups in the lignin. As such, the carbonyl index of all samples increased after 35 days of UV irradiation (Figure 26). Among tested additives, the organic UV absorber (T-479), zinc oxide, and to some extent, cerium oxide proved to be the most effective additives in protecting lignin, which resulted in lower carbonyl group formation. It was shown that zinc oxide could quench free radicals and acts as a radical scavenger.[266, 267] UV absorbers filter the high-energy UV spectrum while radical scavengers neutralize high-energy and destructive free radicals. Therefore, when organic UV absorbers and HALSs were used together, the UV protection was significantly improved compared to using each additive individually.

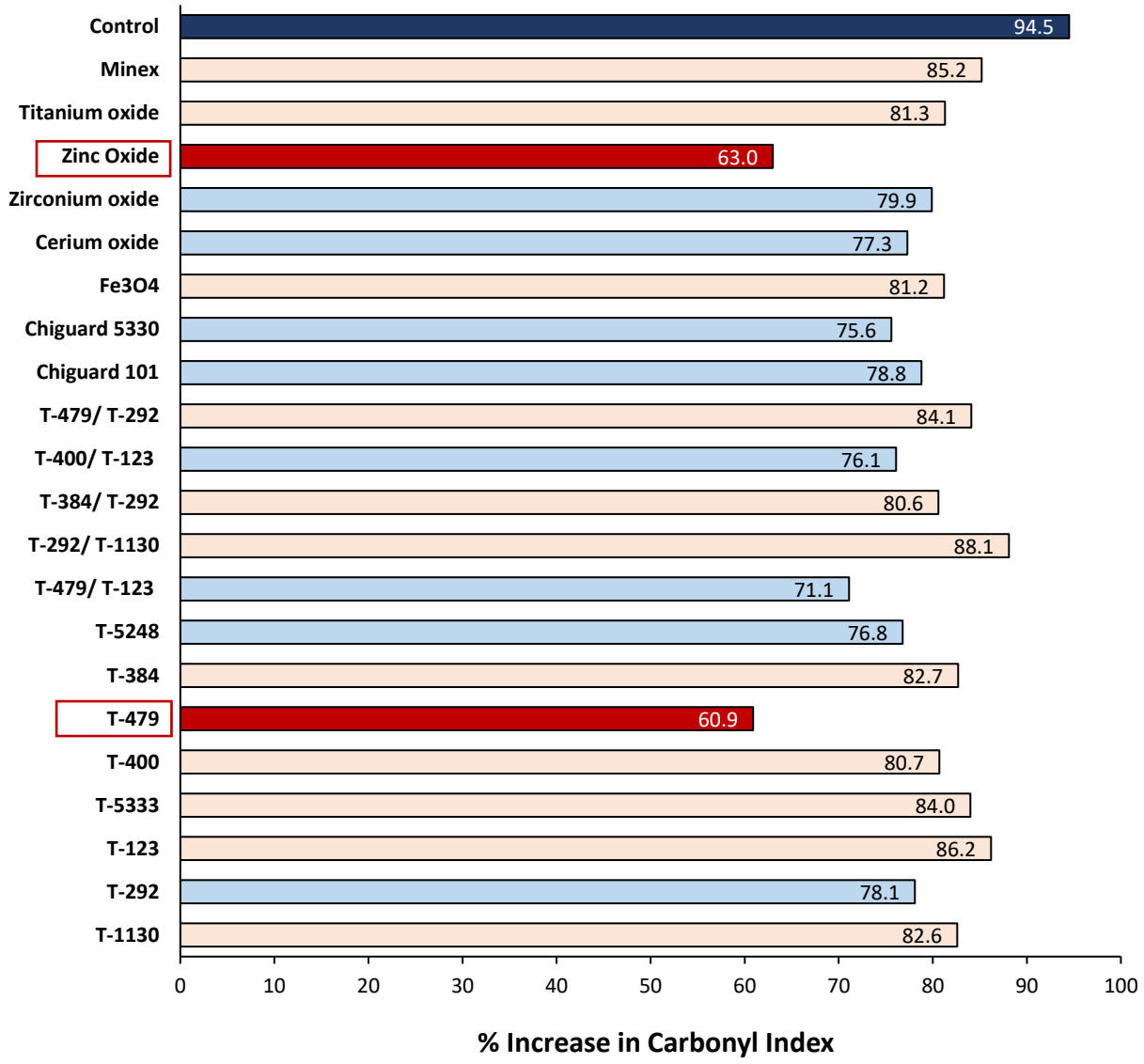

Figure 26. Increase in carbonyl index (%) ($\frac{A\ 1735}{A2921}$) of different samples after 35 days of UV irradiation, (lower numbers are better), the bars with the same color are not significantly different (α=0.5).

In this study, lignin was used as a model compound to evaluate the efficacy of a wide range of light stabilizer additives used in coatings. It was observed that zinc oxide and a mixture of organic UV absorber/HALS were the most effective additives for increasing the photostability of lignin. It was assumed that these additives can potentially increase the UV stability of wood when added to

coating formulations designed for exterior applications. Although other wood components, especially extractives, can also play a role in photodegradation of wood, reducing structural degradation of lignin which absorbs 80-95% of UV-light,[214] is a good starting point in choosing the right additives for formulating clear wood coatings. It is important to point out that the organosolv lignin used in this study has a different structure than native lignin in the wood. It is indisputable that any isolation process will change the structure of lignin; therefore, the additives that have worked in this study might not have the same interaction effect with the lignin on the surface of the wood. That is why the effectiveness of these best-performing additives are being studied (by authors) when added into different resins (alkyd, acrylic, and polyurethane). The performance of coated-wood samples will be monitored during exposure to a combination UV and rain (accelerated weathering).

Some of these additives can still protect the wood surface without chemically bonding with lignin. They can reduce the UV degradation of wood by shielding (dispersion or absorption) the UV light or acting as radical scavengers to capture the formed radicals. Panel et al. [268] reported that the combination of UV absorber and HALS was the most effective treatment for color stabilization of wood in exterior applications. Since similar results were found, studying lignin degradation as a simpler structure than wood seems to be a reliable method to evaluate the performance of newly developed light stabilizers.

6.2 APPENDIX B (Epoxy HNT)

Improving UV-Stability of Epoxy Coating Using Encapsulated Halloysite Nanotubes with Organic UV-Stabilizers and Lignin

Published in Progress in Organic Coatings [269]

Abstract

Epoxy coatings are used in a wide variety of applications due to their excellent chemical, thermal, and mechanical properties. However, their susceptibility to UV degradation has limited their use in exterior applications. Usually organic UV absorbers and stabilizers are added to epoxy systems to improve theirs UV stability, but their performance decreases over time due to the degradation and loss of organic UV-stabilizers. In this study, a novel method was developed to encapsulate organic UV stabilizers and lignin (as a natural UV absorber) into halloysite nanotubes (HNTs). To ensure successful encapsulation, the pristine and filled halloysite nanotubes were characterized quantitatively using thermogravimetric analyzer (TGA), and qualitatively with X-ray photoelectron spectroscopy (XPS). Then, encapsulated nanotubes (HNTs) were added to an epoxy system (1-3 wt%) and their efficacy was evaluated before and after 840 hours of accelerated weathering. Changes in physical, chemical, and thermal properties of coatings were measured using a spectrophotometer, field emission scanning electron microscopy (FE-SEM), electron paramagnetic resonance spectroscopy (EPR), Fourier transform infrared spectroscopy (FTIR), and differential scanning calorimetry (DSC). The results showed that epoxy samples containing 2 wt% HNT-encapsulated with organic UV-stabilizers, and samples containing 1 wt% HNTs encapsulated with lignin had significantly higher UV stability than epoxy resin prepared with the same concentration of these individual components (UV-stabilizers or lignin). This study

demonstrates the efficacy of encapsulated HNTs, with UV stabilizers or lignin, in improving UV stability and extending service life of epoxy coatings.

Keywords: UV stability, halloysite nanotubes, encapsulation, lignin, epoxy

Introduction

Epoxy coatings are widely used in various applications due to their excellent chemical and thermal resistance and their outstanding adhesion to different substrates (metals, woods, and plastics).[270-272] However, in outdoor conditions, these coatings degrade as a result of exposure to UV light. The UV degradation causes chalking, delamination, and discoloration while also negatively affecting the gloss, hardness, and surface roughness of coatings.[273, 274] Although only 5% of the total solar UV radiation reaches the earth's surface (280-400 nm), its high energy can easily induce the formation of free radicals, causing chain scission and secondary oxidative reactions of polymeric chains.[275, 276] Aromatic and ether groups in epoxy resin are photo-initiating sites that are more susceptible to UV degradation.[277] Therefore, one of the main challenges in the coatings industry is to formulate transparent epoxy coatings with exceptional UV stability for exterior applications. To increase the UV stability of epoxy coatings, organic UV stabilizers (including UV absorbers and hindered UV stabilizers), as well as inorganic UV absorbers are added to epoxy formulations. UV-absorbers (UVAs) filter out the short and harmful wavelengths of light before they reach the polymeric chains. UVAs can be categorized into two main groups; 1) benzotriazoles (2-(2-hydroxyphenyl)-benzotriazole) with two absorption peaks at 300 and 350 nm, and 2) hydroxyphenyl triazines (2-hydroxyphenyl-s-triazine), which are newer and have two strong absorption peaks at 300 and 340 nm.[237, 278] Currently, 2-(2-hydroxyphenyl)-benzotriazoles are commonly used as organic UV-absorbers in transparent coating formulations.[232] Most transparent coating formulations contain hindered amine light stabilizers (HALSs), which interact with

radicals and decrease the photooxidative degradation of polymers.[239, 279] Due to high vapor pressure, leaching, and chemical loss by photochemical reactions, the concentration of organic UV stabilizers (both UVAs and HALSs) decreases over time, which reduces their efficacy in service.[237, 238] One way to avoid leaching is to chemically bond UV-absorbers to the resins,[280, 281], which will hinder their migration towards the surface. However, this approach limits the performance of UV stabilizers and requires specific absorbers for each individual resin formulation. Metal oxides are also used as inorganic UV absorbers that can scatter or absorb light. Nanosized metal oxides (<100nm) like zinc and titanium oxide, as well as nano-silica, are commonly used in clear coating formulations.[241, 282-286] Although inorganic UV absorbers are more permanent, they are less efficient than organic UV stabilizers.[287]

Lignin, the most abundant natural aromatic polymer in the world, constitutes 15-35 wt.% of the wood and other plant biomass.[288] Lignin is a natural UV absorber with excellent radical scavenging and antimicrobial properties.[289] However, difficulty in the synthesis and homogeneous dispersion of lignin nanoparticles into coatings,[290, 291] has limited its application at the industrial level.

Encapsulation of UV stabilizers and lignin could be used to potentially solve their weaknesses and in increases their efficiency. To increase the photostability performance of acrylic coatings, Quenant et al.[292] found that the addition of encapsulated poly (methyl methacrylate) microcapsules with UV stabilizers (both UV absorber and HALS) improved the mechanical properties and reduced the discoloration of coated-wood samples after exposure to artificial weathering. Halloysite nanotubes (HNTs) can be used as effective nanocarriers for the encapsulation, and controlled release of chemical and biological compounds, owing to their biocompatible nature as well as their tubular shape.[293] HNTs, natural clay nanoparticles, are nontoxic and have high surface areas.[294, 295] HNTs have been frequently used as additives in epoxy, polyamide, and styrene-

butadiene rubber resins, due to their ability to improve the chemical, thermal, and mechanical properties of composite materials.[296] One study showed that the addition of pristine HNTs to the polylactide resin resulted in a significant decrease in the chemical and physical properties of the coating system after 300 hours of artificial weathering.[297] In another study, the addition of modified HNTs with a surfactant into a polystyrene formulation resulted in improving the UV stability of the resins.[298] Hu et al.[299] showed that immobilization of zinc oxide nano-protrusions on the HNTs' surface, improves the UV shielding performance of nanocellulose films. Another study investigated how zinc oxide immobilization on HNTs affects the photo stability of poly (lactic acid) after 60 days of artificial weathering.[300] It was found that HNT-ZnO nanocomposites showed less discoloration and higher photostability compared to pristine HNT nanocomposites.[300] To the best of our knowledge, there is no study on the encapsulation of organic UV-stabilizers or lignin into HNTs to improve the UV stability of polymers.

The main objective of this study was to examine the UV stability of epoxy resins after the addition of halloysite nanotubes loaded with UVA/HALS or lignin. It was supposed that encapsulation of organic UV stabilizers in HNTs could be an effective method to preserve them in the system. Moreover, it was hypothesized that lignin could potentially serve as an excellent UV absorber by encapsulation. The goal was to improve the efficacy of these organic UV stabilizers and lignin by encapsulating them into a natural nanotube that can easily be added to any transparent coating formulations to extend their exterior service life.

Experimental

Materials

Halloysite nanotubes with the trade name “Hallo Pure” were supplied by I-Minerals Inc. Liquid diglycidyl ether of bisphenol A (Epon Resin 828) with epoxy equivalent weight of 185-192 g/eq was supplied by E.V. Roberts. Isophorone diamine (IPDA) and acetone were purchased from Fisher Scientific Co. UVA T1130, and HALS T292 were provided by BASF. Hardwood organosolv lignin was kindly supplied by Fibria (Lignol), Vancouver, Canada.

Figure 27 shows SEM and TEM images of pristine HNTs at different magnifications. Matauri Bay (MP) HNTs generally include short and stubby tubes with lengths ranging from 100 nm to 3 µm; some long and thin tubes were also observed. As shown in Figure 27, HNTs clump together. The morphological characteristics of HNTs are presented in Table 24. They have tubular shapes, with inner diameters of 15-70 nm and outer diameters of 50-200 nm. The chemical composition is based on $Al_2Si_2O_5(OH)_4$. The surface area of MB HNTs is around 22.10 m^2/g, which is less than other types of HNTs such as patch (PT), Dragonite (DG), and Camel Lake (CLA)).[301]

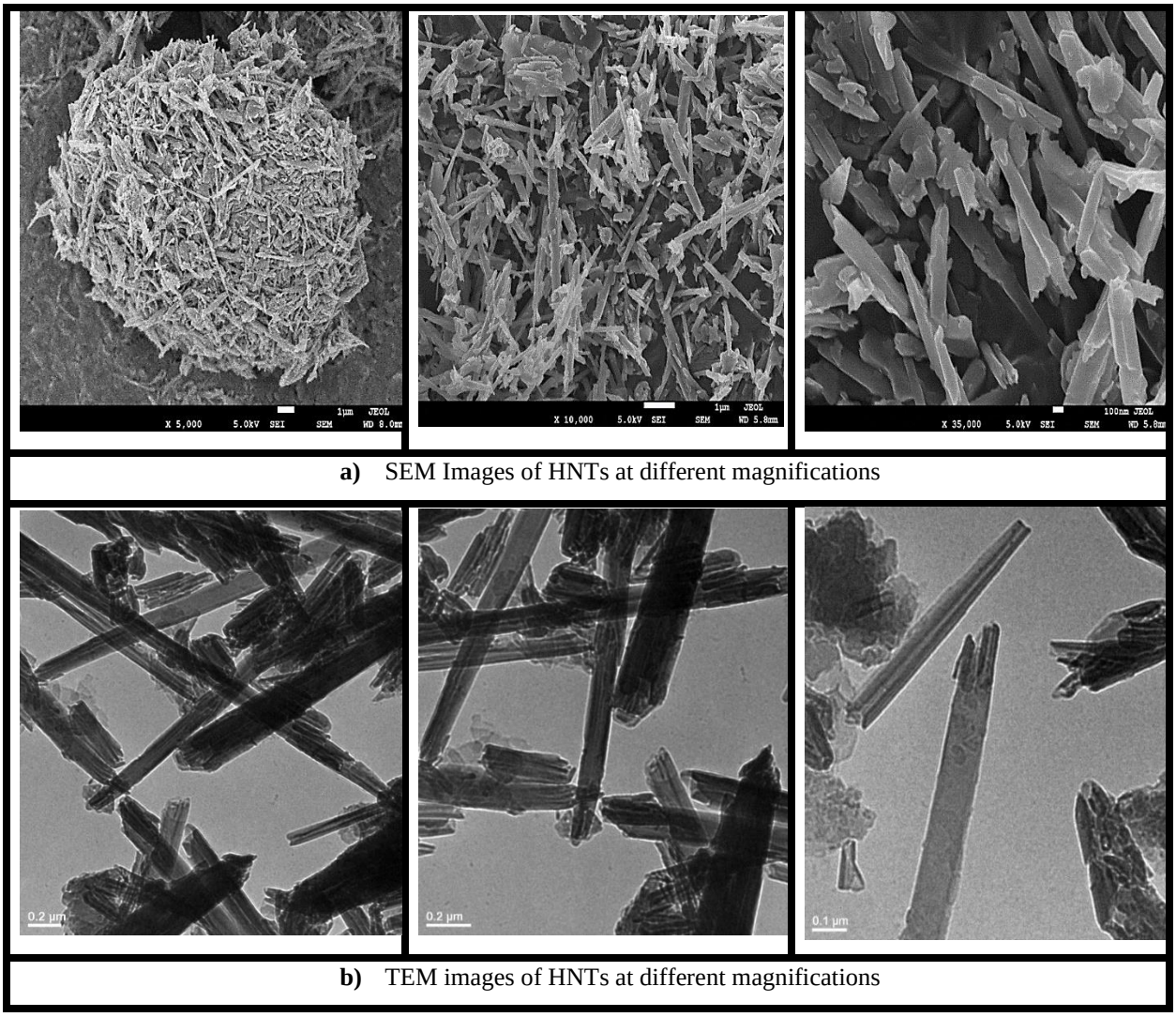

a) SEM Images of HNTs at different magnifications

b) TEM images of HNTs at different magnifications

Figure 27. (a) SEM and (b) TEM images of pristine HNTs with increased magnifications (left to right)

Table 24. Morphological characterization of halloysite nanotubes (HNTs) [301]

HNT-Type	Dominant Particle Shapes	Length (nm)	Inner Diameter (nm)	Outer Diameter (nm)	Aspect Ratio (L/D)	Empirical Formula
Matauri Bay (MB)	Tubular	100−3000	15−70	50−200	12	$Al_2Si_2O_5(OH)_4$

Methods

Encapsulation of HNTs with Organic UV Stabilizers and Lignin

A 400 mg/mL solution of UVA T1130/ HALS T292 (1:1 weight ratio) or lignin was prepared in acetone. T1130 is an organic UV absorber based on hydroxyphenyl benzotriazole, and T292 is a liquid HALS that is widely used for coatings and contains two active compounds, including bis (1, 2, 2, 6, 6-pentamethyl-4-piperidyl) sebacate and methyl 1, 2, 2, 6, 6-pentamethyl-4-piperidyl sebacate. The mixture of UVA/HALS was used based on the manufacturer's recommendation (according to a filed provisional patent) [302]. Acetone was selected as a non-VOC solvent, and it has a low surface tension (25.2 mN/m at 20 °C) [303] can easily solubilize organosolv lignin. Then, 0.6 g HNTs were added to the solution of UVA/HALS, or lignin and acetone and mixed for 48 h at room temperature. Next, the suspension was subjected to a vacuum for 5 min at 76 kPa, until there were no air bubbles coming off from the surface of the solution. This indicated the highest loading (complete encapsulation), which occurs when all the air is removed from inside the nanotubes, and the voids are filled with a solution of UVA/HALS or lignin and acetone. Then, the suspension was centrifugated (5000 rpm for 5min), and the loaded HNTs were washed three times with acetone and with excess DI water to remove any potential residual UVA/HALS or lignin from the surfaces of the HNTs. Figure 28 shows different steps involved in the encapsulation process.

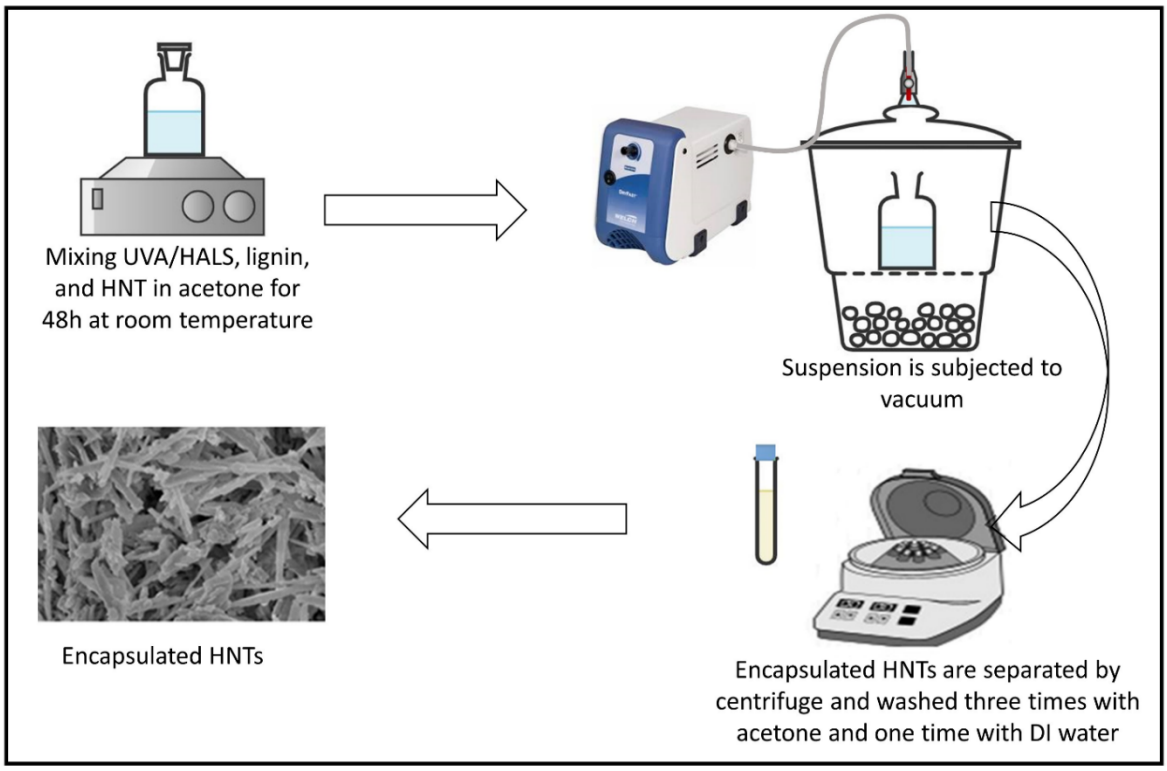

Figure 28. Schematic of HNT-encapsulation process (both UVA/HALS and lignin systems)

Preparation of HNT-Epoxy Nanocomposites

Twelve different sets of samples were prepared as presented in Table 25. To prepare samples containing HNTs, specific amounts of HNTs (1 wt.%, 2 wt.%, or 3 wt.%) were added to the epoxy resin. Then, benzyl alcohol was added as a viscosity reducer (1:10 mass ratio) to improve the dispersion of HNTs into the epoxy resin formulations. Afterward, the resin was placed in a sonication probe at 50% amplitude for 5 min, followed by an ultrasonication bath for 30 min at room temperature (to homogenously disperse HNTs into the epoxy matrix). Further, a curing agent was added (0.22 g IPDA to 1 g epoxy resin) to the solution, and mechanically mixed for 1 min, and later placed in an ultrasonication probe for 2 min. For control samples (without HNTs), the specified amount of epoxy resin, curing agent, benzyl alcohol, and additives (either a pure mixture of UVA/HALS, or lignin) were mixed using a digital overhead stirrer (Caframo) for 2 min at 500

rpm. The mixture was poured into an aluminum pan (10 cm diameter and 0.5 cm height) and heated in an oven at 60 °C for 2 hours (as recommended by the supplier of the epoxy resin). Based on the manufacturer's recommendation, all samples were kept in the dark environment for 7 days at room temperature before further analysis, reaching maximum crosslinking density and preventing potential unwanted reactions of photoactive compounds in the epoxy system.

Table 25. Composition of prepared samples

Sample ID	Type of Additive	Amount of Additive (%)
Epoxy	None	-
UVA/HALS	UVA T1130 and HALS T292 (1:1)	2
Lignin	Hardwood organosolv lignin	2
1% Pristine HNTs	Pristine HNTs	1
2% Pristine HNTs	Pristine HNTs	2
3% Pristine HNTs	Pristine HNTs	3
1% HNT- UVA/HALS	UVA/HALS loaded into HNTs	1
2% HNT-UVA/HALS	UVA/HALS loaded into HNTs	2
3% HNT-UVA/HALS	UVA/HALS loaded into HNTs	3
1% HNT-lignin	Lignin loaded into HNTs	1
2% HNT-lignin	Lignin loaded into HNTs	2
3% HNT-lignin	Lignin loaded into HNTs	3

Characterization

The photostability of the prepared coating samples were evaluated before and after accelerated weathering in a QUV machine (source: UVA 340 nm) at an irradiance of 0.68 W/m^2 with a chamber temperature of 60 °C. The samples were exposed to UV irradiation for a period of 35

days (840 hours) without condensation or a water spray cycle. The samples were evaluated before and after exposure to UV irradiation.

Field emission scanning electron microscopy (JEOL JSM 7500 F) was used to evaluate the morphology of the HNT samples, as well as to study the effect of HNT samples on the UV stability of epoxy coatings. HNTs and epoxy samples were respectively coated with iridium and gold to increase their conductivity for SEM. Also, a small amount of HNTs were dispersed in a methanol solution, and one drop of the mixture was placed into a TEM grid (carbon film 200 mesh, copper) and heated in a vacuum oven at 50 °C prior to TEM (JEOL, JEM-2200FS) analysis. To quantify the loading of organic UV stabilizers and lignin, in the HNT samples, thermogravimetric analysis (TGA) was used. The samples were run from 30°C to 800°C with a heating rate of 10 °C/min, under a nitrogen flow of 25 mL/min for the sample, and 10 mL/min for the balance (TGA TA, Q50). X-ray photoelectron spectroscopy (XPS) and x-ray diffraction (XRD) were used to ensure that the loading of UVA/HALS or lignin into HNTs did not change the structure of the HNTs. The color of the epoxy films, before and after UV exposure was monitored using a spectrophotometer (CM-2300d- Konica Minolta) in SCE mode. The L*a*b* color space before and after 35 days of UV irradiation was quantified to study the effects of UV light exposure on the color change of epoxy coatings.[304]

Electron paramagnetic resonance (EPR) spectroscopy was carried out on small slices of epoxy samples, with a 0.9 mm in thickness, 1 mm wide, and 30 mm long at X-band, on a Bruker E-680X spectrometer equipped with an SHQE–W1 resonator. The resonator was flushed with nitrogen gas during the measurements to maintain the ambient temperature and remove oxygen. Continuous-wave (CW) EPR spectra were detected under non-saturating conditions with 0.5 mW incident microwave power, a microwave frequency of 9.87 GHz, magnetic field modulation with 0.4 mT

amplitude, and 100 kHz frequency, and a data conversion time of 163 ms. For *in situ* EPR experiments, all samples were irradiated by a UVC lamp (25 W) for 5 min. The optical fiber of the lamp was adjusted in front of an EPR resonator 2 cm from the sample probe. The number of radical centers in each sample was determined by double integration of the first derivative cw-EPR spectra preceded by a first-order polynomial baseline correction.

Samples were also analyzed with a Spectrum II PerkinElmer Fourier transform infrared spectrophotometer in attenuated total reflectance mode (FTIR-ATR) to monitor possible chemical changes in epoxy resins, before and after UV exposure. The absorbance mode was used, with wavenumbers ranging from 400-4000 cm^{-1} with 4 cm^{-1} resolution and 32 scans. Glass transition temperatures (T_g) of epoxy samples were measured at different exposure times using a differential scanning calorimeter (DSC 6000, PerkinElmer). 7-10 mg of each epoxy sample was placed in an aluminum pan, and the samples were subjected to a heat/cool/heat cycle with a temperature range of 10-180°C, under a nitrogen flow of 40 mL/min, and a heating rate of 10 °C/min. The second heating curve was used to calculate the T_g.

Results and Discussion

The results of TGA and XPS analysis showed that the UVA/HALS or lignin were successfully loaded into halloysite nanotubes (HNTs). Thermogravimetric analyzer (TGA) was previously used by other researchers to determine the quantity of encapsulation of benzotriazole (as a corrosion inhibitor) into the HNTs as anti-corrosion coatings and salicylic acid (as a biocidal agent) as an antibacterial for food packaging.[305, 306] Five different samples, including (1) pristine HNTs; (2) UVA T1130 and HALS T292 (1:1 mixture); (3) hardwood organosolv lignin; (4) UVA/HALS loaded into HNTs; and (5) lignin loaded into HNTs, were analyzed using TGA. Since the thermal stability of UVA/HALS and lignin are much lower than that of pristine HNTs (due to their mineral

structures), the residual amount of loaded HNT samples were lower than that of pristine HNTs, at levels proportional to the amounts in the encapsulated samples.[306] The results of the TGA analyses are summarized in Table 26 (three replicates were run for each sample). The residual amount of pristine HNTs at 800 °C was around 80 wt.%, while the residual amounts of HNTs loaded with UVA/HALS and lignin were around 68 wt.% and 67 wt.%, respectively. This indicates that about 11 wt.% UVA/HALS and about 13 wt.% lignin were loaded into HNTs. TGA curves of pristine HNTs, a mixture of UVA/HALS, lignin, and loaded HNT samples are shown in Figure 29.

Table 26. Amount of UVA/HALS or lignin loaded into HNTs

Sample Code	% Residual at 800 °C	Loading Amount into HNT (%)
Pristine HNTs	80.5 ± 0.5	-
Mixture of UVA/HALS (T1130-T292)	1.6 ± 0.05	-
Lignin	0.2 ± 0.02	-
Encapsulated UVA/HALS in HNTs	68.1 ± 0.3	10.8 ± 0.2
Encapsulated lignin in HNTs	67.0 ± 0.3	13.3 ± 0.4

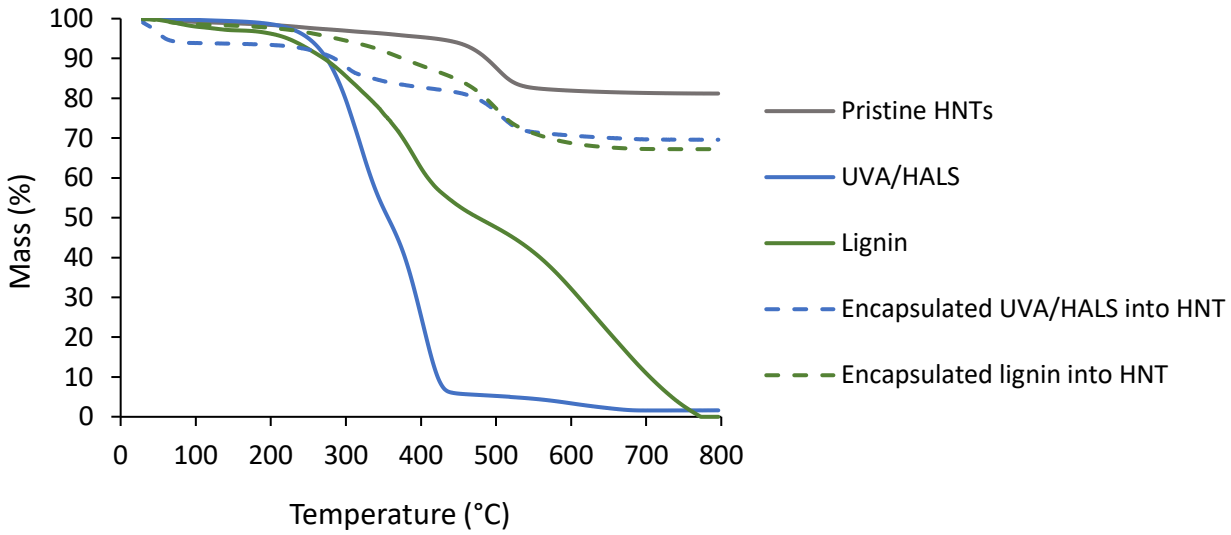

Figure 29. TGA curves of different samples (pristine HNTs, mixture of UVAT-1130/HALS-T282, pure lignin, pristine HNTs, encapsulated UVA/HALS in HNTs, and encapsulated lignin into HNTs)

The XPS analysis was conducted to qualitatively confirm the loading of UVA/HALS and lignin into HNTs.[305] The results of XPS analyses are presented in Table 27. Pristine HNTs are composed of oxygen, aluminum, and silicon. Also, carbon was observed in pristine HNTs, probably due to contamination of the surface.[307] The mixture of UVA/HALS contain C, O, H and N. Additionally, loading lignin into HNTs should significantly increase the carbon and oxygen content in encapsulated samples, because lignin contains around 60% carbon and 35% oxygen.[308] The presence of nitrogen, observed in the loaded UVA/HALS of HNTs, confirms encapsulation of UVA/HALS into HNTs, since only UVA/HALS contain nitrogen in their structures. In addition, for HNTs loaded with lignin, the composition of carbon relative to oxygen increased, which confirms the loading of lignin, as lignin structure contains mainly CHO.

Table 27. XPS analyses results of pristine HNTs and encapsulated samples showing successful encapsulation of UVA/HALS mixture and lignin in HNTs

Sample Code	C%	O%	Al%	Si%	N%
Pristine HNTs	31.11	43.02	6.91	18.96	-
Loaded UVA/HALS in HNTs	55.95	30.06	3.64	8.15	2.19
Loaded lignin in HNTs	61.17	28.88	1.57	8.39	-

Figure 30 illustrates the XRD spectra of three different samples (pristine HNTs, HNT-UVA/HALS, and HNT-lignin). There are two diffraction peaks, at $2\theta = 12.2°$ and $2\theta = 20.1°$, that are related to the 001 and 101 planes in HNTs, respectively. These peaks are attributed to HNTs' tubular morphology, high degree of disorder, small crystalline structures, and interstratifications of the layers with various hydration state [309, 310]. The structure of HNTs did not change after the

loading process since the main peaks of the HNTs are still present. After loading, the intensity and sharpness of some peaks decreased, which is possibly related to the loading of UVA/HALS or lignin into HNTs. Since they are both amorphous compounds, loading of UVA/HALS or lignin decreased the crystallinity of the HNTs.

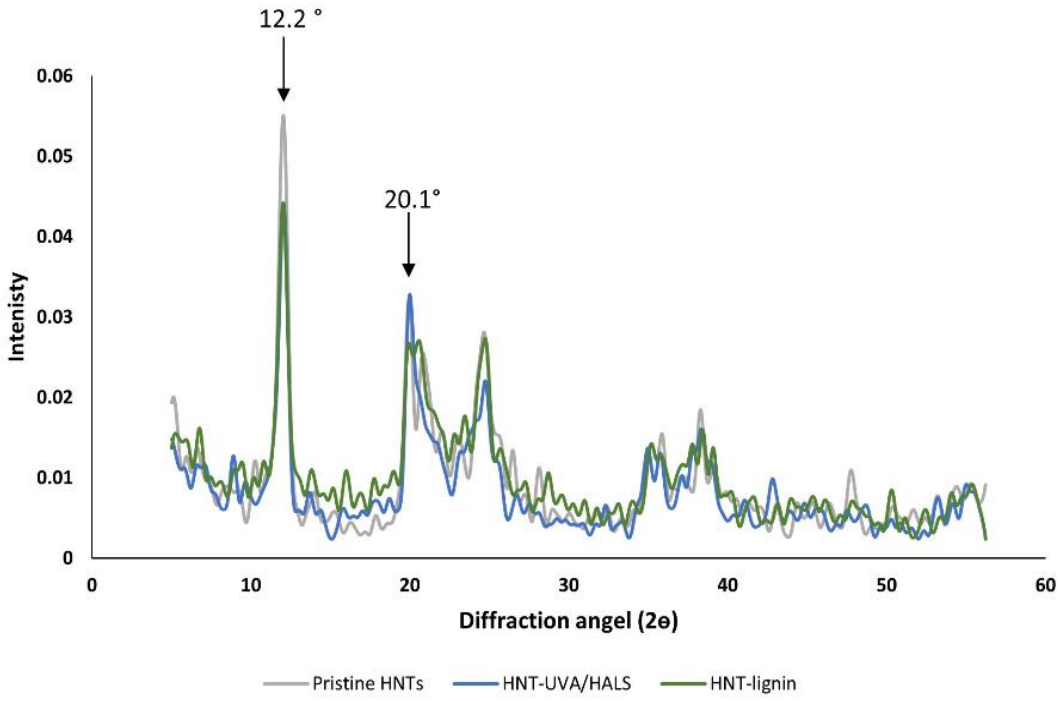

Figure 30. XRD diffraction patterns of the Pristine HNTs, HNT-UVA/HALS, and HNT-lignin

The color changes of the epoxy coatings are due to the increasing numbers of chromophores produced during UV irradiation. Color difference values (ΔE) for different samples after 35 days of UV irradiation are shown in Figure 31. The pure epoxy resin had the highest color change (ΔE=46), while the color change of epoxy resin with the inclusion of 2% pure UVA/HALS (mixture of UVA-T1130/HALS-T292) was 22. Even though the color change of epoxy resin with the addition of 2% lignin was very low (16), the sample was not necessarily more photostable. Rather, the low color change was due to the initial dark color of the lignin itself. By adding 1 wt.% HNT-UVA/HALS, the ΔE of the epoxy resin samples decreased from 46 to 22, which indicated

that the coatings became more photostable. Also, ΔEs of epoxy coatings filled with 1% HNT-lignin (2) and 2% HNT-lignin (6) (indicated using different shades of green) were significantly lower than epoxy resins with pure lignin (46). Hence, these two samples had the highest color stability among the different prepared coatings, even substantially greater than the samples containing the commercial organic UV stabilizers (UVA/HALS). Interestingly, ΔE of samples containing different ratios of pristine HNTs (1, 2 and 3%) (indicated using different shades of grey) are lower than color change of pure epoxy sample (Epoxy). This behavior may be related to the photocatalytic effects of HNTs interaction with the epoxy matrix after UV radiation exposure [304]. The images of some samples before and after 35 days of UV exposure are shown in Figure 32 which has same pattern to the color change data (ΔEs). It was seen that both pure epoxy and UVA/HALS samples underwent huge color changes. On the other side, both samples 2% HNT-UVA/HALS and 2% HNT-lignin showed less color changes.

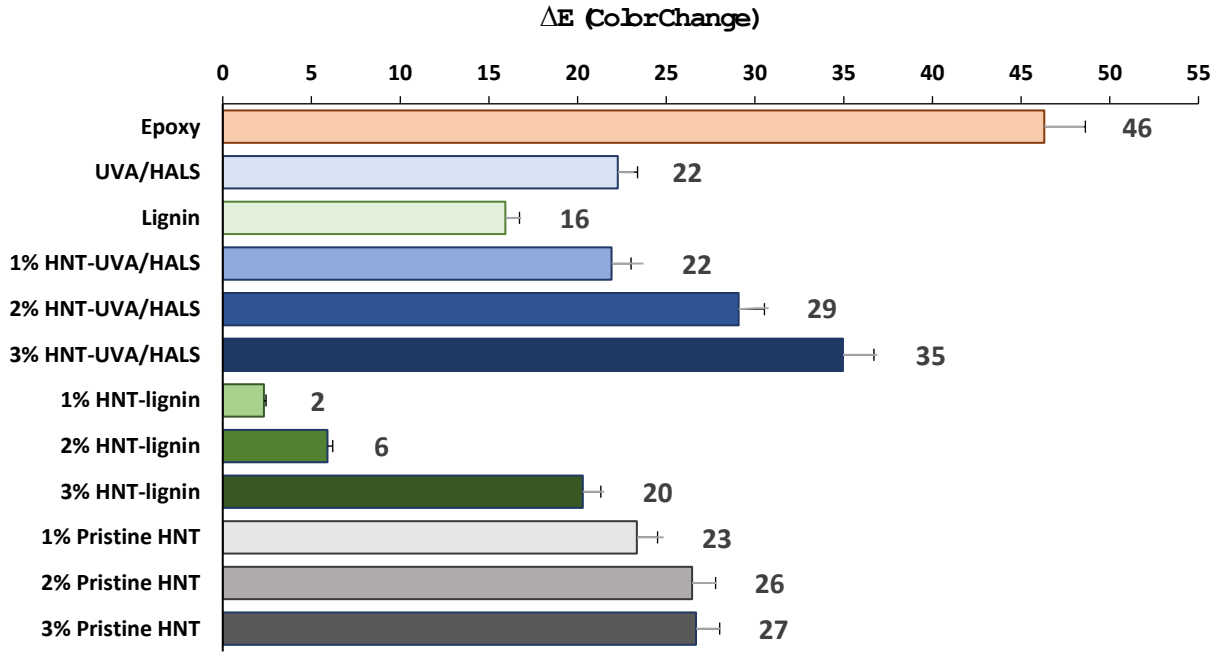

Figure 31. Variations of ΔE* for different samples after exposure to UV irradiation for 35 days (three replicates for each sample)

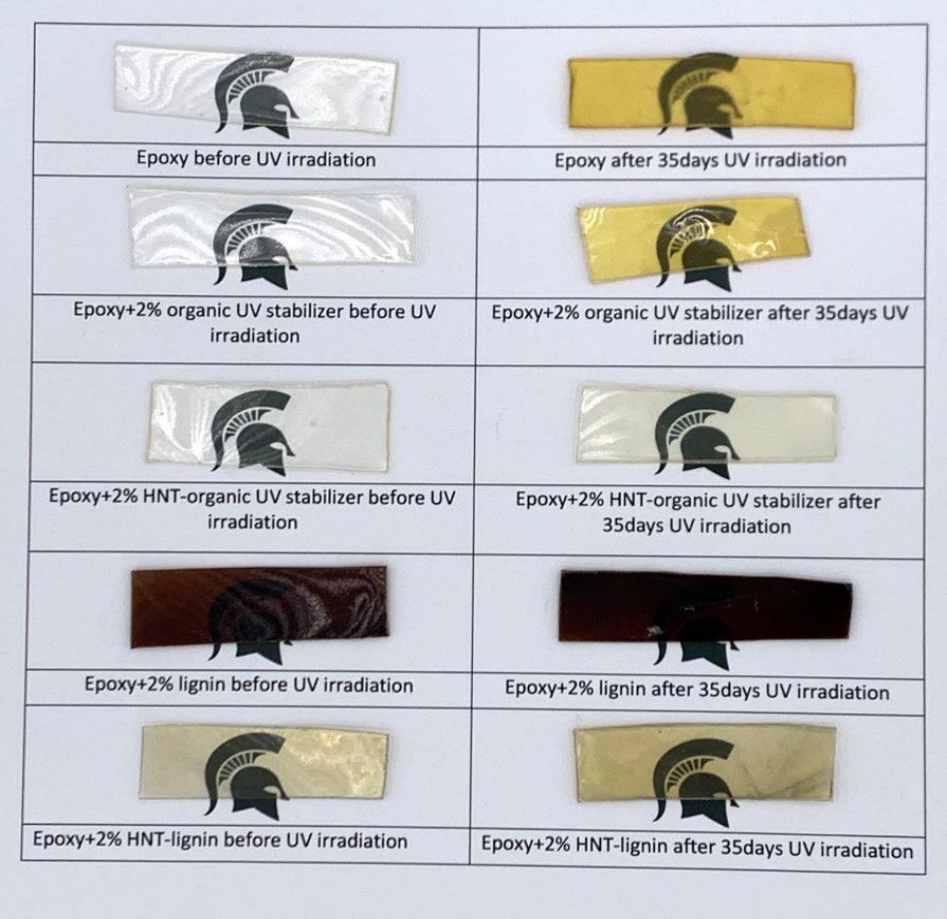

Figure 32. Photos of different epoxy samples before and after UV irradiation

Figure 33 shows FE-SEM micrographs of the pure, UVA/HALS, and lignin epoxy samples before and after 35 days of UV irradiation. After UV exposure, the pure epoxy sample degraded drastically. Several cracks appeared on the sample, and the surface became extremely uneven. This result may be related to the chemical decomposition of epoxy and the release of gases from the epoxy surface, as reported by a previous study [276]. Samples containing pure UVA/HALS (mixture of UVA-T1130/HALS-T292) or lignin showed some visible cracks on their surfaces after UV exposure. The number of cracks on the surface UVA/HALS sample was smaller than that in the

samples containing lignin, indicating that the UVA/HALS samples underwent lower degrees of photodegradation.

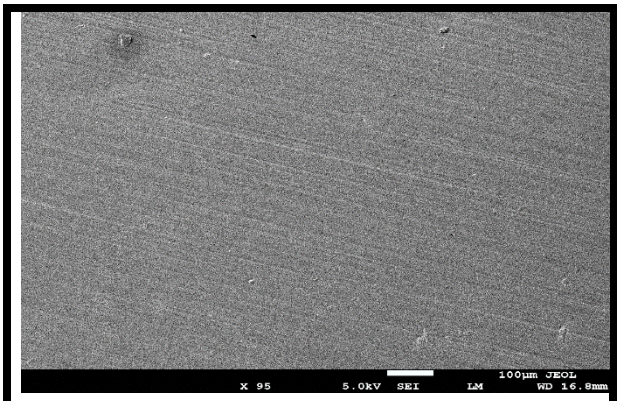

Pure epoxy-before

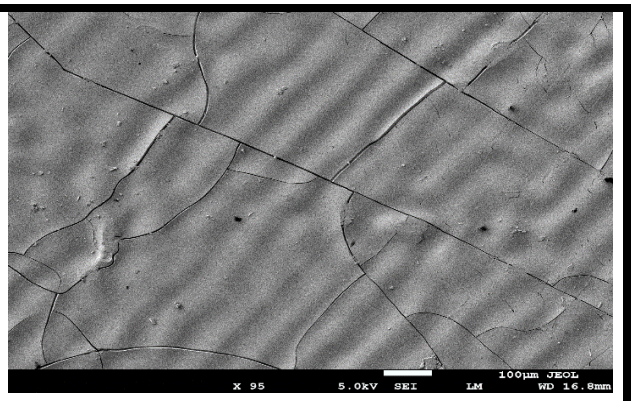

Pure epoxy-after 35 days

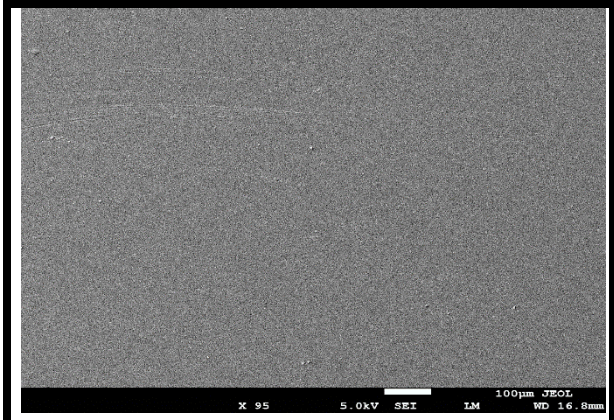

Epoxy with mixture of UVA/HALS-before

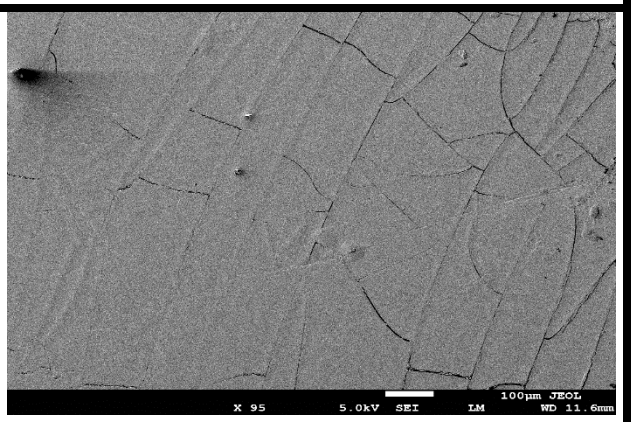

Epoxy with mixture of UVA/HALS-after 35 days

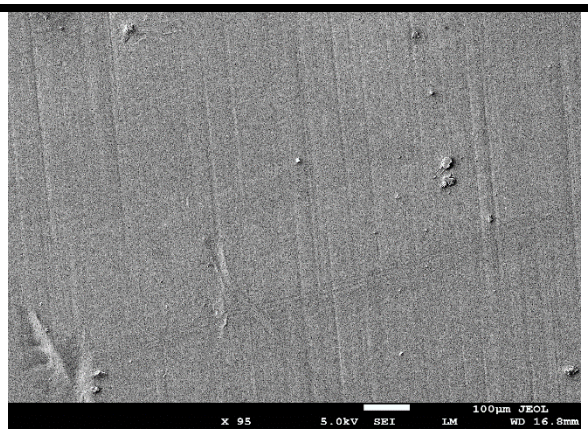

Epoxy with 2% Lignin-before

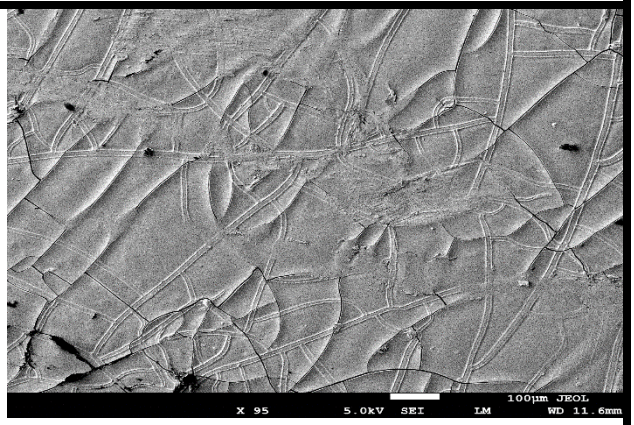

Epoxy with 2% Lignin-after 35 days

Figure 33. FE-SEM micrographs of pure epoxy, epoxy with addition of 2 wt.% pure UVA/HALS, and 2 % lignin before and after 35 days of UV irradiation

Figure 34 shows samples that were filled with different amounts of HNT-encapsulated UVA/HALS. The samples prepared with addition of 2% HNT-UVA/HALS appear more resistant to UV light, since the crack density after UV irradiation is significantly lower than that of other samples.

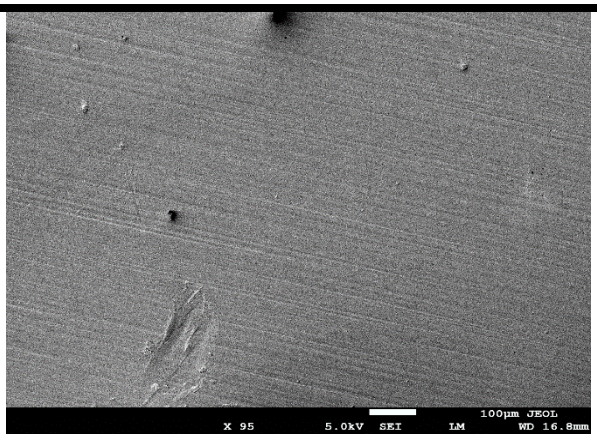

Epoxy with 1% HNT- UVA/HALS-before

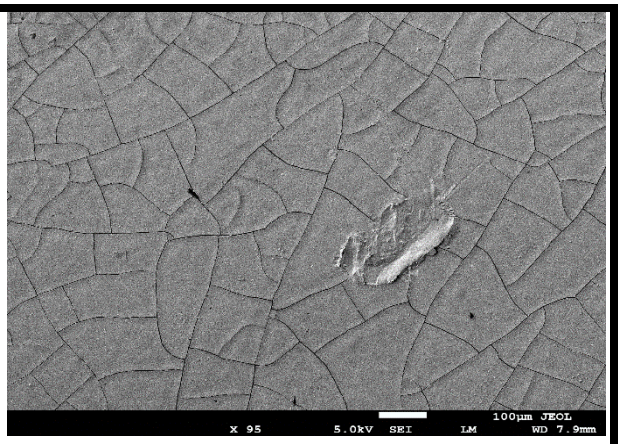

Epoxy with 1% HNT- UVA/HALS-after 35 days

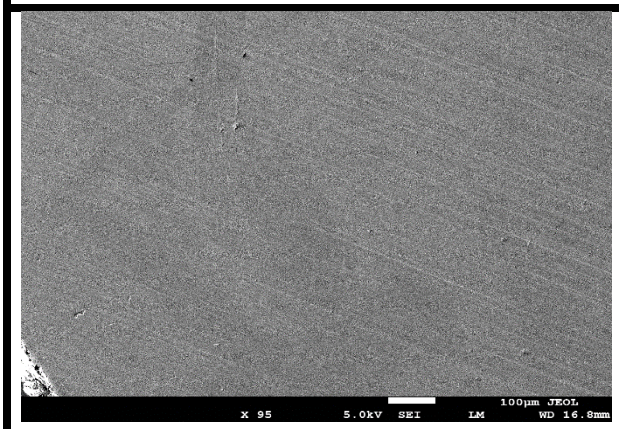

Epoxy with 2% HNT- UVA/HALS-before

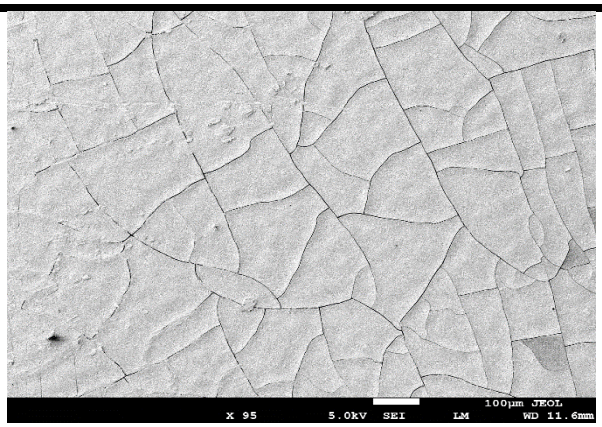

Epoxy with 2% HNT- UVA/HALS-after 35 days

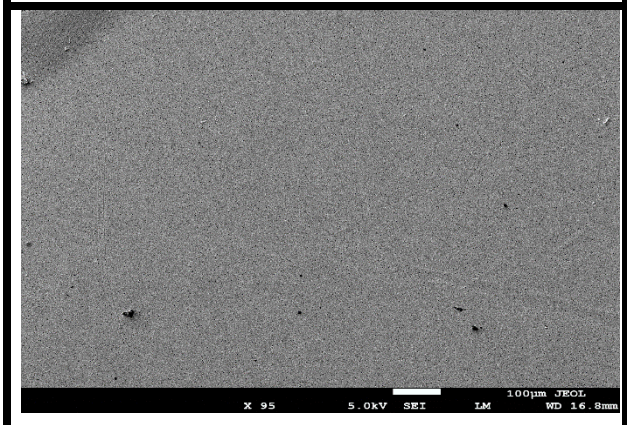

Epoxy with 3% HNT- UVA/HALS-before

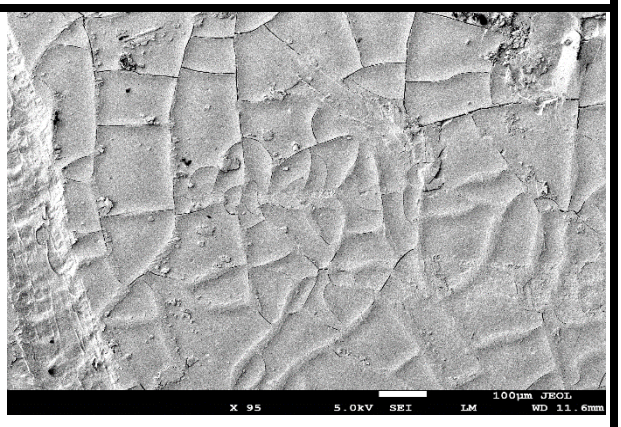

Epoxy with 3% HNT- UVA/HALS-after 35 days

Figure 34. FE-SEM micrographs of epoxy resins with addition of (1-3%) of HNT-UVA/HALS loaded samples before and after 35 days of UV irradiation

Figure 35 displays FE-SEM micrographs of the epoxy resins filled with different amounts (1-3%) of HNT-encapsulated lignin. The results show that the epoxy resin that contained 1% HNTs encapsulated lignin had fewer visible cracks after exposure to UV irradiation, compared with other samples. Increasing the amount of HNTs encapsulated lignin into the epoxy resins increased the frequency of cracks indicating that addition of higher amounts of HNTs encapsulated lignin into the epoxy resins negatively impacts their UV stability.

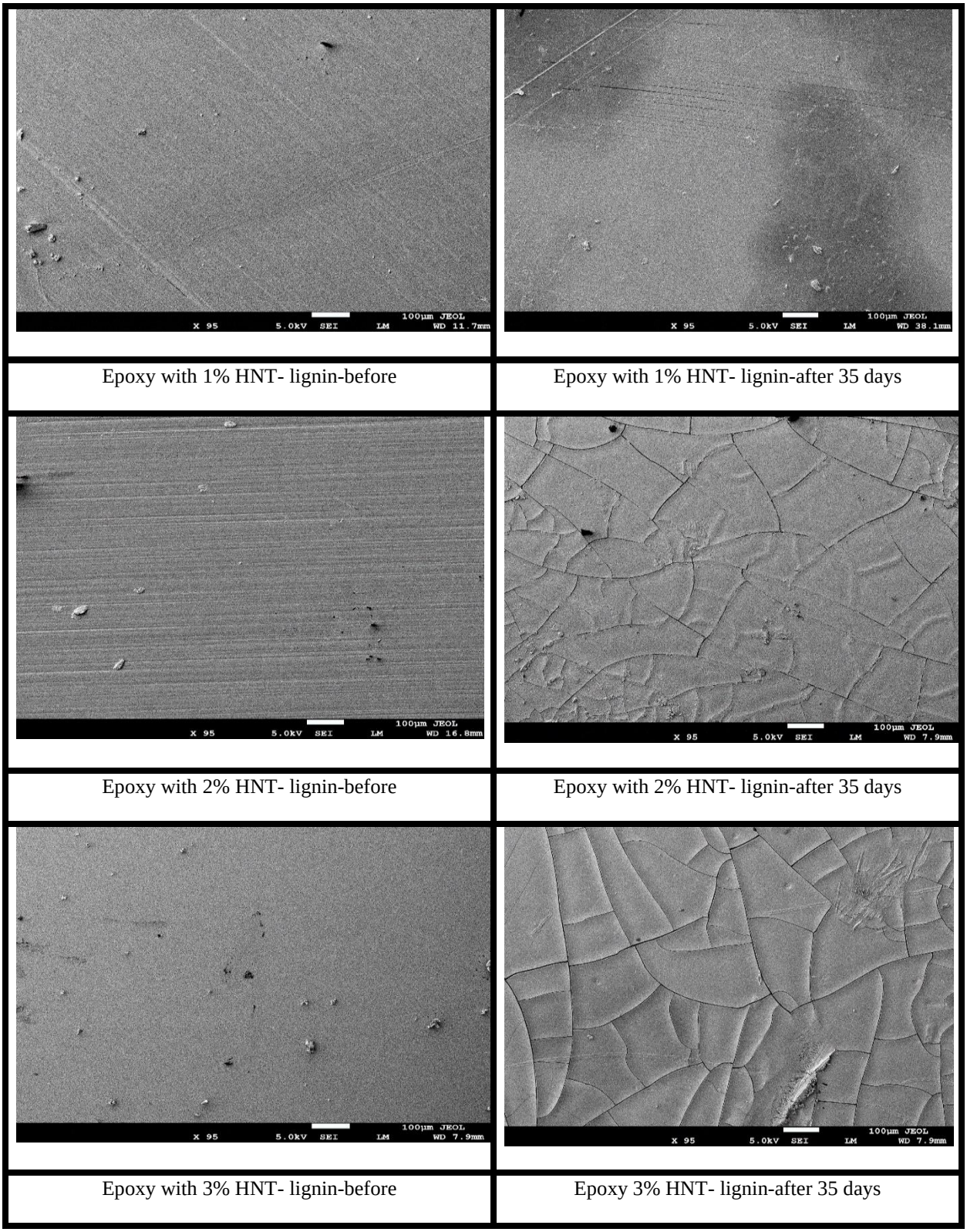

Epoxy with 1% HNT- lignin-before	Epoxy with 1% HNT- lignin-after 35 days
Epoxy with 2% HNT- lignin-before	Epoxy with 2% HNT- lignin-after 35 days
Epoxy with 3% HNT- lignin-before	Epoxy 3% HNT- lignin-after 35 days

Figure 35. FE-SEM micrographs of epoxy samples loaded with different amounts (1-3%) of HNTs encapsulated with lignin, before and after 35 days of UV irradiation

According to the SEM images of all samples, epoxy coatings filled with 2% HNT-UVA/HALS and 1% HNT-lignin had higher photostability than other samples. Note that the sample with 1% HNT-lignin was more photostable (having less visible cracks) than the sample filled with 2% HNT-UVA/HALS. Additionally, the samples containing HNT-UVA/HALS cracked less than the sample containing pure UVA/HALS. It can be suggested that the higher efficiency of the encapsulated systems is due to the fact that encapsulation of UV stabilizers into halloysite nanotubes (HNTs) reduced their migration to the surface of the coatings although, the migration of UV stabilizers to the surface of the coatings was not measured in this study. Lignin has previously been reported to be a good UV absorber and radical scavenger.[311, 312] This study found that photo stability substantially improved when lignin was encapsulated into HNTs versus when pure lignin was directly added to the epoxy coatings.

Electron paramagnetic resonance spectroscopy (EPR) was used to monitor the formation of free radicals in each sample before and after UV exposure. The intensities of various EPR signals, which are directly related to free radical concentrations, were measured in different samples. Figure 36 shows the EPR spectra of pure epoxy collected before irradiation (dark blue trace). The spectrum shows a nonhomogeneous-broadened resonance, typical for an organic radical in the solid-state, centered at approximately g = 2.011.[313, 314] After 5 min of UV irradiation, the EPR signal intensity of pure epoxy increased significantly (Figure 36, red trace) and a new EPR signal characterized by a narrower linewidth was resolved at g = 2.003. The number of paramagnetic centers present in these two samples was determined by double integration of the spectra over their full 30 mT width. Integration values of 104 and 140 were obtained for the “Epoxy-dark” (blue-gray) and “Epoxy-5min” (orange) spectra, respectively, as shown in Figure 36. Parallel sets of EPR spectra are shown in Figures 10b and 10c for the 2% HNT-UVA/HALS and 1% HNT-lignin

samples, respectively. For both samples, radical centers at g = 2.011 and 2.003 were observed prior to illumination. After 5 min of UV irradiation, the EPR signal intensities increased by 20% for 2% HNT-UVA/HALS, and 32% for 1% HNT-lignin (Figure 36). For 2% HNT-UVA/HALS, the observed increase was significantly smaller than the 35% increase observed for the pure-epoxy sample. EPR signal intensities of all samples before and after UV irradiation are shown in Figure 36. Sample with 2% HNT-UVA/HALS had the lowest change in free radical concentration after 5 min UV irradiation. The samples containing lignin, 1% HNT-lignin, 2% HNT-lignin, and 3% HNT-lignin, showed a nearly uniform increase in radical intensity with illumination ranging from 33–42%, essentially independent of doping level. In contrast, the change in radical concentrations upon illumination recorded for the 1% pristine HNT through 3% pristine HNT series showed a steady increase, from 31% at the lower doping level to 92% for the 3% pristine HNT sample.

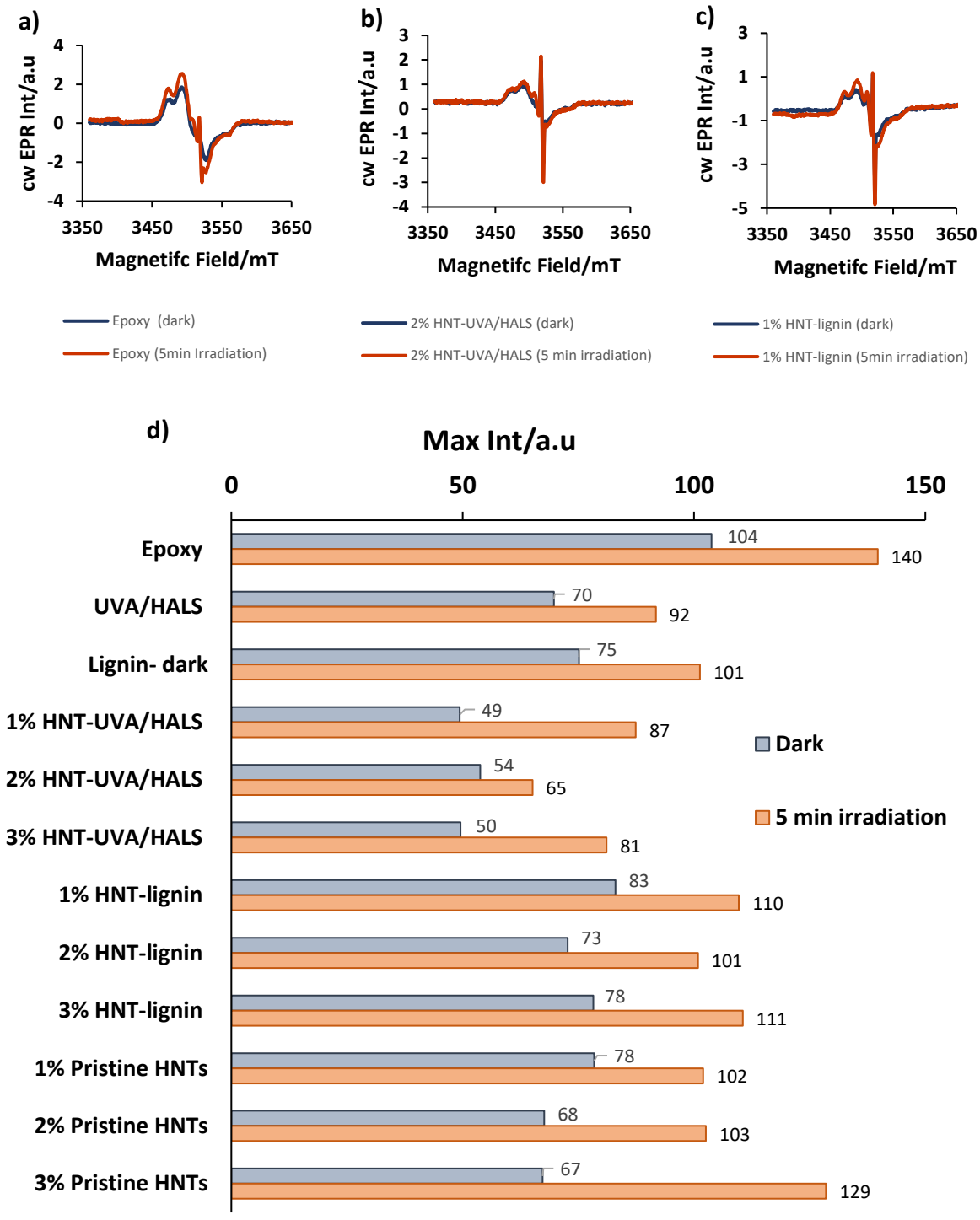

Figure 36. EPR spectra of pure epoxy (a), 2% HNT-UVA/HALS (b), and 1% HNT-lignin (c), before and after 5 min irradiation. d) The intensity of free radicals before and after 5 min UVC irradiation (EPR data) for different samples

After 35 days of UV irradiation, FTIR spectra of all samples were normalized, and carbonyl indexes were calculated (Figure 37) and used to evaluate chemical changes in the samples after UV exposure. The epoxy resin with 2 wt.% pure lignin ("Lignin"), had a carbonyl index of 0.81, which is very high possibly due to the degradation of lignin and formation of quionone.[212] The carbonyl index of pure epoxy and sample with UVA/HALS were 0.74 and 0.59, respectively. The lowest carbonyl indexes were related to the samples containing 1% HNT-UVA/HALS and 1% HNT-lignin which were 0.37 and 0.36, respectively. These results indicate that samples with 1% HNT-UVA/HALS and 1% HNT-lignin underwent less chemical degradation than other samples, complimenting the SEM and EPR results.

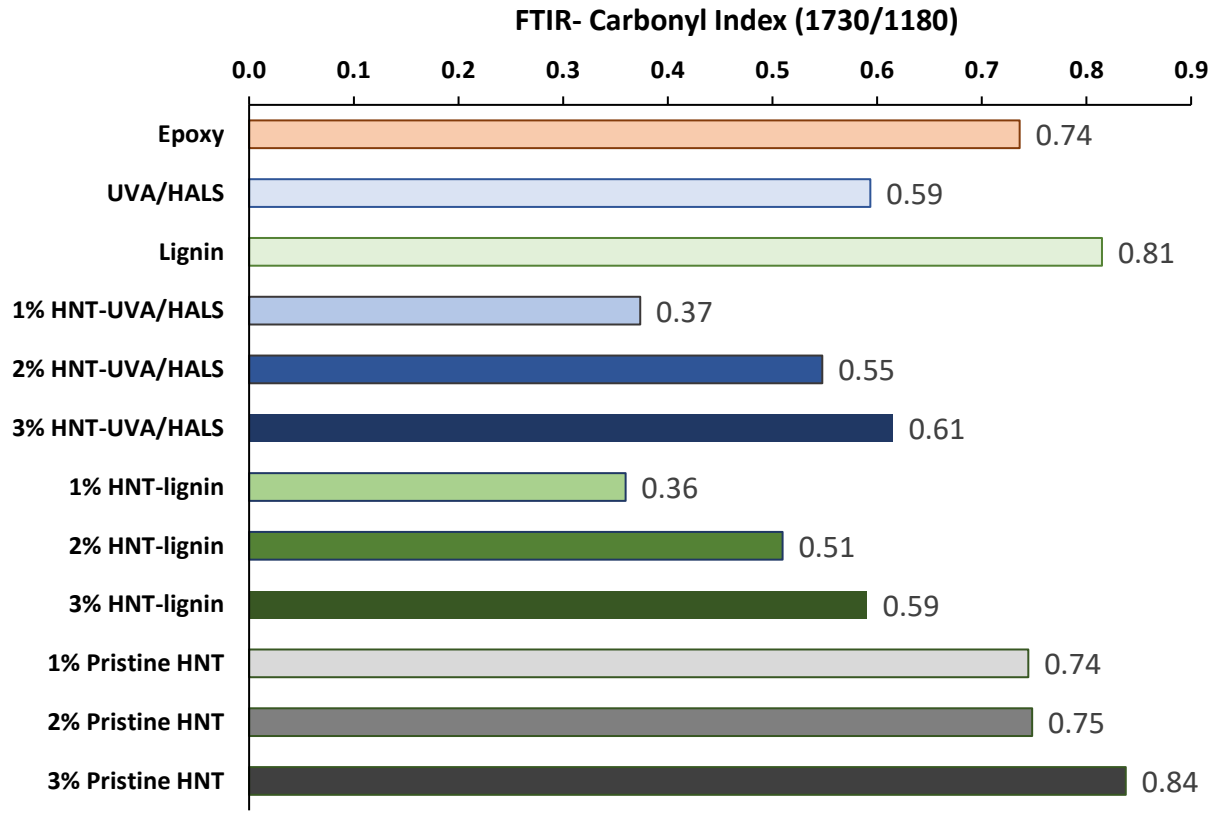

Figure 37. Carbonyl index of various samples obtained from FTIR spectra after 35 days

When polymeric materials are exposed to UV light, their glass transition temperatures (T_g) increase due to the formation of more polar groups (like carbonyls) which hinder chain movements, and breaks up some polymeric chains.[261, 262] The T_g of all samples before and after 35 days of UV irradiation are tabulated in Table 28. Pure epoxy had the highest T_g changes (ΔT_g), as expected, due to its high susceptibility to UV degradation. The addition of organic UV stabilizers to epoxy resin decreased the T_g, while the addition of 2 wt.% lignin did not change the T_g of the epoxy system. In all samples, addition of HNTs increased T_g, due to the inorganic nature of HNTs.[315] Samples that contained HNTs encapsulated lignin, regardless of the loading amount, displayed the lowest change in T_g (smaller ΔT_g). This could well be an indication of the higher photo stability of these samples (especially samples with 1% HNT-lignin) as confirmed by other techniques. In addition, ΔT_g (5.3) of epoxy resin with 1%HNT-UVA/HALS is slightly lower than ΔT_g (6.9) of epoxy resin with pure UVA/HALS, indicating also that encapsulation of UVA/HALS into HNTs reduced the photo degradation of epoxy polymer chains.

Table 28. T_g of different samples before and after 35 days of UV irradiation

Sample ID	T_g °C (Before Irradiation)	T_g °C (After 35 days Irradiation)	ΔT_g
Epoxy	53.1	60.5	7.4
UVA/HALS	51.3	58.2	6.9
Lignin	53.5	60.3	6.8
1% HNT- UVA/HALS	53.6	58.9	5.3
2% HNT-UVA/HALS	56.1	62.6	6.5
3% HNT-UVA/HALS	59.8	63.5	3.7
1% HNT-lignin	57.6	60.4	2.8
2% HNT-lignin	58.2	60.8	2.3
3% HNT-lignin	59.7	60.9	1.2
1% Pristine HNTs	57.1	61.0	3.9
2% Pristine HNTs	57.3	62.8	5.5
3% Pristine HNTs	59.6	62.7	3.1

By monitoring the physical, chemical, and thermal properties of different samples, it was observed that the encapsulation of UVA and HALS into HNTs were an effective method for increasing the photostability of epoxy systems. The highest photostability was achieved when 2 wt.% HNTs encapsulated with UVA/HALS and 1 wt.% HNTs encapsulated with lignin were added to the epoxy system. Our results showed that 1 wt.% HNTs loaded with lignin, a natural UV absorber can effectively be used as a biobased photo stabilizer for epoxy systems. While the higher additions (> 2%) of these encapsulated compounds into epoxy systems resulted in a decrease in photostability, they still performed better than pure epoxy systems. This trend may be related to the photoactivity of HNTs. When the amount of added HNTs increased, the photostability performance decreased, due to an increase in free radical formations caused by the higher UV

absorption (as observed for pristine HNT samples).[300] The addition of pristine HNTs (specifically more than 2%) into epoxy systems negatively impacted the photostability performance of resins (color change, EPR, and FTIR spectroscopy clearly exhibited this trend).

The present research shows that using pristine HNTs in epoxy formulations did not reduce the UV degradation of epoxy resins, as also indicated by another study using HNTs in polylactic acids (PLA).[297] Although pristine HNTs may increase the UV absorption of the system, it does not make it is more photostable. Other published studies used ZnO-HNT systems and found that the addition of these systems improved photostability of natural rubbers and composites.[310, 316] Another study also showed that the encapsulation of UV stabilizers into poly (methyl methacrylate) microcapsules could increase the photostability of water-based acrylic systems,[293] confirming the findings of this study.

REFERENCES

REFERENCES

1. Laurichesse, S.; Avérous, L., Chemical modification of lignins: Towards biobased polymers. *Progress in polymer science* **2014,** *39* (7), 1266-1290.

2. Stewart, D., Lignin as a base material for materials applications: Chemistry, application and economics. *Industrial Crops and Products* **2008,** *27* (2), 202-207.

3. Glasser, W. G.; Barnett, C. A.; Muller, P. C.; Sarkanen, K. V., The chemistry of several novel bioconversion lignins. *Journal of agricultural and Food Chemistry* **1983,** *31* (5), 921-930.

4. Ten, E.; Vermerris, W., Recent developments in polymers derived from industrial lignin. *Journal of Applied Polymer Science* **2015,** *132* (24).

5. Heitner, C.; Dimmel, D.; Schmidt, J., *Lignin and lignans: advances in chemistry*. CRC press: 2016.

6. Sarkanen, K., Classification and distribution. *Lignins-occurrence, formation, structure and reactions* **1971**, 43-94.

7. Boerjan, W.; Ralph, J.; Baucher, M., Lignin biosynthesis. *Annual review of plant biology* **2003,** *54* (1), 519-546.

8. Ragauskas, A.; Beckham, G.; Biddy, M.; Chandra, R.; Chen, F.; Davis, M.; Davison, B.; Dixon, R.; Gilna, P.; Keller, M., GA Tuskan ja CE Wyman. *Science* **2014,** *344*.

9. Behling, R.; Valange, S.; Chatel, G., Heterogeneous catalytic oxidation for lignin valorization into valuable chemicals: what results? What limitations? What trends? *Green Chemistry* **2016,** *18* (7), 1839-1854.

10. Upton, B. M.; Kasko, A. M., Strategies for the conversion of lignin to high-value polymeric materials: review and perspective. *Chem. Rev.* **2016,** *116* (4), 2275-306.

11. Li, C.; Zhao, X.; Wang, A.; Huber, G. W.; Zhang, T., Catalytic transformation of lignin for the production of chemicals and fuels. *Chem. Rev.* **2015,** *115* (21), 11559-624.

12. Zakzeski, J.; Bruijnincx, P. C. A.; Jongerius, A. L.; Weckhuysen, B. M., The catalytic valorization of lignin for the production of renewable chemicals. *Chemical Reviews* **2010,** *110* (6), 3552-3599.

13. Upton, B. M.; Kasko, A. M., Strategies for the conversion of lignin to high-value polymeric materials: review and perspective. *Chem. Rev.* **2016,** *116* (4), 2275-2306.

14. Li, C.; Zhao, X.; Wang, A.; Huber, G. W.; Zhang, T., Catalytic transformation of lignin for the production of chemicals and fuels. *Chem. Rev.* **2015,** *115* (21), 11559-11624.

15. Dessbesell, L.; Paleologou, M.; Leitch, M.; Pulkki, R.; Xu, C. C., Global lignin supply overview and kraft lignin potential as an alternative for petroleum-based polymers. *Renewable and Sustainable Energy Reviews* **2020,** *123*, 109768.

16. Konduri, M. K.; Fatehi, P., Production of water-soluble hardwood kraft lignin via sulfomethylation using formaldehyde and sodium sulfite. *ACS Sustainable Chemistry & Engineering* **2015,** *3* (6), 1172-1182.

17. Kang, S.; Li, X.; Fan, J.; Chang, J., Hydrothermal conversion of lignin: a review. *Renewable and Sustainable Energy Reviews* **2013,** *27*, 546-558.

18. Banu, J. R.; Kavitha, S.; Kannah, R. Y.; Devi, T. P.; Gunasekaran, M.; Kim, S.-H.; Kumar, G., A review on biopolymer production via lignin valorization. *Bioresour. Technol.* **2019,** *290*, 121790.

19. Gosselink, R.; Troosters, T.; Decramer, M., Exercise testing: why, which and how to interpret. *Breathe* **2004,** *1* (2), 120-129.

20. Pouteau, C.; Dole, P.; Cathala, B.; Averous, L.; Boquillon, N., Antioxidant properties of lignin in polypropylene. *Polym. Degrad. Stab.* **2003,** *81* (1), 9-18.

21. Falkehag, S. I. In *Lignin in materials*, Appl. Polym. Symp, 1975; pp 247-257.

22. De Chirico, A.; Armanini, M.; Chini, P.; Cioccolo, G.; Provasoli, F.; Audisio, G., Flame retardants for polypropylene based on lignin. *Polym. Degrad. Stab.* **2003,** *79* (1), 139-145.

23. Dong, X.; Dong, M.; Lu, Y.; Turley, A.; Jin, T.; Wu, C., Antimicrobial and antioxidant activities of lignin from residue of corn stover to ethanol production. *Industrial Crops and Products* **2011,** *34* (3), 1629-1634.

24. Yang, W.; Owczarek, J.; Fortunati, E.; Kozanecki, M.; Mazzaglia, A.; Balestra, G.; Kenny, J.; Torre, L.; Puglia, D., Antioxidant and antibacterial lignin nanoparticles in polyvinyl alcohol/chitosan films for active packaging. *Industrial Crops and Products* **2016,** *94*, 800-811.

25. Li, X. F. In *Preparation and properties of biodegradable sodium lignosulfonate/poly (vinyl alcohol) blend films*, Advanced Materials Research, Trans Tech Publ: 2011; pp 676-681.

26. Sun, G.; Sun, H.; Liu, Y.; Zhao, B.; Zhu, N.; Hu, K., Comparative study on the curing kinetics and mechanism of a lignin-based-epoxy/anhydride resin system. *Polymer* **2007,** *48* (1), 330-337.

27. Huang, J.; Zhang, L., Effects of NCO/OH molar ratio on structure and properties of graft-interpenetrating polymer networks from polyurethane and nitrolignin. *Polymer* **2002,** *43* (8), 2287-2294.

28. Kouisni, L.; Fang, Y.; Paleologou, M.; Ahvazi, B.; Hawari, J.; Zhang, Y.; Wang, X.-M., Kraft lignin recovery and its use in the preparation of lignin-based phenol formaldehyde resins for plywood. *Cellul. Chem. Technol.* **2011,** *45* (7), 515.

29. Kong, F.; Wang, S.; Price, J. T.; Konduri, M. K.; Fatehi, P., Water soluble kraft lignin–acrylic acid copolymer: Synthesis and characterization. *Green Chemistry* **2015,** *17* (8), 4355-4366.

30. Bonini, C.; D'Auria, M.; Emanuele, L.; Ferri, R.; Pucciariello, R.; Sabia, A. R., Polyurethanes and polyesters from lignin. *J. Appl. Polym. Sci.* **2005,** *98* (3), 1451-1456.

31. Araújo, J. D.; Grande, C. A.; Rodrigues, A. E., Vanillin production from lignin oxidation in a batch reactor. *Chem. Eng. Res. Des.* **2010,** *88* (8), 1024-1032.

32. Mialon, L.; Vanderhenst, R.; Pemba, A. G.; Miller, S. A., Polyalkylenehydroxybenzoates (PAHBs): Biorenewable aromatic/aliphatic polyesters from lignin. *Macromol. Rapid Commun.* **2011,** *32* (17), 1386-1392.

33. Tarabanko, V.; Chelbina, Y. V.; Kudryashev, A.; Tarabanko, N., Separation of vanillin and syringaldehyde produced from lignins. *Sep. Sci. Technol.* **2013,** *48* (1), 127-132.

34. Villar, J. C.; Caperos, A.; García-Ochoa, F., Oxidation of hardwood kraft-lignin to phenolic derivatives with oxygen as oxidant. *Wood Science and Technology* **2001,** *35* (3), 245-255.

35. Yuan, Z.; Klinger, G. E.; Nikafshar, S.; Cui, Y.; Fang, Z.; Alherech, M.; Goes, S.; Anson, C.; Singh, S. K.; Bals, B., Effective Biomass Fractionation through Oxygen-Enhanced Alkaline–Oxidative Pretreatment. *ACS Sustainable Chemistry & Engineering* **2021,** *9* (3), 1118-1127.

36. Kadla, J.; Kubo, S.; Venditti, R.; Gilbert, R.; Compere, A.; Griffith, W., Lignin-based carbon fibers for composite fiber applications. *Carbon* **2002,** *40* (15), 2913-2920.

37. Park, W. H.; Lee, J. K.; Kwon, K. J., Cure behavior of an epoxy-anhydride-imidazole system. *Polym. J.* **1996,** *28* (5), 407-411.

38. Petrie, E. M., *Epoxy adhesive formulations*. McGraw Hill Professional: 2005.

39. Achilias, D. S.; Karabela, M. M.; Varkopoulou, E. A.; Sideridou, I. D., Cure kinetics study of two epoxy systems with fourier tranform infrared spectroscopy (FTIR) and differential scanning calorimetry (DSC). *Journal of Macromolecular Science, Part A* **2012,** *49* (8), 630-638.

40. Kimura, H.; Matsumoto, A.; Hasegawa, K.; Ohtsuka, K.; Fukuda, A., Epoxy resin cured by bisphenol A based benzoxazine. *J. Appl. Polym. Sci.* **1998,** *68* (12), 1903-1910.

41. Strehmel, V.; Scherzer, T., Structural investigation of epoxy amine networks by mid-and near-infrared spectroscopy. *European polymer journal* **1994,** *30* (3), 361-368.

42. Benyahya, S.; Aouf, C.; Caillol, S.; Boutevin, B.; Pascault, J. P.; Fulcrand, H., Functionalized green tea tannins as phenolic prepolymers for bio-based epoxy resins. *Industrial Crops and Products* **2014,** *53*, 296-307.

43. Ma, S.; Liu, X.; Jiang, Y.; Tang, Z.; Zhang, C.; Zhu, J., Bio-based epoxy resin from itaconic acid and its thermosets cured with anhydride and comonomers. *Green Chemistry* **2013,** *15* (1), 245-254.

44. García-Espiñeira, M.; Tejeda-Benítez, L.; Olivero-Verbel, J., Toxic effects of bisphenol a, propyl paraben, and triclosan on Caenorhabditis elegans. *International journal of environmental research and public health* **2018,** *15* (4), 684.

45. Flint, S.; Markle, T.; Thompson, S.; Wallace, E., Bisphenol A exposure, effects, and policy: a wildlife perspective. *Journal of environmental management* **2012,** *104*, 19-34.

46. Aouf, C.; Nouailhas, H.; Fache, M.; Caillol, S.; Boutevin, B.; Fulcrand, H., Multi-functionalization of gallic acid. Synthesis of a novel bio-based epoxy resin. *Eur. Polym. J.* **2013,** *49* (6), 1185-1195.

47. Turker, M. S., Banning Bisphenol A in the United States and Canada: Epigenetic Science, the Precautionary Principle, and a Missed Opportunity to Protect the Fetus. *J. Health & Biomedical L.* **2012,** *8*, 173.

48. Amen-Chen, C.; Pakdel, H.; Roy, C., Production of monomeric phenols by thermochemical conversion of biomass: a review. *Bioresour. Technol.* **2001,** *79* (3), 277-299.

49. Quaranta, E.; Minischetti, C. C.; Tartaro, G., Chemical Recycling of Poly (bisphenol A carbonate) by Glycolysis under 1, 8-Diazabicyclo [5.4. 0] undec-7-ene Catalysis. *ACS omega* **2018,** *3* (7), 7261-7268.

50. Sun, R.; Sun, X.; Wang, S.; Zhu, W.; Wang, X., Ester and ether linkages between hydroxycinnamic acids and lignins from wheat, rice, rye, and barley straws, maize stems, and fast-growing poplar wood. *Industrial Crops and Products* **2002,** *15* (3), 179-188.

51. Wan, J.; Gan, B.; Li, C.; Molina-Aldareguia, J.; Kalali, E. N.; Wang, X.; Wang, D.-Y., A sustainable, eugenol-derived epoxy resin with high biobased content, modulus, hardness and low flammability: synthesis, curing kinetics and structure–property relationship. *Chemical Engineering Journal* **2016,** *284*, 1080-1093.

52. Liu, X.; Huang, W.; Jiang, Y.; Zhu, J.; Zhang, C., Preparation of a bio-based epoxy with comparable properties to those of petroleum-based counterparts. *Express Polymer Letters* **2012,** *6* (4).

53. Nikafshar, S.; Zabihi, O.; Hamidi, S.; Moradi, Y.; Barzegar, S.; Ahmadi, M.; Naebe, M., A renewable bio-based epoxy resin with improved mechanical performance that can compete with DGEBA. *RSC advances* **2017,** *7* (14), 8694-8701.

54. Aouf, C.; Lecomte, J.; Villeneuve, P.; Dubreucq, E.; Fulcrand, H., Chemo-enzymatic functionalization of gallic and vanillic acids: synthesis of bio-based epoxy resins prepolymers. *Green chemistry* **2012,** *14* (8), 2328-2336.

55. Ferdosian, F.; Yuan, Z.; Anderson, M.; Xu, C. C., Sustainable lignin-based epoxy resins cured with aromatic and aliphatic amine curing agents: Curing kinetics and thermal properties. *Thermochimica acta* **2015,** *618*, 48-55.

56. El Mansouri, N.-E.; Yuan, Q.; Huang, F., Synthesis and characterization of kraft lignin-based epoxy resins. © *BioResources, 2011, vol. 6, núm. 3, p. 2492-2503* **2011**.

57. Sasaki, C.; Wanaka, M.; Takagi, H.; Tamura, S.; Asada, C.; Nakamura, Y., Evaluation of epoxy resins synthesized from steam-exploded bamboo lignin. *Industrial crops and products* **2013,** *43*, 757-761.

58. Jablonskis, A.; Arshanitsa, A.; Arnautov, A.; Telysheva, G.; Evtuguin, D., Evaluation of Ligno Boost™ softwood kraft lignin epoxidation as an approach for its application in cured epoxy resins. *Industrial Crops and Products* **2018,** *112*, 225-235.

59. Xue, B.; Tang, R.; Xue, D.; Guan, Y.; Sun, Y.; Zhao, W.; Tan, J.; Li, X., Sustainable alternative for bisphenol A epoxy resin high-performance and recyclable lignin-based epoxy vitrimers. *Industrial Crops and Products* **2021,** *168*, 113583.

60. Over, L. C.; Grau, E.; Grelier, S.; Meier, M. A.; Cramail, H., Synthesis and characterization of epoxy thermosetting polymers from glycidylated organosolv lignin and Bisphenol a. *Macromol. Chem. Phys.* **2017,** *218* (4), 1600411.

61. Singh, A.; Yadav, K.; Sen, A. K., Sal (Shorea Robusta) leaves lignin epoxidation and its use in epoxy based coatings. *American Journal of Polymer Science* **2012,** *2* (1), 14-18.

62. Zhu, Y.; Li, Z.; Wang, X.; Ding, N.; Tian, Y., Preparation and Application of Lignin-Based Epoxy Resin from Pulping Black Liquor. *ChemistrySelect* **2020,** *5* (12), 3494-3502.

63. Nicastro, K. H.; Kloxin, C. J.; Epps III, T. H., Potential lignin-derived alternatives to bisphenol a in diamine-hardened epoxy resins. *ACS Sustainable Chemistry & Engineering* **2018,** *6* (11), 14812-14819.

64. Ferdosian, F.; Yuan, Z.; Anderson, M.; Xu, C. C., Chemically modified lignin through epoxidation and its thermal properties. *J-FOR* **2012,** *2*, 11-15.

65. Chen, C.; Zhu, M.; Li, M.; Fan, Y.; Sun, R.-C., Epoxidation and etherification of alkaline lignin to prepare water-soluble derivatives and its performance in improvement of enzymatic hydrolysis efficiency. *Biotechnology for biofuels* **2016,** *9* (1), 87.

66. Zhao, S.; Abu-Omar, M. M., Synthesis of renewable thermoset polymers through successive lignin modification using lignin-derived phenols. *ACS Sustainable Chemistry & Engineering* **2017,** *5* (6), 5059-5066.

67. Zhao, S.; Abu-Omar, M. M., Renewable epoxy networks derived from lignin-based monomers: effect of cross-linking density. *ACS Sustainable Chemistry & Engineering* **2016,** *4* (11), 6082-6089.

68. van de Pas, D. J.; Torr, K. M., Biobased epoxy resins from deconstructed native softwood lignin. *Biomacromolecules* **2017,** *18* (8), 2640-2648.

69. Maiorana, A.; Spinella, S.; Gross, R. A., Bio-Based Epoxy Resins from Diphenolate Esters—Replacing the Diglycidyl Ether of Bisphenol A. In *Green Polymer Chemistry: Biobased Materials and Biocatalysis*, ACS Publications: 2015; pp 371-386.

70. Hollande, L.; Do Marcolino, I.; Balaguer, P.; Domenek, S.; Gross, R. A.; Allais, F., Preparation of renewable epoxy-amine resins with tunable thermo-mechanical properties, wettability and degradation abilities from lignocellulose-and plant oils-derived components. *Frontiers in Chemistry* **2019,** *7*, 159.

71. Mattar, N.; de Anda, A. R.; Vahabi, H.; Renard, E.; Langlois, V., Resorcinol-Based Epoxy Resins Hardened with Limonene and Eugenol Derivatives: From the Synthesis of Renewable Diamines to the Mechanical Properties of Biobased Thermosets. *ACS Sustainable Chemistry & Engineering* **2020,** *8* (34), 13064-13075.

72. Maiorana, A.; Spinella, S.; Gross, R. A., Bio-based alternative to the diglycidyl ether of bisphenol A with controlled materials properties. *Biomacromolecules* **2015,** *16* (3), 1021-1031.

73. Ménard, R.; Caillol, S.; Allais, F., Ferulic acid-based renewable esters and amides-containing epoxy thermosets from wheat bran and beetroot pulp: Chemo-enzymatic synthesis and thermo-mechanical properties characterization. *Industrial Crops and Products* **2017,** *95*, 83-95.

74. Maiorana, A.; Reano, A. F.; Centore, R.; Grimaldi, M.; Balaguer, P.; Allais, F.; Gross, R. A., Structure property relationships of biobased n-alkyl bisferulate epoxy resins. *Green Chemistry* **2016,** *18* (18), 4961-4973.

75. http://www.marketsandmarkets.com/PressReleases/polyurethane-coatings.asp.

76. Dodge, J., Polyurethanes and polyureas. *Synthetic Methods in Step-Growth Polymers. United States of America: John Wiley & Sons* **2003**, 197-258.

77. Meier-Westhues, H.-U., *Polyurethanes: coatings, adhesives and sealants*. European Coatings: 2019.

78. Insight, P. https://www.plasticsinsight.com/resin-intelligence/resin-prices/polyurethane/%0A%0Ahttps://investor.covestro.com/securedl/14391.

79. Muller, P. C.; Kelley, S. S.; Glasser, W. G., Engineering plastics from lignin. IX. Phenolic resin synthesis and characterization. *The Journal of Adhesion* **1984,** *17* (3), 185-206.

80. Saraf, V. P.; Glasser, W. G.; Wilkes, G. L.; McGrath, J. E., Engineering plastics from lignin. VI. Structure–property relationships of PEG-containing polyurethane networks. *Journal of applied polymer science* **1985,** *30* (5), 2207-2224.

81. Wang, Y.-Y.; Cai, C. M.; Ragauskas, A. J., Recent advances in lignin-based polyurethanes. *Tappi Journal* **2017,** *16* (4).

82. Alinejad, M.; Henry, C.; Nikafshar, S.; Gondaliya, A.; Bagheri, S.; Chen, N.; Singh, S. K.; Hodge, D. B.; Nejad, M., Lignin-based polyurethanes: Opportunities for bio-based foams, elastomers, coatings and adhesives. *Polymers* **2019,** *11* (7), 1202.

83. Chung, H.; Washburn, N. R., Improved lignin polyurethane properties with lewis acid treatment. *ACS applied materials & interfaces* **2012,** *4* (6), 2840-2846.

84. Delebecq, E.; Pascault, J.-P.; Boutevin, B.; Ganachaud, F., On the versatility of urethane/urea bonds: reversibility, blocked isocyanate, and non-isocyanate polyurethane. *Chem. Rev.* **2013,** *113* (1), 80-118.

85. Areskogh, D.; Li, J.; Gellerstedt, G.; Henriksson, G., Structural modification of commercial lignosulphonates through laccase catalysis and ozonolysis. *Industrial Crops and Products* **2010,** *32* (3), 458-466.

86. Vishtal, A. G.; Kraslawski, A., Challenges in industrial applications of technical lignins. *BioResources* **2011,** *6* (3), 3547-3568.

87. Farkas, A.; Mills, G., Catalytic effects in isocyanate reactions. In *Advances in Catalysis*, Elsevier: 1962; Vol. 13, pp 393-446.

88. Duval, A.; Lawoko, M., A review on lignin-based polymeric, micro-and nano-structured materials. *React. Funct. Polym.* **2014,** *85*, 78-96.

89. Sadeghifar, H.; Argyropoulos, D. S., Correlations of the antioxidant properties of softwood kraft lignin fractions with the thermal stability of its blends with polyethylene. *ACS Sustainable Chemistry & Engineering* **2015,** *3* (2), 349-356.

90. Gierer, J., Chemistry of delignification. *Wood Science and technology* **1985,** *19* (4), 289-312.
91. Meng, X.; Crestini, C.; Ben, H.; Hao, N.; Pu, Y.; Ragauskas, A. J.; Argyropoulos, D. S., Determination of hydroxyl groups in biorefinery resources via quantitative 31 P NMR spectroscopy. *Nature Protocols* **2019,** *14* (9), 2627-2647.

92. Sarkanen, K.; Ludwig, C.; Lignins-Occurrence, F., Structure and Reactions. Wiley-Interscience, New York: 1971.

93. Poletto, M., Assessment of the thermal behavior of lignins from softwood and hardwood species. *Maderas. Ciencia y tecnología* **2017,** *19* (1), 63-74.

94. Aldaeus, F.; Olsson, A.-M.; Stevanic, J. S., Miniaturized determination of ash content in kraft lignin samples using oxidative thermogravimetric analysis. *Nordic Pulp & Paper Research Journal* **2017,** *32* (2), 280-282.

95. TAPPI, T., 211 om–93 (1993).". *Ash in wood, pulp, paper and paperboard: Combustion at 525*.

96. 84(2021), A. D.-. Standard Test Method for Ash in Wood. 2021.

97. Element, C., Method 3051A microwave assisted acid digestion of sediments, sludges, soils, and oils. *Z. Für Anal. Chem* **2007,** *111*, 362-366.

98. Asgari, F.; Argyropoulos, D. S., Fundamentals of oxygen delignification. Part II. Functional group formation/elimination in residual kraft lignin. *Can. J. Chem.* **1998,** *76* (11), 1606-1615.

99. Granata, A.; Argyropoulos, D. S., 2-Chloro-4, 4, 5, 5-tetramethyl-1, 3, 2-dioxaphospholane, a reagent for the accurate determination of the uncondensed and condensed phenolic moieties in lignins. *J. Agric. Food. Chem.* **1995,** *43* (6), 1538-1544.

100. Crestini, C.; Lange, H.; Bianchetti, G., Detailed chemical composition of condensed tannins via quantitative 31P NMR and HSQC analyses: Acacia catechu, Schinopsis balansae, and Acacia mearnsii. *Journal of natural products* **2016,** *79* (9), 2287-2295.

101. Melone, F.; Saladino, R.; Lange, H.; Crestini, C., Tannin structural elucidation and quantitative 31P NMR analysis. 2. Hydrolyzable tannins and proanthocyanidins. *Journal of agricultural and food chemistry* **2013,** *61* (39), 9316-9324.

102. Spyros, A.; Dais, P., Application of 31P NMR spectroscopy in food analysis. 1. Quantitative determination of the mono-and diglyceride composition of olive oils. *Journal of agricultural and food chemistry* **2000,** *48* (3), 802-805.

103. Fronimaki, P.; Spyros, A.; Christophoridou, S.; Dais, P., Determination of the diglyceride content in Greek virgin olive oils and some commercial olive oils by employing 31P NMR spectroscopy. *Journal of agricultural and food chemistry* **2002,** *50* (8), 2207-2213.

104. Hatzakis, E.; Agiomyrgianaki, A.; Dais, P., Detection and Quantification of Free Glycerol in Virgin Olive Oil by 31 P-NMR Spectroscopy. *Journal of the American Oil Chemists' Society* **2010,** *87* (1), 29-34.

105. Akim, L. G.; Argyropoulos, D. S.; Jouanin, L.; Leplé, J.-C.; Pilate, G.; Pollet, B.; Lapierre, C., Quantitative 31P NMR spectroscopy of lignins from transgenic poplars. *Holzforschung* **2001,** *55* (4), 386-390.

106. Li, M.; Yoo, C. G.; Pu, Y.; Ragauskas, A. J., 31P NMR chemical shifts of solvents and products impurities in biomass pretreatments. *ACS Sustainable Chemistry & Engineering* **2018,** *6* (1), 1265-1270.

107. Olarte, M. V. Base-catalyzed depolymerization of lignin and hydrodeoxygenation of lignin model compounds for alternative fuel production. Georgia Institute of Technology, 2011.

108. Ibbett, R.; Gaddipati, S.; Davies, S.; Hill, S.; Tucker, G., The mechanisms of hydrothermal deconstruction of lignocellulose: new insights from thermal–analytical and complementary studies. *Bioresour. Technol.* **2011,** *102* (19), 9272-9278.

109. Nguyen, N. A.; Bowland, C. C.; Bonnesen, P. V.; Littrell, K. C.; Keum, J. K.; Naskar, A. K., Fractionation of Lignin for Selective Shape Memory Effects at Elevated Temperatures. *Materials* **2020,** *13* (8), 1940.

110. Sjöström, E.; Alén, R., *Analytical methods in wood chemistry, pulping, and papermaking*. Springer Science & Business Media: 2013.

111. Lora, J., Industrial commercial lignins: sources, properties and applications. In *Monomers, polymers and composites from renewable resources*, Elsevier: 2008; pp 225-241.

112. Areskogh, D.; Li, J.; Gellerstedt, G. r.; Henriksson, G., Investigation of the molecular weight increase of commercial lignosulfonates by laccase catalysis. *Biomacromolecules* **2010,** *11* (4), 904-910.

113. Chakar, F. S.; Ragauskas, A. J., Review of current and future softwood kraft lignin process chemistry. *Industrial Crops and Products* **2004,** *20* (2), 131-141.

114. Neimo, L., Papermaking chemistry (Book 4). *Papermaking science and technology* **1999**.

115. Gottumukkala, L. D.; Mathew, A. K.; Abraham, A.; Sukumaran, R. K., Biobutanol Production: Microbes, Feedstock, and Strategies. In *Biofuels: Alternative Feedstocks and Conversion Processes for the Production of Liquid and Gaseous Biofuels*, Elsevier: 2019; pp 355-377.

116. Buranov, A. U.; Mazza, G., Lignin in straw of herbaceous crops. *Industrial crops and products* **2008,** *28* (3), 237-259.
117. Wörmeyer, K.; Ingram, T.; Saake, B.; Brunner, G.; Smirnova, I., Comparison of different pretreatment methods for lignocellulosic materials. Part II: Influence of pretreatment on the properties of rye straw lignin. *Bioresour. Technol.* **2011,** *102* (5), 4157-4164.

118. Azeez, M. A., Pulping of non-woody biomass. *Pulp and Paper Processing* **2018**, 55-86.

119. Chan, K.; Argyropoulos, D.; White, D.; Yeager, G.; Hay, A., Facile quantitative analysis of hydroxyl end groups of poly (2, 6-dimethyl-1, 4-phenylene oxide) s by 31P NMR spectroscopy. *Macromolecules* **1994,** *27* (22), 6371-6375.

120. Argyropoulos, D. S., Quantitative phosphorus-31 NMR analysis of six soluble lignins. *J. Wood Chem. Technol.* **1994,** *14* (1), 65-82.

121. Zawadzki, M.; Ragauskas, A., N-hydroxy compounds as new internal standards for the 31P-NMR determination of lignin hydroxy functional groups. *Holzforschung* **2001,** *55* (3), 283-285.

122. Erdtman, H., Lignins: Occurrence, formation, structure and reactions, KV Sarkanen and CH Ludwig, Eds., John Wiley & Sons, Inc., New York, 1971. 916 pp. $35.00. *Journal of Polymer Science Part B: Polymer Letters* **1972,** *10* (3), 228-230.

123. Izydorczyk, M. S.; Biliaderis, C. G., Cereal arabinoxylans: advances in structure and physicochemical properties. *Carbohydr. Polym.* **1995,** *28* (1), 33-48.

124. Gellerstedt, G.; Henriksson, G., Lignins: major sources, structure and properties. In *Monomers, polymers and composites from renewable resources*, Elsevier: 2008; pp 201-224.

125. Gierer, J. *The reactions of lignin during pulping. A description and comparison of conventional pulping processes*; Svenska Traforskingings Institute Stockholm: 1970.

126. Constant, S.; Wienk, H. L.; Frissen, A. E.; de Peinder, P.; Boelens, R.; Van Es, D. S.; Grisel, R. J.; Weckhuysen, B. M.; Huijgen, W. J.; Gosselink, R. J., New insights into the structure and composition of technical lignins: a comparative characterisation study. *Green Chemistry* **2016,** *18* (9), 2651-2665.

127. Vázquez, G.; Antorrena, G.; González, J.; Freire, S., The influence of pulping conditions on the structure of acetosolv eucalyptus lignins. *J. Wood Chem. Technol.* **1997,** *17* (1-2), 147-162.

128. Faix, O., Fourier transform infrared spectroscopy. In *Methods in lignin chemistry*, Springer: 1992; pp 83-109.

129. Pandey, K., A study of chemical structure of soft and hardwood and wood polymers by FTIR spectroscopy. *J. Appl. Polym. Sci.* **1999,** *71* (12), 1969-1975.

130. Yang, X.; Ma, F.; Zeng, Y.; Yu, H.; Xu, C.; Zhang, X., Structure alteration of lignin in corn stover degraded by white-rot fungus Irpex lacteus CD2. *International Biodeterioration & Biodegradation* **2010,** *64* (2), 119-123.

131. Derkacheva, O.; Sukhov, D. In *Investigation of lignins by FTIR spectroscopy*, Macromolecular Symposia, Wiley Online Library: 2008; pp 61-68.

132. Gidh, A. V.; Decker, S. R.; Vinzant, T. B.; Himmel, M. E.; Williford, C., Determination of lignin by size exclusion chromatography using multi angle laser light scattering. *J. Chromatogr. A* **2006,** *1114* (1), 102-110.

133. Baumberger, S.; Abaecherli, A.; Fasching, M.; Gellerstedt, G.; Gosselink, R.; Hortling, B.; Li, J.; Saake, B.; de Jong, E., Molar mass determination of lignins by size-exclusion chromatography: towards standardisation of the method. *Holzforschung* **2007,** *61* (4), 459-468.

134. Dence, C. W., *Methods in lignin chemistry*. Springer-Verlag: 1992.

135. Huijgen, W.; Telysheva, G.; Arshanitsa, A.; Gosselink, R.; De Wild, P., Characteristics of wheat straw lignins from ethanol-based organosolv treatment. *Industrial Crops and Products* **2014,** *59*, 85-95.

136. Sulaeva, I.; Zinovyev, G.; Plankeele, J.-M.; Sumerskii, I.; Rosenau, T.; Potthast, A., Fast track to molar-mass distributions of technical lignins. *ChemSusChem* **2017,** *10* (3), 629-635.

137. Brunow, G., Methods to reveal the structure of lignin. *Biopolymers Online: Biology• Chemistry• Biotechnology• Applications* **2005,** *1*.

138. Hatakeyama, H., Thermal analysis of lignin by differential scanning calorimetry. *Cellul. Chem. Technol.* **1972,** *6*, 521-529.

139. Hatakeyama, H.; Tsujimoto, Y.; Zarubin, M. J.; Krutov, S. M.; Hatakeyama, T., Thermal decomposition and glass transition of industrial hydrolysis lignin. *Journal of Thermal Analysis and Calorimetry* **2010,** *101* (1), 289-295.

140. Olsson, A. M. a. S., L., The effect of lignin composition on the viscoelastic properties of wood. *Nord Pulp Paper Res J.* **1997,** *12* (3), 140-144.

141. Li, H.; McDonald, A. G., Fractionation and characterization of industrial lignins. *Industrial Crops and Products* **2014,** *62*, 67-76.

142. Belgacem, M. N. G., A., Lignins as Components of Macromolecular Materials. *In Monomers, polymers and composites from renewable resources* **2008**, 243-271.

143. Nikafshar, S.; Wang, J.; Dunne, K.; Sangthonganotai, P.; Nejad, M., Choosing the Right Lignin to Fully Replace Bisphenol A in Epoxy Resin Formulation. *ChemSusChem* **2021,** *14* (4), 1184.

144. Malutan, T.; Nicu, R.; Popa, V. I., Lignin modification by epoxidation. *BioResources* **2008,** *3* (4), 1371-13767.

145. Nejad, M.; Nikafshar, S. U.S. Provisional Patent Application, filed December 22, 2020.

146. International, A., ASTM D 1652-97: Standard Test Methods for Epoxy Content of Epoxy Resins. Catalog: 1997.

147. Fang, Z.; Nikafshar, S.; Hegg, E. L.; Nejad, M., Biobased Divanillin as a Precursor for Formulating Biobased Epoxy Resin. *ACS Sustainable Chemistry & Engineering* **2020**.

148. Gioia, C.; Colonna, M.; Tagami, A.; Medina, L.; Sevastyanova, O.; Berglund, L. A.; Lawoko, M., Lignin-based epoxy resins: unravelling the relationship between structure and material properties. *Biomacromolecules* **2020**.

149. Fache, M.; Darroman, E.; Besse, V.; Auvergne, R.; Caillol, S.; Boutevin, B., Vanillin, a promising biobased building-block for monomer synthesis. *Green Chemistry* **2014,** *16* (4), 1987-1998.

150. Li, B.; Zhou, M.; Huo, W.; Cai, D.; Qin, P.; Cao, H.; Tan, T., Fractionation and oxypropylation of corn-stover lignin for the production of biobased rigid polyurethane foam. *Industrial Crops and Products* **2020,** *143*, 111887.

151. Xin, J.; Li, M.; Li, R.; Wolcott, M. P.; Zhang, J., Green epoxy resin system based on lignin and tung oil and its application in epoxy asphalt. *ACS Sustainable Chemistry & Engineering* **2016,** *4* (5), 2754-2761.

152. Savonnet, E.; Grau, E.; Grelier, S.; Defoort, B.; Cramail, H., Divanillin-Based Epoxy Precursors as DGEBA Substitutes for Biobased Epoxy Thermosets. *ACS Sustainable Chemistry & Engineering* **2018,** *6* (8), 11008-11017.

153. Chiu, Y.-C.; Chou, I.-C.; Tseng, W.-C.; Ma, C.-C. M., Preparation and thermal properties of diglycidylether sulfone epoxy. *Polym. Degrad. Stab.* **2008,** *93* (3), 668-676.

154. Domínguez, J.; Oliet, M.; Alonso, M.; Gilarranz, M.; Rodríguez, F., Thermal stability and pyrolysis kinetics of organosolv lignins obtained from Eucalyptus globulus. *Industrial crops and products* **2008,** *27* (2), 150-156.

155. Hafiezal, M. R. M.; Khalina, A.; Zurina, Z. A.; Azaman, M. D. M.; Hanafee, Z. M., Thermal and flammability characteristics of blended jatropha bio-epoxy as matrix in carbon fiber–reinforced polymer. *Journal of Composites Science* **2019,** *3* (1), 6.

156. Harvey, B. G.; Guenthner, A. J.; Meylemans, H. A.; Haines, S. R.; Lamison, K. R.; Groshens, T. J.; Cambrea, L. R.; Davis, M. C.; Lai, W. W., Renewable thermosetting resins and thermoplastics from vanillin. *Green Chemistry* **2015,** *17* (2), 1249-1258.

157. Yang, Y.; Deng, Y.; Tong, Z.; Wang, C., Renewable lignin-based xerogels with self-cleaning properties and superhydrophobicity. *ACS Sustainable Chemistry & Engineering* **2014,** *2* (7), 1729-1733.

158. Tellers, J.; Jamali, M.; Willems, P.; Tjeerdsma, B.; Sbirrazzuoli, N.; Guigo, N., Cross-linking behavior of eutectic hardeners from natural acid mixtures. *Green Chemistry* **2021,** *23* (1), 536-545.

159. Zakzeski, J.; Bruijnincx, P. C.; Jongerius, A. L.; Weckhuysen, B. M., The catalytic valorization of lignin for the production of renewable chemicals. *Chem. Rev.* **2010,** *110* (6), 3552-3599.

160. Crestini, C.; Lange, H.; Sette, M.; Argyropoulos, D. S., On the structure of softwood kraft lignin. *Green Chemistry* **2017,** *19* (17), 4104-4121.

161. GELLERSTEDT, G.; GIERER, J., The Reactions of Lignin during Neutral Sulphite Cooking. *Acta Chem. Scand.* **1968,** *22* (8), 2510-2518.

162. Gioia, C.; Lo Re, G.; Lawoko, M.; Berglund, L., Tunable thermosetting epoxies based on fractionated and well-characterized lignins. *J. Am. Chem. Soc.* **2018,** *140* (11), 4054-4061.

163. Gioia, C.; Colonna, M.; Tagami, A.; Medina, L.; Sevastyanova, O.; Berglund, L. A.; Lawoko, M., Lignin-based epoxy resins: Unravelling the relationship between structure and material properties. *Biomacromolecules* **2020,** *21* (5), 1920-1928.

164. Clary, J.; Feron, V.; Van Velthuijsen, J., Safety assessment of lactate esters. *Regulatory toxicology and pharmacology* **1998,** *27* (2), 88-97.

165. Paul, S.; Pradhan, K.; R Das, A., Ethyl lactate as a green solvent: a promising bio-compatible media for organic synthesis. *Current Green Chemistry* **2016,** *3* (1), 111-118.

166. Clark, J. H.; Tavener, S. J., Alternative solvents: shades of green. *Organic process research & development* **2007,** *11* (1), 149-155.

167. MacKinnon, A. J.; Jenkins, S. D.; McGrail, P. T.; Pethrick, R. A., A dielectric, mechanical, rheological and electron microscopy study of cure and properties of a thermoplastic-modified epoxy resin. *Macromolecules* **1992,** *25* (13), 3492-3499.

168. Núñez-Regueira, L.; Gracia-Fernández, C.; Gómez-Barreiro, S., Use of rheology, dielectric analysis and differential scanning calorimetry for gel time determination of a thermoset. *Polymer* **2005,** *46* (16), 5979-5985.

169. Park, B.-D.; Riedl, B.; Hsu, E. W.; Shields, J., Differential scanning calorimetry of phenol–formaldehyde resins cure-accelerated by carbonates. *Polymer* **1999,** *40* (7), 1689-1699.

170. Vickers, N. J., Animal communication: when i'm calling you, will you answer too? *Current biology* **2017,** *27* (14), R713-R715.

171. Prime, R. B., Thermoset in Thermal Characterization of Polymeric Materials. 1997.

172. Winter, H. H., Can the gel point of a cross-linking polymer be detected by the G′–G ″crossover? *Polymer Engineering & Science* **1987,** *27* (22), 1698-1702.

173. Vyazovkin, S.; Sbirrazzuoli, N., Mechanism and kinetics of epoxy− amine cure studied by differential scanning calorimetry. *Macromolecules* **1996,** *29* (6), 1867-1873.

174. Teil, H.; Page, S.; Michaud, V.; Månson, J. A., TTT-cure diagram of an anhydride-cured epoxy system including gelation, vitrification, curing kinetics model, and monitoring of the glass transition temperature. *J. Appl. Polym. Sci.* **2004,** *93* (4), 1774-1787.

175. Cadenato, A.; Salla, J.; Ramis, X.; Morancho, J.; Marroyo, L.; Martin, J., Determination of gel and vitrification times of thermoset curing process by means of TMA, DMTA and DSC techniques: TTT diagram. *J. Therm. Anal. Calorim.* **1997,** *49* (1), 269-279.

176. Flory, P. J., *Principles of polymer chemistry*. Cornell University Press: 1953.

177. Stockmayer, W., Errata: Molecular distribution in condensation polymers. *J. Polym. Sci* **1953,** *11*, 424.

178. Shechter, L.; Wynstra, J.; Kurkjy, R. P., Glycidyl ether reactions with amines. *Industrial & Engineering Chemistry* **1956,** *48* (1), 94-97.

179. Thomas, S.; Sinturel, C.; Thomas, R., *Micro and nanostructured epoxy/rubber blends*. John Wiley & Sons: 2014.

180. Hong, S.-G.; Wu, C.-S., DSC and FTIR analyses of the curing behavior of epoxy/dicy/solvent systems on hermetic specimens. *J. Therm. Anal. Calorim.* **2000,** *59* (3), 711-719.

181. Wang, Z.; Yang, X.; Zhou, Y.; Liu, C., Mechanical and thermal properties of polyurethane films from peroxy-acid wheat straw lignin. *BioResources* **2013,** *8* (3), 3833-3843.

182. Thring, R.; Vanderlaan, M.; Griffin, S., Polyurethanes from Alcell® lignin. *Biomass and Bioenergy* **1997,** *13* (3), 125-132.

183. Klein, S. E.; Rumpf, J.; Kusch, P.; Albach, R.; Rehahn, M.; Witzleben, S.; Schulze, M., Unmodified kraft lignin isolated at room temperature from aqueous solution for preparation of highly flexible transparent polyurethane coatings. *RSC advances* **2018,** *8* (71), 40765-40777.

184. Griffini, G.; Passoni, V.; Suriano, R.; Levi, M.; Turri, S., Polyurethane Coatings Based on Chemically Unmodified Fractionated Lignin. *ACS Sustainable Chemistry & Engineering* **2015,** *3* (6), 1145-1154.

185. Mahmood, N.; Yuan, Z.; Schmidt, J.; Xu, C. C., Depolymerization of lignins and their applications for the preparation of polyols and rigid polyurethane foams: A review. *Renewable and Sustainable Energy Reviews* **2016,** *60*, 317-329.

186. Klein, S. E.; Alzagameem, A.; Rumpf, J.; Korte, I.; Kreyenschmidt, J.; Schulze, M., Antimicrobial activity of lignin-derived polyurethane coatings prepared from unmodified and demethylated lignins. *Coatings* **2019,** *9* (8), 494.

187. Wang, Z.; Yang, X.; Zhou, Y.; Liu, C., *Mechanical and Thermal Properties of Polyurethane Films from Peroxy-acid Wheat Straw Lignin*. 2013; Vol. 8.

188. Manock, H., New developments in polyurethane and PU/acrylic dispersions. *Pigment & resin technology* **2000**.

189. Szycher, M., Waterborne polyurethanes. *Handbook of Polyurethanes, 2nd ed.; Szycher, M., Ed* **2012**, 417-448.

190. Fu, C.; Zheng, Z.; Yang, Z.; Chen, Y.; Shen, L., A fully bio-based waterborne polyurethane dispersion from vegetable oils: From synthesis of precursors by thiol-ene reaction to study of final material. *Prog. Org. Coat.* **2014,** *77* (1), 53-60.

191. Liu, L.; Lu, J.; Zhang, Y.; Liang, H.; Liang, D.; Jiang, J.; Lu, Q.; Quirino, R. L.; Zhang, C., Thermosetting polyurethanes prepared with the aid of a fully bio-based emulsifier with high bio-content, high solid content, and superior mechanical properties. *Green Chemistry* **2019,** *21* (3), 526-537.

192. Liang, H.; Feng, Y.; Lu, J.; Liu, L.; Yang, Z.; Luo, Y.; Zhang, Y.; Zhang, C., Bio-based cationic waterborne polyurethanes dispersions prepared from different vegetable oils. *Industrial Crops and Products* **2018,** *122*, 448-455.

193. Man, L.; Feng, Y.; Hu, Y.; Yuan, T.; Yang, Z., A renewable and multifunctional eco-friendly coating from novel tung oil-based cationic waterborne polyurethane dispersions. *Journal of Cleaner Production* **2019,** *241*, 118341.

194. Patel, C. J.; Mannari, V., Air-drying bio-based polyurethane dispersion from cardanol: Synthesis and characterization of coatings. *Prog. Org. Coat.* **2014,** *77* (5), 997-1006.

195. Lai, Y.; Qian, Y.; Yang, D.; Qiu, X.; Zhou, M., Preparation and performance of lignin-based waterborne polyurethane emulsion. *Industrial Crops and Products* **2021,** *170*, 113739.

196. Krishna, S. H.; Assary, R. S.; Rashke, Q. A.; Schmidt, Z. R.; Curtiss, L. A.; Dumesic, J. A.; Huber, G. W., Mechanistic insights into the hydrogenolysis of levoglucosanol over bifunctional platinum silica–alumina catalysts. *ACS Catalysis* **2018,** *8* (5), 3743-3753.

197. Mouterde, L. M.; Allais, F.; Stewart, J. D., Enzymatic reduction of levoglucosenone by an alkene reductase (OYE 2.6): a sustainable metal-and dihydrogen-free access to the bio-based solvent Cyrene®. *Green Chemistry* **2018,** *20* (24), 5528-5532.

198. McElroy, C. R.; Farmer, T. J.; Duncan, T.; Raverty, W.; Hunta, A. J.; Clark, J. H., Dihydrolevoglucosenone (Cyrene) as a bio-based alternative for dipolar aprotic solvents1. *Chem. Commun* **2014,** *50*, 9650-9652.

199. Mistry, L.; Mapesa, K.; Bousfield, T. W.; Camp, J. E., Synthesis of ureas in the bio-alternative solvent Cyrene. *Green Chemistry* **2017,** *19* (9), 2123-2128.

200. Zhang, J.; White, G. B.; Ryan, M. D.; Hunt, A. J.; Katz, M. J., Dihydrolevoglucosenone (Cyrene) as a green alternative to N, N-dimethylformamide (DMF) in MOF synthesis. *ACS Sustainable Chemistry & Engineering* **2016,** *4* (12), 7186-7192.

201. Hughes, L.; McElroy, C. R.; Whitwood, A. C.; Hunt, A. J., Development of pharmaceutically relevant bio-based intermediates though aldol condensation and Claisen–Schmidt reactions of dihydrolevoglucosenone (Cyrene®). *Green Chemistry* **2018,** *20* (19), 4423-4427.

202. Ray, P.; Hughes, T.; Smith, C.; Hibbert, M.; Saito, K.; Simon, G. P., Development of bio-acrylic polymers from Cyrene™: transforming a green solvent to a green polymer. *Polymer Chemistry* **2019,** *10* (24), 3334-3341.

203. Meng, X.; Pu, Y.; Li, M.; Ragauskas, A. J., A biomass pretreatment using cellulose-derived solvent Cyrene. *Green Chemistry* **2020,** *22* (9), 2862-2872.

204. Evans, P. D., Weathering of wood and wood composites. In *Handbook of wood chemistry and wood composites*, CRC Press: 2012; pp 166-231.

205. Hon, D. N. S., ESCA study of oxidized wood surfaces. *Journal of Applied Polymer Science* **1984,** *29* (9), 2777-2784.

206. Turkulin, H.; Sell, J., Structural and fractographic study on weathered wood. **1997**.

207. Nejad, M.; Cooper, P., Exterior wood coatings. Part-1: Performance of semitransparent stains on preservative-treated wood. *Journal of coatings technology and research* **2011,** *8* (4), 449-458.

208. Hayoz, P.; Peter, W.; Rogez, D., A new innovative stabilization method for the protection of natural wood. *Progress in organic coatings* **2003,** *48* (2-4), 297-309.

209. Sakakibara, A.; Sano, Y., Chemistry of lignin. *Wood and cellulosic chemistry* **2000,** *2*, 109-173.

210. Davidson, R. S., The photodegradation of some naturally occurring polymers. *Journal of Photochemistry and Photobiology B: Biology* **1996,** *33* (1), 3-25.

211. Kutz, M., *Handbook of environmental degradation of materials*. William Andrew: 2018.

212. Müller, U.; Rätzsch, M.; Schwanninger, M.; Steiner, M.; Zöbl, H., Yellowing and IR-changes of spruce wood as result of UV-irradiation. *Journal of Photochemistry and Photobiology B: Biology* **2003,** *69* (2), 97-105.

213. Williams, R. S., Weathering of wood. *Handbook of wood chemistry and wood composites* **2005,** *7*, 139-185.

214. Hon, D. N.-S.; Shiraishi, N., *Wood and cellulosic chemistry, revised, and expanded*. CRC press: 2000.

215. Umezawa, T., Chemistry of extractives. *Wood and cellulosic chemistry* **2000,** *2*, 213-242.

216. Funaoka, K.; Kuroda, Y.; Kai, Y.; Kondo, T., On the phenolic constituents from Cryptomeria japonica D. Don. I. Isolation and a few characteristics of two phenolic substances. *Mokuzai Gakkaishi* **1963,** *9*, 139-141.

217. Abe, Z., The color change of sugi (Cryptomeria japonica D. Don) heartwood from reddish brown to black. I. The color changes and its causes. *Mokuzai Gakkaishi* **1994,** *40*, 1119-1125.

218. Chang, S.-T.; Wang, S.-Y.; Su, Y.-C.; Huang, S.-L.; Kuo, Y.-H., Chemical constituents and mechanisms of discoloration of Taiwania (Taiwania cryptomerioides Hayata) Heartwood. The structure reconfirmation and conversion mechanism of Taiwanin A. **1999**.

219. Pandey, K. K., A note on the influence of extractives on the photo-discoloration and photo-degradation of wood. *Polym. Degrad. Stab.* **2005,** *87* (2), 375-379.

220. Kataoka, Y.; Kiguchi, M.; Williams, R. S.; Evans, P. D. In *The effects of wavelength on photodegradation depth profiles in Japanese cedar (Cryptomeria japonica D. Don) earlywood*, Proceedings of the Fifth International Woodcoatings Congress: Enhancing Service Life, 2006 October 17-18, Prague, Czech Republic. Middlesex, UK: PRA Coatings Technology Centre, c2006: 11 p.: ISBN: 9780955131745: 095513174X, 2006; pp 1-11.

221. Kalnins, M. A., Surface characteristics of wood as they affect durability of finishes. Part II. Photochemical degradation of wood. *U.S. Forest Service Res. Pap. FPL 57, Madison, WI, U.S. Department of Agriculture,* **1966,** *57*, 23–57.

222. Hon, D.-S.; Chang, S.-T.; Feist, W., Participation of singlet oxygen in the photodegradation of wood surfaces. *Wood Science and Technology* **1982,** *16* (3), 193-201.

223. Hon, D. N.-S., Weathering and photochemistry of wood. *Wood and cellulosic chemistry* **2001,** *2*, 512-546.

224. Chang, S.-T.; Hon, D. N.-S.; Feist, W. C., Photodegradation and photoprotection of wood surfaces. *Wood and Fiber Science* **2007,** *14* (2), 104-117.

225. Evans, P.; Schmalzl, K., A quantitative weathering study of wood surfaces modified by chromium VI and iron III compounds. Part 1. Loss in zero-span tensile strength and weight of thin wood veneers. *Holzforschung-International Journal of the Biology, Chemistry, Physics and Technology of Wood* **1989,** *43* (5), 289-292.

226. Schmalzl, K.; Evans, P., Wood surface protection with some titanium, zirconium and manganese compounds. *Polym. Degrad. Stab.* **2003,** *82* (3), 409-419.

227. Rowell, R. M.; RM, R.; WD, E., Weathering of chemically modified southern pine. **1981**.

228. Feist, W. C.; Rowell, R. M.; Ellis, W. D., Moisture sorption and accelerated weathering of acetylated and methacrylated aspen. *Wood and Fiber Science* **2007,** *23* (1), 128-136.

229. Evans, P.; Owen, N.; Schmid, S.; Webster, R., Weathering and photostability of benzoylated wood. *Polym. Degrad. Stab.* **2002,** *76* (2), 291-303.

230. Rowell, R.; Feist, W.; Ellis, W., Weathering of chemically modified southern pine [Polymer lumen fill treatments]. *Wood Science* **1981,** *13*, 202-208.

231. Xie, Y.; Krause, A.; Militz, H.; Mai, C., Weathering of uncoated and coated wood treated with methylated 1, 3-dimethylol-4, 5-dihydroxyethyleneurea (mDMDHEU). *Holz als Roh-und Werkstoff* **2008,** *66* (6), 455.

232. Nikafshar, S.; Zabihi, O.; Ahmadi, M.; Mirmohseni, A.; Taseidifar, M.; Naebe, M., The effects of UV light on the chemical and mechanical properties of a transparent epoxy-diamine system in the presence of an organic UV absorber. *Materials* **2017,** *10* (2), 180.

233. Saha, S.; Kocaefe, D.; Boluk, Y.; Pichette, A., Surface degradation of CeO2 stabilized acrylic polyurethane coated thermally treated jack pine during accelerated weathering. *Applied surface science* **2013,** *276*, 86-94.

234. Forsthuber, B.; Grüll, G., The effects of HALS in the prevention of photo-degradation of acrylic clear topcoats and wooden surfaces. *Polymer degradation and stability* **2010,** *95* (5), 746-755.

235. Van den Bulcke, J.; Rijckaert, V.; Van Acker, J.; Stevens, M., Adhesion and weathering performance of waterborne coatings applied to different temperate and tropical wood species. *JCT research* **2006,** *3* (3), 185-192.

236. Saiter, J.; Delahaye, N.; Liziard, M.; Podgorski, L., Characterization of alkyd based thermosetting resins. *J. Therm. Anal.* **1995,** *45* (5), 1145-1151.

237. Schaller, C.; Rogez, D.; Braig, A., Hydroxyphenyl-s-triazines: advanced multipurpose UV-absorbers for coatings. *Journal of Coatings Technology and Research* **2008,** *5* (1), 25-31.

238. Decker, C.; Biry, S.; Zahouily, K., Photostabilisation of organic coatings. *Polymer degradation and stability* **1995,** *49* (1), 111-119.

239. Klemchuk, P. P.; Gande, M. E.; Cordola, E., Hindered amine mechanisms: Part III—investigations using isotopic labelling. *Polymer degradation and stability* **1990,** *27* (1), 65-74.

240. Morris, P.; McFarling, S. In *Enhancing the performance of transparent coatings by UV protective pretreatments*, Proceedings of the International Research Group on Wood Protection Meeting, Tromsø, Norway, 2006; pp 18-22.

241. Salla, J.; Pandey, K. K.; Srinivas, K., Improvement of UV resistance of wood surfaces by using ZnO nanoparticles. *Polymer Degradation and Stability* **2012,** *97* (4), 592-596.

242. Nkeuwa, W. N.; Riedl, B.; Landry, V., Wood surfaces protected with transparent multilayer UV-cured coatings reinforced with nanosilica and nanoclay. Part II: Application of a standardized test method to study the effect of relative humidity on scratch resistance. *Journal of Coatings Technology and Research* **2014,** *11* (6), 993-1011.

243. Evans, P. D.; Haase, J. G.; Seman, A. S.; Kiguchi, M., The search for durable exterior clear coatings for wood. *Coatings* **2015,** *5* (4), 830-864.

244. de Meijer, M.; Nienhuis, J., Influence of internal stress and extensibility on the exterior durability of wood coatings. *Prog. Org. Coat.* **2009,** *65* (4), 498-503.

245. Passauer, L.; Schubert, J.; Schulz, T.; Flade, P.; Weiß, B.; Burkhardt, H., Artificial weathering of surfaces from laminated phenol-formaldehyde resin impregnated compressed wood: impact of top veneer type and overlay application. *European Journal of Wood and Wood Products* **2021,** *79* (3), 567-578.

246. Tolvaj, L.; Mitsui, K., Correlation between hue angle and lightness of light irradiated wood. *Polym. Degrad. Stab.* **2010,** *95* (4), 638-642.

247. Mandlekar, N.; Cayla, A.; Rault, F.; Giraud, S.; Salaün, F.; Malucelli, G.; Guan, J.-P., An overview on the use of lignin and its derivatives in fire retardant polymer systems. *Lignin–Trends and Applications. InTech* **2018**, 207-231.

248. 927-6, E., Paints and varnishes. Coating materials and coating systems for exterior wood. Part 3: Natural weathering test. European Committee for Standardization Brussels: 2006.

249. Anderson, E. L.; Pawlak, Z.; Owen, N. L.; Feist, W. C., Infrared studies of wood weathering. Part I: Softwoods. *Appl. Spectrosc.* **1991,** *45* (4), 641-647.

250. Pandey, K. K., Study of the effect of photo-irradiation on the surface chemistry of wood. *Polymer degradation and Stability* **2005,** *90* (1), 9-20.

251. Kline, L. M.; Hayes, D. G.; Womac, A. R.; Labbe, N., Simplified determination of lignin content in hard and soft woods via UV-spectrophotometric analysis of biomass dissolved in ionic liquids. *BioResources* **2010,** *5* (3), 1366-1383.

252. Stark, N. M.; Matuana, L. M., Surface chemistry and mechanical property changes of wood-flour/high-density-polyethylene composites after accelerated weathering. *J. Appl. Polym. Sci.* **2004,** *94* (6), 2263-2273.

253. Popescu, C.-M.; Popescu, M.-C.; Vasile, C., Structural analysis of photodegraded lime wood by means of FT-IR and 2D IR correlation spectroscopy. *International journal of biological macromolecules* **2011,** *48* (4), 667-675.

254. Ganne-Chédeville, C.; Jääskeläinen, A.-S.; Froidevaux, J.; Hughes, M.; Navi, P., Natural and artificial ageing of spruce wood as observed by FTIR-ATR and UVRR spectroscopy. *Holzforschung* **2012,** *66* (2), 163-170.

255. Rowell, R., The chemistry of solid wood. *The chemistry of solid wood.* **1984**.

256. Feist, W. C.; Hon, D. N.-S., Chemistry of weathering and protection. *The chemistry of solid wood* **1984,** *207*, 401-451.

257. Argyropoulos, D. S.; Sun, Y., Photochemically induced solid-state degradation, condensation, and rearrangement reactions in lignin model compounds and milled wood lignin. *Photochem. Photobiol.* **1996,** *64* (3), 510-517.

258. Castellan, A.; Zhu, J.; Colombo, N.; Nourmamode, A.; Davidson, R.; Dunn, L., An approach to understanding the mechanism of protection of bleached high-yield pulps against photoyellowing by reducing agents using the lignin model dimer: 3, 4-dimethoxy-a-(2′-methoxyphenoxy)-acetophenone. *Journal of Photochemistry and Photobiology A: Chemistry* **1991,** *58* (2), 263-273.

259. Holmbom, B., Analysis of chemical changes caused by exposure to light and bleaching of spruce groundwood. *Mitteilungen der Bundesforschungsanstalt fuer Forst-und Holzwirtschaft (Germany, FR)* **1991**.

260. Azadfalah, M.; Mirshokraei, S. A.; JAHAN, L. A.; PARSAPAZHOUH, D., Analysis of photodegraded lignin on cellulose matrix by means of FTIR spectroscopy and high pressure size exclusion chromatography. **2008**.

261. Aloui, F.; Ahajji, A.; Irmouli, Y.; George, B.; Charrier, B.; Merlin, A., Inorganic UV absorbers for the photostabilisation of wood-clearcoating systems: Comparison with organic UV absorbers. *Applied surface science* **2007,** *253* (8), 3737-3745.

262. Hill, L.; Korzeniowski, H.; Ojunga-Andrew, M.; Wilson, R., Accelerated clearcoat weathering studied by dynamic mechanical analysis. *Progress in organic coatings* **1994,** *24* (1-4), 147-173.

263. Wang, J.; Deng, Y.; Qian, Y.; Qiu, X.; Ren, Y.; Yang, D., Reduction of lignin color via one-step UV irradiation. *Green Chemistry* **2016,** *18* (3), 695-699.

264. Dao, N. N.; Dai Luu, M.; Nguyen, Q. K.; Kim, B. S., UV absorption by cerium oxide nanoparticles/epoxy composite thin films. *Advances in Natural Sciences: Nanoscience and Nanotechnology* **2011,** *2* (4), 045013.

265. Jia, H.; Wang, H.; Chen, W., The combination effect of hindered amine light stabilizers with UV absorbers on the radiation resistance of polypropylene. *Radiat. Phys. Chem.* **2007,** *76* (7), 1179-1188.

266. Soren, S.; Kumar, S.; Mishra, S.; Jena, P. K.; Verma, S. K.; Parhi, P., Evaluation of antibacterial and antioxidant potential of the zinc oxide nanoparticles synthesized by aqueous and polyol method. *Microbial Pathogenesis* **2018,** *119*, 145-151.

267. Kumar, B.; Smita, K.; Cumbal, L.; Debut, A., Green approach for fabrication and applications of zinc oxide nanoparticles. *Bioinorganic chemistry and applications* **2014,** *2014*.

268. Pánek, M.; Oberhofnerová, E.; Hýsek, Š.; Šedivka, P.; Zeidler, A., Colour stabilization of oak, spruce, larch and douglas fir heartwood treated with mixtures of nanoparticle dispersions and UV-stabilizers after exposure to UV and VIS-radiation. *Materials* **2018,** *11* (9), 1653.

269. Nikafshar, S.; McCracken, J.; Dunne, K.; Nejad, M., Improving UV-Stability of epoxy coating using encapsulated halloysite nanotubes with organic UV-Stabilizers and lignin. *Progress in Organic Coatings* **2021,** *151*, 105843.

270. Awaja, F.; Pigram, P. J., Surface molecular characterisation of different epoxy resin composites subjected to UV accelerated degradation using XPS and ToF-SIMS. *Polymer Degradation and Stability* **2009,** *94* (4), 651-658.

271. Musto, P.; Abbate, M.; Pannico, M.; Scarinzi, G.; Ragosta, G., Improving the photo-oxidative stability of epoxy resins by use of functional POSS additives: A spectroscopic, mechanical and morphological study. *Polymer* **2012,** *53* (22), 5016-5036.

272. Jin, F.-L.; Li, X.; Park, S.-J., Synthesis and application of epoxy resins: A review. *Journal of Industrial and Engineering Chemistry* **2015,** *29*, 1-11.

273. Makki, H.; Adema, K. N.; Hendrix, M. M.; Peters, E. A.; Laven, J.; Van Der Ven, L. G.; Van Benthem, R. A.; de With, G., Weathering of a polyester-urethane clearcoat: lateral inhomogeneities. *Polymer Degradation and Stability* **2015,** *122*, 180-186.

274. Adema, K. N.; Makki, H.; Peters, E. A.; Laven, J.; van der Ven, L. G.; van Benthem, R. A.; de With, G., The influence of the exposure conditions on the chemical and physical changes of polyester–urethane coatings during photodegradation. *Polymer Degradation and Stability* **2016,** *123*, 13-25.

275. Nguyen, T. V.; Tri, P. N.; Nguyen, T. D.; El Aidani, R.; Trinh, V. T.; Decker, C., Accelerated degradation of water borne acrylic nanocomposites used in outdoor protective coatings. *Polymer Degradation and Stability* **2016,** *128*, 65-76.

276. Rabek, J. F., *Polymer photodegradation: mechanisms and experimental methods*. Springer Science & Business Media: 2012.

277. Asmatulu, R.; Mahmud, G. A.; Hille, C.; Misak, H. E., Effects of UV degradation on surface hydrophobicity, crack, and thickness of MWCNT-based nanocomposite coatings. *Progress in Organic Coatings* **2011,** *72* (3), 553-561.

278. Chou, P.-L.; Chang, H.-T.; Yeh, T.-F.; Chang, S.-T., Characterizing the conservation effect of clear coatings on photodegradation of wood. *Bioresource technology* **2008,** *99* (5), 1073-1079.

279. Pospisil, J.; Klemchuk, P. P., *Oxidation inhibition in organic materials*. CRC Press: 1989; Vol. 1.

280. Kiguchi, M.; Evans, P.; Ekstedt, J.; Williams, R.; Kataoka, Y., Improvement of the durability of clear coatings by grafting of UV-absorbers on to wood. *Surface coatings international Part B: Coatings transactions* **2001,** *84* (4), 263.

281. Olsson, S.; Johansson, M.; Westin, M.; Östmark, E., Grafting of 2-hydroxy-4 (2, 3-epoxypropoxy)-benzophenone and epoxidized soybean oil to wood: Reaction conditions and effects on the color stability of Scots pine. *Polymer degradation and stability* **2012,** *97* (9), 1779-1786.

282. Parimalam, M.; Islam, M. R.; Yunus, R. M., Effects of nanosilica, zinc oxide, titatinum oxide on the performance of epoxy hybrid nanocoating in presence of rubber latex. *Polymer Testing* **2018,** *70*, 197-207.

283. Islam, M.; Yahaya, A.; Isa, N., Effects of zinc oxide on pretreated multiwalled-carbon-nanotube-reinforced biobased polyesters. *Journal of Applied Polymer Science* **2017,** *134* (12).

284. Parimalam, M.; Islam, M.; Yunus, R.; Rashidi, N., Effects of Colloidal Nanosilica on Epoxy-based Nanocomposite Coatings. *Progress in Color, Colorants and Coatings* **2019,** *12* (2), 71-82.

285. Parimalam, M.; Islam, M. R.; Yunus, R. M., Effects of nanosilica and titanium oxide on the performance of epoxy–amine nanocoatings. *Journal of Applied Polymer Science* **2019,** *136* (35), 47901.

286. Li, Y.-Q.; Fu, S.-Y.; Mai, Y.-W., Preparation and characterization of transparent ZnO/epoxy nanocomposites with high-UV shielding efficiency. *Polymer* **2006,** *47* (6), 2127-2132.

287. Manaia, E. B.; Kaminski, R. C. K.; Corrêa1, M. A.; Chiavacci, L. A., Inorganic UV filters. *Brazilian Journal of Pharmaceutical Sciences* **2013,** *49* (2), 201-209.

288. Kai, D.; Tan, M. J.; Chee, P. L.; Chua, Y. K.; Yap, Y. L.; Loh, X. J., Towards lignin-based functional materials in a sustainable world. *Green Chemistry* **2016,** *18* (5), 1175-1200.

289. Beisl, S.; Friedl, A.; Miltner, A., Lignin from micro-to nanosize: applications. *International journal of molecular sciences* **2017,** *18* (11), 2367.

290. Hilburg, S. L.; Elder, A. N.; Chung, H.; Ferebee, R. L.; Bockstaller, M. R.; Washburn, N. R., A universal route towards thermoplastic lignin composites with improved mechanical properties. *Polymer* **2014,** *55* (4), 995-1003.

291. Guo, X.; Xin, J.; Huang, J.; Wolcott, M. P.; Zhang, J., Preparation and toughening of mechanochemically modified lignin-based epoxy. *Polymer* **2019,** *183*, 121859.

292. Queant, C.; Blanchet, P.; Landry, V.; Schorr, D., Comparison of two encapsulation systems of UV stabilizers on the UV protection efficiency of wood clear coats. *Journal of Polymer Engineering* **2018,** *39* (1), 94-103.

293. Lvov, Y.; Wang, W.; Zhang, L.; Fakhrullin, R., Halloysite clay nanotubes for loading and sustained release of functional compounds. *Advanced Materials* **2016,** *28* (6), 1227-1250.

294. De Silva, R.; Pasbakhsh, P.; Goh, K.; Chai, S.-P.; Chen, J., Synthesis and characterisation of poly (lactic acid)/halloysite bionanocomposite films. *Journal of Composite Materials* **2014,** *48* (30), 3705-3717.

295. Lvov, Y. M.; Shchukin, D. G.; Möhwald, H.; Price, R. R., Halloysite Clay Nanotubes for Controlled Release of Protective Agents. *ACS Nano* **2008,** *2* (5), 814-820.

296. Ismail, H.; Pasbakhsh, P.; Fauzi, M. A.; Bakar, A. A., Morphological, thermal and tensile properties of halloysite nanotubes filled ethylene propylene diene monomer (EPDM) nanocomposites. *Polymer Testing* **2008,** *27* (7), 841-850.

297. Kaynak, C.; Kaygusuz, I., Consequences of accelerated weathering in polylactide nanocomposites reinforced with halloysite nanotubes. *Journal of Composite Materials* **2016,** *50* (3), 365-375.

298. Tzounis, L.; Herlekar, S.; Tzounis, A.; Charisiou, N. D.; Goula, M.; Stamm, M., Halloysite nanotubes noncovalently functionalised with SDS anionic surfactant and PS-b-P4VP block copolymer for their effective dispersion in polystyrene as UV-blocking nanocomposite films. *Journal of Nanomaterials* **2017,** *2017*.

299. Hu, D.; Zhang, Z.; Liu, M.; Lin, J.; Chen, X.; Ma, W., Multifunctional UV-shielding nanocellulose films modified with halloysite nanotubes-zinc oxide nanohybrid. *Cellulose* **2020,** *27* (1), 401-413.

300. Lim, K.; Chow, W.; Pung, S., Accelerated Weathering and UV Protection-Ability of Poly (lactic acid) Nanocomposites Containing Zinc Oxide Treated Halloysite Nanotube. *Journal of Polymers and the Environment* **2019,** *27* (8), 1746-1759.

301. Cervini-Silva, J.; Nieto-Camacho, A.; Palacios, E.; Montoya, J. A.; Gómez-Vidales, V.; Ramírez-Apán, M. T., Anti-inflammatory and anti-bacterial activity, and cytotoxicity of halloysite surfaces. *Colloids and Surfaces B: Biointerfaces* **2013,** *111*, 651-655.

302. Nejad, M.; Nikafshar, S. Nanotube-Encapsulated UV Stabilizers. 2019.

303. Lee, M.; Mun, C.; Kim, D.-H.; Chang, S.-C.; Park, S.-G., Analyte-concentrating 3D hybrid plasmonic nanostructures for use in highly sensitive chemical sensors. *RSC advances* **2016,** *6* (94), 92120-92126.

304. Guo, H.; Klose, D.; Hou, Y.; Jeschke, G.; Burgert, I., Highly efficient UV protection of the biomaterial wood by a transparent TiO2/Ce xerogel. *ACS applied materials & interfaces* **2017,** *9* (44), 39040-39047.

305. He, Y.; Xu, W.; Tang, R.; Zhang, C.; Yang, Q., pH-Responsive nanovalves based on encapsulated halloysite for the controlled release of a corrosion inhibitor in epoxy coating. *RSC Advances* **2015,** *5* (110), 90609-90620.

306. Makaremi, M.; Pasbakhsh, P.; Cavallaro, G.; Lazzara, G.; Aw, Y. K.; Lee, S. M.; Milioto, S., Effect of morphology and size of halloysite nanotubes on functional pectin bionanocomposites for food packaging applications. *ACS applied materials & interfaces* **2017,** *9* (20), 17476-17488.

307. Meng, Y.; Wang, M.; Tang, M.; Hong, G.; Gao, J.; Chen, Y., Preparation of robust superhydrophobic halloysite clay nanotubes via mussel-inspired surface modification. *Applied Sciences* **2017,** *7* (11), 1129.

308. Demir, M.; Farghaly, A. A.; Decuir, M. J.; Collinson, M. M.; Gupta, R. B., Supercapacitance and oxygen reduction characteristics of sulfur self-doped micro/mesoporous bio-carbon derived from lignin. *Materials Chemistry and Physics* **2018,** *216*, 508-516.

309. Rooj, S.; Das, A.; Thakur, V.; Mahaling, R. N.; Bhowmick, A. K.; Heinrich, G., Preparation and properties of natural nanocomposites based on natural rubber and naturally occurring halloysite nanotubes. *Materials & Design* **2010,** *31* (4), 2151-2156.

310. Haroosh, H. J.; Dong, Y.; Chaudhary, D. S.; Ingram, G. D.; Yusa, S.-i., Electrospun PLA: PCL composites embedded with unmodified and 3-aminopropyltriethoxysilane (ASP) modified halloysite nanotubes (HNT). *Applied Physics A* **2013,** *110* (2), 433-442.

311. Yang, W.; Dominici, F.; Fortunati, E.; Kenny, J.; Puglia, D., Effect of lignin nanoparticles and masterbatch procedures on the final properties of glycidyl methacrylate-g-poly (lactic acid) films before and after accelerated UV weathering. *Industrial Crops and Products* **2015,** *77*, 833-844.

312. Yearla, S. R.; Padmasree, K., Preparation and characterisation of lignin nanoparticles: evaluation of their potential as antioxidants and UV protectants. *Journal of Experimental Nanoscience* **2016,** *11* (4), 289-302.

313. Sarathi, R.; Kumar, P. R.; Sahu, R., Analysis of surface degradation of epoxy nanocomposite due to tracking under AC and DC voltages. *Polymer degradation and stability* **2007,** *92* (4), 560-568.

314. Bährle, C.; Nick, T. U.; Bennati, M.; Jeschke, G.; Vogel, F., High-field electron paramagnetic resonance and density functional theory study of stable organic radicals in lignin: influence of the extraction process, botanical origin, and protonation reactions on the radical g tensor. *The Journal of Physical Chemistry A* **2015,** *119* (24), 6475-6482.

315. Prashantha, K.; Lacrampe, M.-F.; Krawczak, P., Processing and characterization of halloysite nanotubes filled polypropylene nanocomposites based on a masterbatch route: effect of halloysites treatment on structural and mechanical properties. *Express Polymer Letters* **2011,** *5* (4).

316. Rooj, S.; Das, A.; Thakur, V.; Mahaling, R.; Bhowmick, A. K.; Heinrich, G., Preparation and properties of natural nanocomposites based on natural rubber and naturally occurring halloysite nanotubes. *Materials & Design* **2010,** *31* (4), 2151-2156.